

Goldsmiths Research Online

*Goldsmiths Research Online (GRO)
is the institutional research repository for
Goldsmiths, University of London*

Citation

Javaheri Javid, Mohammad Ali. 2019. Aesthetic Automata: Synthesis and Simulation of Aesthetic Behaviour in Cellular Automata. Doctoral thesis, Goldsmiths, University of London [Thesis]

Persistent URL

<https://research.gold.ac.uk/id/eprint/27681/>

Versions

The version presented here may differ from the published, performed or presented work. Please go to the persistent GRO record above for more information.

If you believe that any material held in the repository infringes copyright law, please contact the Repository Team at Goldsmiths, University of London via the following email address: gro@gold.ac.uk.

The item will be removed from the repository while any claim is being investigated. For more information, please contact the GRO team: gro@gold.ac.uk

**AESTHETIC AUTOMATA:
SYNTHESIS AND SIMULATION OF
AESTHETIC BEHAVIOUR IN
CELLULAR AUTOMATA**

Mohammad Ali Javaheri Javid

A thesis submitted in partial fulfillment
of the requirements for the degree of

Doctor of Philosophy

in

Computer Science

Department of Computing
Goldsmiths, University of London

Declaration of Authorship

I, Mohammad Ali Javaheri Javid hereby declare that this thesis and the work presented in it is entirely my own. Where I have consulted the work of others, this is always clearly stated.

Signed:

Date:

Acknowledgements

I would like to express my gratitude to those people who have made this thesis possible: to Prof. Robert Zimmer, my first supervisor, for providing so many valuable comments, and for outstanding guides for the progress of this thesis; to Prof. Mark d'Inverno, my second supervisor, for his support and encouragement; to Dr. Tim Blackwell for his detailed, fruitful comments and stimulating discussions. I would also like to thank to all my family, especially my parents, for their love and generous support, without which this thesis could never have been produced. Very special thanks to Dr. Mohammad Majid al-Rifaie for providing enlightening discussions, feedback and an impeccable support. I am also grateful to Prof. Dr. Thomas Jacobsen of Helmut Schmidt University for sharing his experimental stimuli and data. While undertaking this research, I could count on the support of many people, who helped me to discuss concepts and ideas. They are too numerous to be listed here, but my heartfelt thanks go to each one of them.

Finally, I would like to dedicate this thesis to Dr. Javad Nurbakhsh and Dr. Alireza Nurbakhsh, the masters of love, to whom I owe my very life.

Abstract

This thesis addresses the computational notion of aesthetics in the framework of multi-state two-dimensional cellular automata (2D CA). The measure of complexity is a core concept in computational approaches to aesthetics. Shannon's information theory provided an objective measure of complexity, which led to the emergence of various informational theories of aesthetics. However, entropy fails to take into account the spatial characteristics of 2D patterns; these characteristics are fundamental in addressing the aesthetic problem, in general, and of CA-generated patterns, in particular. This thesis proposes two empirically evaluated alternative measures of complexity, taking into account the spatial characteristics of 2D patterns and experimental studies on human aesthetic perception in the visual domain. The measures are extended to robustly quantify the complexity of multi-state 2D CA-generated patterns.

The first model, spatial complexity, is based on the probabilistic spatial distribution of homogeneous/heterogeneous neighbouring cells over the lattice of a multi-state 2D cellular automaton. The second model is based on algorithmic information theory (Kolmogorov complexity) which is extended to estimate the complexity of 2D patterns. The spatial complexity measure presents performance advantage over information-theoretic models, specifically in discriminating symmetries and the orientation in CA-generated patterns, enabling more accurate measurement of complexity in relation to aesthetic evaluations of 2D patterns.

A series of experimental stimuli with various structural characteristics and levels of complexity were generated by seeding 3-state 2D CA with different initial configurations for psychological experiments. The results of experimentation demonstrate the presence of correlation between spatial complexity measures and aesthetic judgements of experimental stimuli. The same results were obtained for the estimations of Kolmogorov complexity of experimental stimuli.

Table of Contents

| | |
|--|-----------|
| Declaration of Authorship | 2 |
| Acknowledgements | 3 |
| Abstract | 4 |
| Table of Contents | 6 |
| List of Figures | 6 |
| List of Tables | 8 |
| 1 Introduction | 10 |
| 1.1 Aesthetic Automata | 12 |
| 1.2 Motivation | 13 |
| 1.3 Objectives and Scope | 14 |
| 1.4 Methodological Approach | 16 |
| 1.5 Contributions | 16 |
| 1.6 Thesis Structure | 17 |
| 2 Cellular Automata and Art | 18 |
| 2.1 Behaviour Simulator Automata | 18 |
| 2.2 Self-Replicating Automata | 20 |
| 2.3 Mathematical Foundations | 21 |
| 2.4 Behaviour Analysis | 26 |
| 2.5 Syntheses with CA | 28 |
| 2.6 Mechanism of Pattern Formation | 29 |
| 2.7 Artistic Applications of CA | 33 |
| 3 Informational Aesthetics | 39 |
| 3.1 Aesthetics as Science of Sensation | 41 |
| 3.1.1 Measuring Sensations | 41 |
| 3.2 Computing Aesthetic Sensation | 45 |
| 3.2.1 Informational Theories of Aesthetics | 47 |
| 4 Quantifying Spatial Complexity | 50 |
| 4.1 Conceptual Model | 51 |
| 4.2 Spatial Complexity Measure | 51 |
| 4.3 Kolmogorov Complexity of 2D Patterns | 55 |
| 4.4 Experiments and Results | 58 |
| 4.5 Summary | 68 |

| | |
|--|------------|
| 5 Experiments and Results | 69 |
| 5.1 Objectives | 69 |
| 5.2 Experiment I | 70 |
| 5.2.1 Method | 70 |
| 5.2.2 Material | 70 |
| 5.2.3 Procedure | 71 |
| 5.2.4 Results | 72 |
| 5.2.5 Procedure for the Extended Study | 72 |
| 5.2.6 Results and Analysis | 73 |
| 5.3 Experiment II | 77 |
| 5.3.1 Method | 77 |
| 5.3.2 Material | 77 |
| 5.3.3 Procedure | 84 |
| 5.3.4 Results and Analysis | 85 |
| 5.4 Discussions | 89 |
| 6 Conclusion | 90 |
| 6.1 Further Directions | 96 |
| Appendices | 97 |
| A Space-Time Diagrams of Cellular Automaton 4.6 | 98 |
| B Publications | 126 |
| Bibliography | 128 |

List of Figures

| | | |
|------|---|----|
| 2.1 | The formation of torus space from a lattice with periodic boundary conditions. | 22 |
| 2.2 | Illustration of von Neumann (a) and Moore (b) neighbourhood templates. | 23 |
| 2.3 | The space-time diagram depicts the behaviour of a cellular automaton as a sequence of configurations. | 24 |
| 2.4 | All the possible configurations of an outer-totalistic von Neumann neighbourhood. | 25 |
| 2.5 | All the possible configurations of an outer-totalistic Moore neighbourhood. | 25 |
| 2.6 | A 12 cell square IC used to seed cellular automaton 2.4 and a 5 cell Glider IC used to seed cellular automaton 2.5. | 29 |
| 2.7 | Space-time diagram of the cellular automaton 2.4 with the 12 cell square IC. | 30 |
| 2.8 | Space-time diagram of the cellular automaton 2.5 with the Glider IC. | 31 |
| 2.9 | Samples of multi-state 2D CA patterns generated by the author. | 32 |
| 2.10 | Samples of commercial products using CA-generated patterns. | 38 |
| 3.11 | The inverted-U curve illustrating the relationship between stimuli complexity and appraisal. | 43 |
| 3.12 | Schematic plot of the relationship between complexity and pleasantness of stimuli adapted from Berlyne. | 44 |
| 3.13 | Aesthetic measures of sample polygonal forms. | 46 |
| 4.14 | The measurements of H for structurally different patterns. | 50 |
| 4.15 | The spectrum of spatial complexity. | 51 |
| 4.16 | Calculations of $\overline{G}_{r,s}$ for a 2D pattern composed of black and white cells. | 53 |
| 4.17 | Six different templates applied for the estimation of K in 2D plane. | 56 |
| 4.18 | The measurements of H , \overline{G}_s , $\Delta\overline{G}_s$ and K for structurally different patterns. | 57 |
| 4.19 | Four different ICs used to seed cellular automaton 4.6. | 58 |
| 4.20 | The space-time diagram of cellular automaton 4.6 for a sample of time steps starting from the single cell IC (4.19(a)). | 59 |
| 4.21 | The measurements of $\Delta\overline{G}_s$ for 4.19(a) (single cell) IC. | 59 |
| 4.22 | The space-time diagram of the cellular automaton 4.6 for a sample of time steps starting from 4.19(b) IC. | 60 |
| 4.23 | The measurements of $\Delta\overline{G}_s$ for 4.19(b) IC. | 61 |
| 4.24 | The space-time diagram of the cellular automaton 4.6 for a sample of time steps starting from 4.19(c) IC. | 61 |
| 4.25 | The measurements of $\Delta\overline{G}_s$ for 4.19(c) IC. | 62 |
| 4.26 | The measurements of H for 4.19(a), 4.19(b), 4.19(c) and 4.19(d) ICs. | 62 |
| 4.27 | Comparison of the measurement of $\Delta\overline{G}_{P_d}$ for 4.19(a) and 4.19(b) ICs. | 63 |
| 4.28 | Comparison of the measurement of $\Delta\overline{G}_{S_d}$ for 4.19(a) and 4.19(b) ICs. | 63 |

| | | |
|------|---|-----|
| 4.29 | The comparison of H , $\overline{G}s$, $\Delta\overline{G}s$ and K for cellular automaton 4.6 conformations at $t = 40$ for 4.19(b) and 4.19(c) ICs. | 64 |
| 4.30 | The space-time diagram of the cellular automaton 4.6 for a sample of time steps for the random IC (4.19(d)) | 65 |
| 4.31 | The measurements of $\Delta\overline{G}s$ for 4.19(d) IC. | 65 |
| 4.32 | The estimations of K for 4.19(a), 4.19(b), 4.19(c) and 4.19(d) ICs. . . | 66 |
| 4.33 | The measurements of μGs for 4.19(a), 4.19(b), 4.19(c) and 4.19(d) ICs. . . | 66 |
| 5.34 | Samples of stimuli patterns adopted from Jacobsen and Höfel. | 71 |
| 5.35 | Mean aesthetic judgements of stimuli patterns and their ranking. | 72 |
| 5.36 | A sample of the calculations of spatial complexity, $\mu(G)s$, K and H for two stimuli patterns. | 73 |
| 5.37 | The measurement of $\mu(G)s$, K and H for stimuli patterns ordered based on their ranking. | 74 |
| 5.38 | The measurement of $\mu(G)s$, K and H for stimuli patterns ordered based on their ranking. | 75 |
| 5.39 | The spectrum of spatial complexity considered for the generation of 10 experimental patterns | 77 |
| 5.40 | Generated patterns with various structural characteristics reflecting the spectrum of spatial complexity 4.15. | 78 |
| 5.41 | The measurements of spatial complexity measure, $\mu(G)s$, K and H for the generated patterns with various structural characteristics. . . | 79 |
| 5.42 | The measurements of spatial complexity measure, $\mu(G)s$, K and H for the generated patterns with various structural characteristics. . . | 80 |
| 5.43 | The measurements of spatial complexity measure, $\mu(G)s$, K and H for the generated patterns with various structural characteristics. . . | 81 |
| 5.44 | The measurements of spatial complexity measure, $\mu(G)s$, K and H for the generated patterns with various structural characteristics. . . | 82 |
| 5.45 | The measurements of spatial complexity measure, $\mu(G)s$, K and H for the generated patterns with various structural characteristics. . . | 83 |
| 5.46 | The plot of $\mu(G)s$, K and H for the generated survey patterns. | 84 |
| 5.47 | The order of patterns used in the survey. | 84 |
| 5.48 | The total ratings and the aggregated scores for the patterns. | 86 |
| 5.49 | The aggregated scores of survey patterns. | 87 |
| 5.50 | The arrangement of patterns in descending order of their aggregated scores. | 87 |
| 6.51 | The spectrum of spatial complexity. | 91 |
| A.1 | The space-time diagram of cellular automaton 4.6 for 200 time steps starting from the single cell IC (4.19(a)). | 104 |
| A.2 | The space-time diagram of cellular automaton 4.6 for 200 time steps starting from 4.19(b) IC. | 111 |
| A.3 | The space-time diagram of cellular automaton 4.6 for 200 time steps starting from 4.19(c) IC. | 118 |
| A.4 | The space-time diagram of cellular automaton 4.6 for 200 time steps starting from the random IC (4.19(d)). | 125 |

List of Tables

| | | |
|------|--|----|
| 2.1 | Update rule of GoL cellular automaton. | 25 |
| 2.2 | Comparison of the size of rule spaces for two state 2D CA using formulas. | 26 |
| 2.3 | Parametrising CA rules space by λ parameter. | 27 |
| 2.4 | Update rule of cellular automaton 2.4. | 29 |
| 2.5 | Update rule of cellular automaton 2.5. | 30 |
| 4.6 | Update rule of cellular automaton 4.6. | 58 |
| 4.7 | Calculations of r for different ICs. | 67 |
| 5.8 | The results of Pearson correlation coefficient test between μGs , K , H and pattern ranking along with mean aesthetic ratings of the 252 stimuli patterns. | 76 |
| 5.9 | The distribution of age groups and genders for 68 collected valid responses. | 85 |
| 5.10 | The results of survey. | 85 |
| 5.11 | Assigned weight to each scale. | 85 |
| 5.12 | The results of Spearman rank correlation test (r_s) between μGs , K , H and the aggregated scores of survey patterns. | 88 |

1. Introduction

*“How lovely, how beautiful!
Your face!*

*What coyness lies in those eyes
and eyebrows!” [1]*

– Dr. Javad Nurbakhsh

Beauty has an affective power encountering it in natural instances initiates an immediate perceptual experience of *pleasure* and *delight*. Our attraction to beauty and innate ability to extract information on the aesthetic qualities of objects drive our efforts in the creation of various synthetic instances of beauty, either in the forms of artworks or objects of design.

Human creation of synthetic forms and objects can be traced back to prehistoric eras. What is known as *prehistoric art* was created in preliterate period on the walls of caves or shells using ochre, bone and charcoal for a variety of possible purposes: communication, recording events or aesthetic purposes. We continue to engage ourselves with the creation of synthetic forms, exploiting the capabilities of modern tools made available by technological advances.

While early humans employed organic materials for the creation of their synthetic forms, nowadays we tend to employ *digital tools* to create our *digital forms* on *digital media* for almost the same purposes. The introduction of direct graphical manipulation and interactive tools in the early 1960s transformed human-computer interaction and made digital machines more accessible to non-technical artists who did not have the knowledge of punch card programming, and utilised computers to *partially automate artistic processes* [2].

Using a computer to partially automate an artistic process has brought me, a non-artist, some understanding of the effect of certain features on

the appearance of a face. It is the understanding that can be gained from computer drawings that is more valuable than mere production of a drawing for shop use [2, p.110].

The availability of interactive graphical tools along with high level languages specifically designed for graphic generation created a new form of art known as *computer art*, or, according to Max Bense “*artificial art*” [3].

The partial automation of artistic processes using computers exposes us to a very distinct visual perceptual space through the experience of synthetic instances of beauty. As noted by Michael Noll, one of the early pioneers of computer art:

In the computer, man has created not just an inanimate tool but an intellectual and active creative partner that, when fully exploited, could be used to produce wholly new art forms and possibly new aesthetic experiences [4, p.89].

The advancement of computer tools and contributions from techniques developed in Artificial Intelligence (AI) and Artificial Life (ALife) fields have shifted the automation of artistic processes towards a more *autonomous artistic process* where AI and ALife enabled techniques make decisions within a defined domain in situations that are not pre-determined.

The autonomy of computer art heavily relies on ALife techniques among others. The field of ALife is inspired by biological systems and exploits computer technology to synthesize and simulate common processes and behaviours of living organisms based on the principles of bottom-up synthesis. Many ALife techniques (collectively referred to as generative tools) have been contributed either for the creation of computer art or for addressing problems concerning the autonomy of artistic processes.

Evolutionary computation in [5, 6, 7, 8, 9, 10, 11, 12, 13, 14, 15], swarm intelligence in [16, 17, 18], ant colony in [11], Lindenmayer systems [19] in [20, 21, 22, 23] and reaction-diffusion systems in [24] are some examples of ALife based art syntheses.

1.1 Aesthetic Automata

Cellular Automata (CA), among other generative tools, have contributed to the creation of many forms of computer art. In the 1960s the idea of using CA as an artistic tool emerged from the works of Knowlton and Schwartz, who produced “*Pixillation*”, one of the early computer generated animations [25, 26].

The concept of cellular automaton, one of the early biologically inspired systems, was developed in the late 1940s by John von Neumann and Stanislaw Ulam as a material independent framework to simulate the self-replicating behaviour of biological systems.

Although CA was a known computational paradigm within the computer science community and several research efforts followed John von Neumann’s idea of self-replicating automata [27], it remained neglected for decades [28] until Gardner published an account of John Conway’s “Game of Life” (GoL) as a “new solitaire game” in 1970 [29]. The GoL is a simple binary cellular automaton with two states, 0 and 1, which are interpreted as *dead* or *live*. But despite its simplicity, the GoL is capable of generating complex and emergent behaviour. The popularity of the GoL drew the attention of the wider community of digital artists and designers to the unexplored potential of CA in generating rich digital content from the iteration of simple deterministic rules.

The computer arts of Struycken [30] and Brown [31] and evolutionary architecture of Frazer [32] are some examples of CA driven computer arts. Moreover, CA have been used for music composition, for example, Xenakis [33] and Miranda [34].

The main characteristics of CA that make them particularly interesting to digital artists are their ability to generate visually appealing and very complex patterns on the basis of very simple rules. This fact has been noted by Wolfram, who himself produced some CA art in the 1980s, “even a program that may have extremely simple rules will often be able to generate pictures that have striking aesthetic qualities—sometimes reminiscent of nature, but often unlike anything ever seen before.” [35, p.11].

1.2 Motivation

Aesthetic qualities are an integral part of the creation of various forms of art (painting, sculpture, music, dance), product [36] and architectural designs [37], information visualization [38], usability studies [39, 40] and human computer interaction (HCI) [41]. The combined exponential increase in the processing capacity of hardware devices and the richness of software tools available to the research and practice of computer graphics and visualisation, on one hand, and the application of computers as an artistic tool along with the significance of aesthetic qualities in developing graphical contents on other hand, have contributed to the emergence of a new field called *computational aesthetics* in computer science.

The notion of computational aesthetics is defined as “the research of computational methods that can make applicable aesthetic decisions in a similar fashion as humans can” [42, p.16]. From a merely computational perspective, the research revolves around developing aesthetic measures as functions which compute the aesthetic value of an object [digital object] [43]; however, in a wider perspective it integrates computer science with philosophy, biology, psychology, and art. Furthermore, the field investigates both tools to enhance the expressiveness of fine and applied arts, as well as theoretical approaches that further our understanding of aesthetic evaluation, perception and meaning [44].

The general approach of digital art in visual domains is based on utilising generative tools to create a large pool of imagery followed by subjective aesthetic evaluation and selection by the artist. Given that the generative tools can generate thousands of pieces of imagery with different characteristics in a short period of time, the process of aesthetic evaluation and selection would be a time consuming process for human users. Hence automating the aesthetic evaluation and selection process in a way which is capable of making aesthetic judgements conforming to human aesthetic perception is fundamental to computational aesthetics. Therefore, the ultimate goal of computational aesthetics is to close the loop of generation and evaluation where both processes are functions of computational methods.

The primary motivation of this research has come from our earlier study with multi-state 2D CA models where visually appealing behaviours were observed [45]. Although CA with binary states can exhibit complex behaviours, experiments with multi-state 2D CA models have shown that adding more states significantly increases

the complexity of behaviour, thus, generating very complex patterns occasionally with high aesthetic qualities [45].

There have been interesting attempts to develop means of controlling the emergence of aesthetic behaviour in CA [46, 8, 47, 48, 49]. A recent work offers insights in the production of art works using CA models and intended to inspire artists to take on cellular automata as their creative tool [50]. Despite the popularity of CA models among digital artists and a great deal of research conducted on the theoretical and practical areas of CA, the subject of the quantitative aesthetic evaluation of CA behaviour is left mostly unexplored.

1.3 Objectives and Scope

This study builds its grounds on the theories of aesthetics which associate the aesthetic perception with the degree of stimulus complexity. These theories can be divided (roughly) in two main categorises:

1. Theories which consider *inverse* relationship between stimulus complexity and aesthetic preference,
2. Theories which consider *direct* relationship between stimulus complexity and aesthetic preference.

The aesthetic measure of Birkhoff [51] is an example of inverse relationship theories which has influenced most computational notions of aesthetics. Theories considering direct relationship between stimulus complexity and aesthetic preference are mostly developed from empirical studies of aesthetics, such as the “arousal theory” of Berlyne [52].

We assume a direct relationship between stimulus complexity and aesthetic preference taking into account the findings of experimental studies. In addition, it is assumed that a decrease in the degree of complexity would lead to some form of order, whereas an increase would lead to randomness. Therefore, a single measure of complexity would be sufficient for the computational notions of aesthetics. This assumption is in contrast with Birkhoff’s separation of order and complexity in his aesthetic measure.

The scope of this research is limited to (1) multi-state 2D CA and (2) visual aesthetics. It follows the tradition of parametrising aesthetic objects based on an

objective measure of complexity. Therefore, the broad aim is to address aesthetic problems in two dimensions and particularly within the framework of 2D CA by investigating the possibility of formulating a complexity measure for aesthetic evaluation of CA-generated patterns. The measure of complexity is required to meet the following criteria:

1. The measure uses only information available within the framework of 2D CA, such as the number of cells and their states, size of lattice and neighbourhood template. This constraint considers the generated patterns of CA to be internal objects of CA environment.
2. The measure reflects on the structural characteristics of CA patterns (i.e. homogeneity/heterogeneity of cells and their spatial distribution over the lattice of CA).

Given these criteria, informational theories of complexity are capable of parametrising structurally different 2D CA patterns. Despite great debate and differentiation over the terms “*aesthetic*”, “*beautiful*” and “*attractive*” in philosophy and other disciplines, these terms are used interchangeably throughout this thesis.

1.4 Methodological Approach

This research is conducted within two distinctive methods:

- (1) Rational Aesthetics: A scientific approach to address aesthetic problems.
- (2) Bottom-up Synthesis: Aesthetic as a global behaviour is a result of local interactions or rules in CA.

In the absence of scientific theories of aesthetics, any methodological approach of computational aesthetics is inherently empirical and experimental [53]. Therefore, the validity of the models is assessed by conducting experiments with human subjects to evaluate the following general hypotheses:

Hypothesis 1: *The aesthetic value of a cellular automaton pattern depends on the sum of mean information gains of cells having homogeneous/heterogeneous neighbouring cells over the lattice of a cellular automaton.*

Hypothesis 2: *The aesthetic value of a cellular automaton pattern depends on the estimation of the Kolmogorov complexity of a cellular automaton pattern.*

1.5 Contributions

This thesis has made a number of contributions to the fields of computer science and computational aesthetics. These contributions are listed below:

1. The development of a *spatial complexity spectrum*, taking into account human intuitive perception of complexity and structural characteristics of 2D patterns. The model is bound by two extreme points of complete *order* and *disorder*. It facilitates the mapping of the complexity of 2D patterns based on their structural characteristics between the two extremes.
2. Developing *spatial complexity measure*, capable of discriminating symmetries and their orientation in a 2D plane. It also is capable of reflecting on the spatial distribution of a cell over the lattice of 2D CA. The model is based on information gain measure in [54, 55, 56].
3. Extending algorithmic information theory of Kolmogorov [57] for estimating the complexity of patterns in 2D plane.

1.6 Thesis Structure

The structure of this thesis is organised as follows:

Chapter 2: Cellular Automata and Art

This chapter reviews the historical development of automata and CA. Formal definitions are then provided, with an analysis of CA behaviour followed by a review of some applications of CA. Finally, the contributions of various CA models for the creation of computer arts are reviewed.

Chapter 3: Informational Aesthetics

In this chapter, the relationship between aesthetics and complexity is examined. The notion of complexity from Shannon's information theory perspective is analysed, and its influence on informational theories of aesthetics is discussed.

Chapter 4: Quantifying Spatial Complexity

This chapter covers analysis of entropic approaches for aesthetic evaluation purposes. An in-depth analysis of entropic measure for 2D patterns with examples are provided. In the framework of the objectives of this study, a spatial complexity spectrum is formulated then two models of spatial complexity and Kolmogorov complexity are developed. The effectiveness of the models in discriminating symmetries and their orientation in 2D plane are then evaluated using a set of experiments.

Chapter 5: Experiments and Results

This chapter covers the details of the two experiments and their results on the correlation between entropy, spatial complexity and Kolmogorov complexity measures with human aesthetic judgement.

Chapter 6: Conclusion

This chapter covers the findings of this thesis by summarising the results of the experiments and exploring further applications of the developed models.

2. Cellular Automata and Art

Cellular Automaton is one of the first biologically inspired systems. Decades of research in Cellular Automaton has created a vast amount of literature dealing with the theoretical and practical aspects of CA. This chapter will not serve as comprehensive coverage of literature, but a selective set of relevant and core contributions to the research of CA which are closely related to the topic of this thesis. It reviews the historical development of automata and CA. Formal definitions are provided with an analysis of CA behaviour followed by a review of some applications of CA. Finally, the contributions of various CA models for the creation of computer arts are reviewed.

2.1 Behaviour Simulator Automata

Designing and building mechanical automata to perform a range of functions according to a predetermined set of instructions have been the subject of many endeavours since antiquity. The term *automaton* (pl. *automata*, *automatons*) is derived from the Greek word *autómatos* meaning “self-acting” formed from the combination of *autos* meaning “self” and *matos* meaning “thinking and animated”. Initially, automata referred to a mechanical device that is self-operating (acting without human agency) after it has been set in motion [58].

Designing automata as self-performing mechanical machines generating the behaviour of living beings has been the subject of many studies. They were built to either perform functional tasks (e.g. time keeping and calculations) or for entertainment purposes (e.g. theatrical automata and musical automata). The *Antikythera* mechanism is an example of functional automata and is considered the earliest known analogue computer, designed between 150 – 100 BC to mechanically

calculate the positions of astronomical objects [59]. Descartes (1596 – 1650) evaluated the functioning of animals, and much of humans, as being explainable in terms of the automata of his day (i.e. clockwork and hydraulic automata) but drew a line at the cognitive functions of the brain [60].

During the 17th century, Pascal (1623 – 1662) designed and built *Pascaline*, a mechanical calculator which was capable of performing addition and subtraction. Leibniz (1646 – 1716), inspired by Pascal’s work, designed *Leibnitz’s Wheel* which could perform multiplication and division as well.

In the 18th century Jacques de Vaucanson (1709 – 1789) designed *Digesting Duck*, an automaton capable of digestion. Some of the most significant automata of this period were designed by Pierre Jaquet-Droz (1721 – 1790) by focusing on the simulation of human behaviour like *The Writer*, *The Musician* and *The Draughtsman*. His *Writer* automata was a special case among the others since it was *programmable automata*. Charles Babbage’s (1791 – 1871) *Difference Engine* was an attempt to build an automaton to remove the errors of human computers on creating mathematical tables.

In the 20th century, the design of automata shifted towards the simulation of mankind’s cognitive power by focusing on “information processing automata”. The purpose was to mechanically automate the task of large scale calculations (e.g. military data processing) assigned to human computers . These calculations could sometimes be very complex and introduce errors with serious consequences. Since then, *automata* referred to a class of electromechanical devices that transform information from one form into another on the basis of predetermined instructions [58].

Building information processing automata was far more complex than the classical automata known at the time. This is because it needed to undertake the kind of tasks which are usually performed by human cognition. There was a gap in the knowledge for understanding both the biological and logical principles underlying the operations of the human brain in terms of an information processing automaton.

In addressing *Hilbert’s decision problem* (i.e. the possibility of solving all mathematical problems using algorithms), Turing invented an abstract machine which he called *automatic machine* (now commonly referred to as *The Turing Machine*) [61]. Turing’s machine laid the foundations for the development of information processing automata which was exclusive to biological systems.

2.2 Self-Replicating Automata

On 20 September, 1948 John von Neumann delivered a lecture titled “*The General and Logical Theory of Automata*” at the Hixon Symposium in Pasadena, California. In this lecture he outlined a model of an *Automaton* as a machine that its behaviour follows *logical axioms*. This model was abstracted from the observations of living organisms to conceptualize an *artificial automaton*. He then used this general model to address the specific problem of *self-replication* with reference to Turing’s computing machine.

For the question which concerns me here, that of “*self-reproduction*” of automata, Turing’s procedure is too narrow in one respect only. His automata are purely computing machines. Their output is a piece of tape with zeros and ones on it. What is needed for the construction to which I referred is an automaton whose output is other automata...

The problem of self-reproduction can then be stated like this: *Can one build an aggregate out of such elements in such a manner that if it is put into a reservoir, in which there float all these elements in large numbers, it will then begin to construct other aggregates, each of which will at the end turn out to be another automaton exactly like the original one?* This is feasible, and the principle on which it can be based is closely related to Turing’s principle outlined earlier [62, p.28].

To achieve a self-replicating automaton, von Neumann explored (1) *kinematic machine*, (2) *cellular machine*, (3) *neuron type machine*, (4) *continuous machine*, and (5) *probabilistic machine* [63]. His kinematic machine was a physically realised floating machine in a pool of elements with long sequences of instructions and a constructor arm to reach necessary elements and assemble an identical copy of itself. This physical machine needed to address many problems before it could actually begin assembling a replica of itself.

Stanislaw Ulam was also interested in the concept of self-replication. He would sit in a coffeehouse in Lwów in 1929, speculating on the possibility of artificial automata reproducing themselves [64]. At the time, he was working with a lattice network as a mathematical model to study crystal growth. He suggested the use of a lattice network as a material independent framework to investigate the possibility

of self-reproduction [65]. The integration of the lattice network model with the logic of self-replication formulated the initial model of *Cellular Automata*. It is fair to say that the *cellular* part comes from Ulam, and the *automata* part from von Neumann [66].

The machinery of cellular automata (CA) is based on the local interaction of each automaton (cell) with its immediate neighbourhood automata (cells) according to a set of rules. The interaction of automata at a local level generates the emergent behaviour, sometimes with attractive complexity, at the global level. The first theoretical model of self-replicating cellular automaton was a 2D lattice of cells with 29 states for each cell and 5-cell neighbourhood. Later, Longan showed that a self-replication can be achieved with only 8 states (known as *Langton's Loop* [67]). Byl then showed that self-replication is possible with a mere 6 states [68] (known as *Byl's Loop*).

2.3 Mathematical Foundations

Since the mathematics of *crystalline structures* contributed to the mathematical foundation of CA with lattice networks model by Ulam, most mathematical formulations in CA are inherited from *lattices (order theory)*, *crystallography* and *finite state automaton*.

Definition 2.1. *A deterministic finite state automaton is formally defined [69] as a quintuple of \mathcal{M} such that:*

$$\mathcal{M} = \langle Q, \Sigma, \delta, q_0, F \rangle, \quad (2.1)$$

1. Q is a finite set of *states*,
2. Σ is a finite set of symbols as *input alphabet*,
3. $\delta : Q \times \Sigma \mapsto Q$ is the *state transition function*,
4. $q_0 \in Q$ is the *start* or *initial state*,
5. $F \subseteq Q$ is a set of *accepting* or *final states*.

The state transaction function δ takes two arguments as $q \in Q$ and an input symbol $a \in \Sigma$ and then maps them to final state $q_1 \in Q$ (i.e, $\delta(q, a) = q_1$). The term “deterministic” refers to the fact that for each input there is one and only one state to which the automaton can be transmitted from its current state.

Definition 2.2. A lattice L is a regular tiling of space by a unit cell.

The *Euclidean* plane is considered so the lattice L is over Z^2 . Lattices can have *square*, *hexagonal* or *triangle* for their unit cells. A lattice can be *infinite* with *aperiodic boundary conditions*, or *finite* with *periodic boundary conditions*. A finite lattice with periodic boundary conditions where the opposite borders (up and down with left and right) are connected forms a torus space (Fig. 2.1).

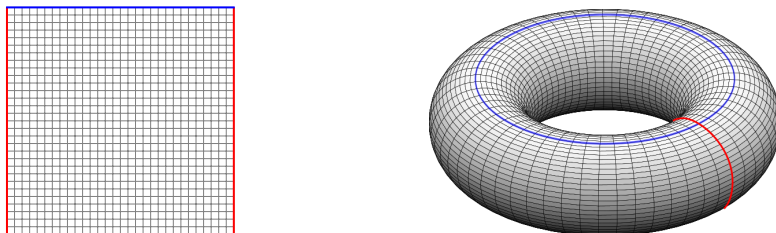


Fig. 2.1. The formation of torus space from a lattice with periodic boundary conditions.

Definition 2.3. A cellular automaton is a regular tiling of a lattice with uniform deterministic finite state automata.

A cellular automaton \mathcal{A} is specified by a quadruple $\langle L, S, \mathcal{N}, f \rangle$ where:

1. L is a finite square lattice of cells (i, j) ,
2. $S = \{1, 2, \dots, k\}$ is set of states. Each cell (i, j) in L has a state $s \in S$,
3. \mathcal{N} is neighbourhood, as specified by a set of lattice vectors $\{e_a\}$, $a = \{1, 2, \dots, N\}$.

The neighbourhood of cell $r = (i, j)$ is $\{r + e_1, r + e_2, \dots, r + e_N\}$,

4. f is state transition function (update rule). f computes the state s_1^{t+1} of a given cell from the states (s_1, s_2, \dots, s_N) of cells in its neighbourhood: $s_1^{t+1} = f(s_1, s_2, \dots, s_N)$.

Remark 2.1. A mapping that satisfies $f(s_q, s_q, \dots, s_q) = s_q$ where $s_q \in S$ is called a *quiescent state*.

Remark 2.2. A cell is considered to be in its own neighbourhood so that one of $\{e_a\}$ is the zero vector $(0, 0)$. With an economy of notation, the cells in the neighbourhood of (i, j) can be numbered from 1 to N ; the neighbourhood states of (i, j) can therefore be denoted (s_1, s_2, \dots, s_N) .

Remark 2.3. When periodic boundary conditions are applied at the edges of the lattice, complete neighbourhoods exist for every cell in L .

Remark 2.4. If a lattice is considered as a set, then its elements are deterministic finite automata such that $L = \{a_1, a_2, \dots, a_n\}$.

The state transition function f maps from the set of neighbourhood states $S^{|N|}$ where $|N|$ is the cardinality of neighbourhood set, to the set of states $S = \{s_1, \dots, s_N\}$ *synchronously* in *discrete time* intervals of $t = \{0, 1, 2, 3, \dots, N\}$ where t_0 is the *initial time* of cellular automaton. The state of each cell at time $(t + 1)$ is determined by the states of immediate neighbouring cells (nearest neighbourhood) at time (t) given a neighbourhood template. Two common neighbourhoods are the five-cell mapping von Neumann neighbourhood ($f : S^5 \mapsto S, \{(0, 0), (\pm 1, 0), (0, \pm 1)\}$, Eq. 2.2, Fig. 2.2(a)) and the nine-cell mapping Moore neighbourhood ($f : S^9 \mapsto S, \{(0, 0), (\pm 1, 0), (0, \pm 1), (\pm 1, \pm 1)\}$, Eq. 2.3, Fig. 2.2(b)).

$$s_{i,j}^{t+1} = f \left(\begin{array}{ccc} & s_{(i,j+1)}^t & \\ s_{(i-1,j)}^t & s_{(i,j)}^t & s_{(i+1,j)}^t \\ & s_{(i,j-1)}^t & \end{array} \right) \quad (2.2)$$

$$s_{i,j}^{t+1} = f \left(\begin{array}{ccc} s_{(i-1,j+1)}^t & s_{(i,j+1)}^t & s_{(i+1,j+1)}^t \\ s_{(i-1,j)}^t & s_{(i,j)}^t & s_{(i+1,j)}^t \\ s_{(i-1,j-1)}^t & s_{(i,j-1)}^t & s_{(i+1,j-1)}^t \end{array} \right) \quad (2.3)$$

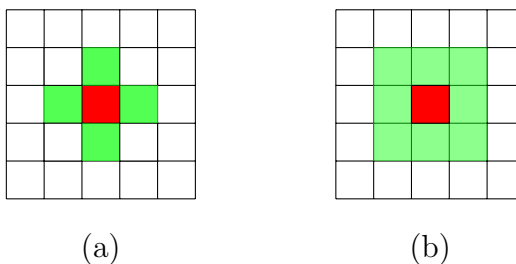


Fig. 2.2. Illustration of von Neumann (a) and Moore (b) neighbourhood templates.

The collection of states for all cells in L is known as a *configuration* (C). The global rule F maps the whole automaton forward in time; it is the synchronous application of f to each cell. The behaviour of a particular \mathcal{A} is the sequence $(c^0, c^1, c^2, \dots, c^{T-1})$, where c^0 is the initial configuration (IC) at $t = 0$. The graphical representation of the sequence of configurations as the behaviour of a

cellular automata by assigning a colour for cell state (cell) over the lattice L is called a *space-time diagram*. The space-time diagrams add another dimension as *time* to depict the spatio-temporal dynamics of CA behaviour (Fig. 2.3).

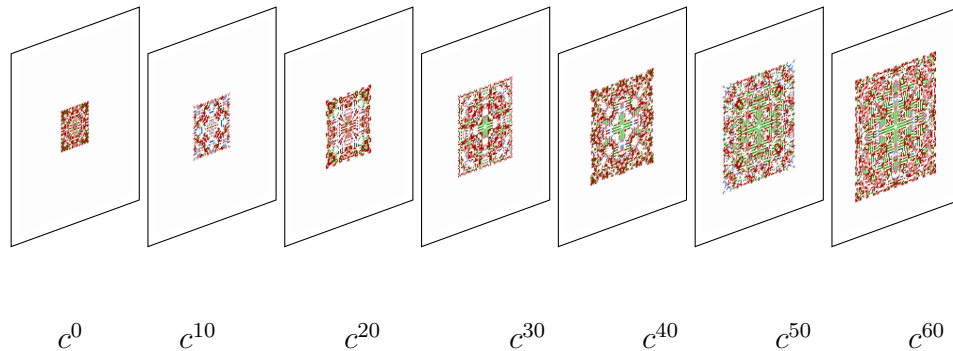


Fig. 2.3. The space-time diagram depicts the behaviour of a cellular automaton as a sequence of configurations.

Remark 2.5. Since the lattice, time intervals and states are all discrete values, a cellular automaton in this scope can be considered a *discrete dynamical system*.

The total number of possible state transition functions as the size of rule space Φ can be obtained from

$$\Phi = |S|^{|S|^{|N|}}, \quad (2.4)$$

where $|S|$ is the cardinality of S and $|N|$ is the cardinality of N . For instance, given a two state ($|S|= 2$) mapping with a Moore neighbourhood template ($|N|= 9$), $\Phi = 2^{2^9} = 2^{512} \approx 1.3 \times 10^{154}$. In order to put this number in perspective, it can be noted that the number of atoms in a visible universe is $\approx 10^{80}$. This excessively large number of state transition functions can neither be stored in any modern computer nor be algorithmically defined. A general approach to overcome this problem is to define a subset(s) of all possible state transition functions via a formula.

Two commonly applied formulas to generate such subsets are *totalistic* rules and *outer totalistic* rules, where the state of each cell is updated according to the sum of the states of the neighbouring cells in a given template. Eq. 2.5 and Eq. 2.6 show the generation of totalistic (tot) and outer-totalistic (outer-tot) rules for a Moore neighbourhood template. Conway's GoL is an example of an outer-totalistic Moore neighbourhood cellular automaton (Table. 2.1).

$$\text{Totalistic rules: } s_{i,j}^{t+1} = f_{tot}(\sigma), \quad (2.5)$$

where

$$\sigma = \sum \left\{ \begin{array}{ccc} s_{(i-1,j+1)}^t & s_{(i,j+1)}^t & s_{(i+1,j+1)}^t \\ s_{(i-1,j)}^t & s_{(i,j)}^t & s_{(i+1,j)}^t \\ s_{(i-1,j-1)}^t & s_{(i,j-1)}^t & s_{(i+1,j-1)}^t \end{array} \right\}.$$

$$\text{Outer-totalistic rules: } s_{i,j}^{t+1} = f_{outot}(\sigma), \quad (2.6)$$

where

$$\sigma = \sum \left\{ \begin{array}{ccc} s_{(i-1,j+1)}^t & s_{(i,j+1)}^t & s_{(i+1,j+1)}^t \\ s_{(i-1,j)}^t & & s_{(i+1,j)}^t \\ s_{(i-1,j-1)}^t & s_{(i,j-1)}^t & s_{(i+1,j-1)}^t \end{array} \right\}.$$

Game of Life Cellular Automaton

\mathcal{N} : Moore neighbourhood

$f : S^9 \mapsto S$

$$f_{(s_{i,j})}^t = s_{(i,j)}^{t+1} = \left\{ \begin{array}{ll} 1 & \text{if } s_{(i,j)}^t = 1 \text{ and } \sigma = 2, 3 \\ 1 & \text{if } s_{(i,j)}^t = 0 \text{ and } \sigma = 3 \\ 0 & \text{otherwise} \end{array} \right\}$$

Table 2.1: Update rule of GoL cellular automaton.



Fig. 2.4. All the possible configurations of an outer-totalistic von Neumann neighbourhood.

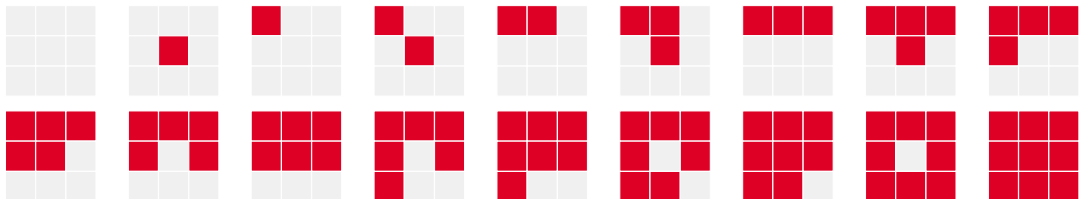


Fig. 2.5. All the possible configurations of an outer-totalistic Moore neighbourhood.

Fig. 2.4 illustrates all the possible configurations of an outer-totalistic Moore neighbourhood and Fig. 2.5 illustrates all the possible configurations of an outer-totalistic von Neumann neighbourhood. Table 2.2 demonstrates the reduction of the size of rule space by defining formulas to generate a subset of state transaction functions.

| Rule type | von Neumann (5) | Moore (9) |
|------------------|--|---|
| All | $2^{2^5} = 2^{32} \approx 4 \times 10^9$ | $2^{2^9} = 2^{512} \approx 1.3 \times 10^{154}$ |
| Totalistic | $2^5 = 32$ | $2^9 = 512$ |
| Totalistic | $3^5 = 243$ | $3^9 = 19683$ |
| Totalistic | $4^5 = 1024$ | $4^9 = 262144$ |
| Outer Totalistic | $2^{10} = 1024$ | $2^{18} = 262144$ |

Table 2.2: Comparison of the size of rule spaces for two state 2D CA using formulas.

2.4 Behaviour Analysis

Behavioural studies of CA deal with two kinds problems: (1) forward problems, where given a cellular automaton rule, determining a corresponding behaviour, and (2) backward problems, where given the behaviour of a cellular automaton, finding the corresponding rule(s) [70].

Wolfram noted that the behaviour of one-dimensional CA (1D CA) starting from a random initial configuration falls into four qualitative classes [71]:

Class 1 Evolution leads to a homogeneous state.

1D CA in this class always evolves to a homogeneous arrangement, with every cell being in the same state, never to change again.

Class 2 Evolution leads to a set of separated simple stable or periodic structures.

CA in the second class form periodic structures that endlessly cycle through a fixed number of states.

Class 3 Evolution leads to a chaotic pattern.

CA in the third class form random-like patterns that are a lot like the static white noise in a bad television channel.

Class 4 Evolution leads to complex localized structures, sometimes long-lived.

CA in the fourth class form complex patterns with localized structure that move through space in time. The patterns must eventually become homogeneous, like Class 1, or periodic like Class 2.

For the quantitative analysis of CA behaviour, Langton [72] introduced λ parametrisation scheme to quantitatively evaluate the behaviour of Wolfram's four classes [73]. The λ parameter measures how many neighbourhood states are mapped onto a non-quiescent state by a particular transition function. He considered all of the rules that defined the mapping from one neighbourhood configuration into another. Some of these rules will map a cell into the quiescent state, while others will map into the other states. It is possible to split these two rule types into two distinct sets, with the union of the sets being all of the rules. Considering that the total number of entries in the rule table is equal to K^{2r+l} . Letting the number of rules that map to the quiescent state be N_q , we can define a special parameter as the fraction of all the rules that map to a non-quiescent state Eg. 2.7. Table 2.3 show how rules space can be parametrised using λ .

$$\lambda = \frac{K^N - N_q}{N} \quad (2.7)$$

| λ | all rules | chaotic rules | complex rules |
|-----------|-----------|---------------|---------------|
| 0 | 1 | 0 | 0 |
| 1/8 | 8 | 0 | 0 |
| 1/4 | 28 | 2 | 0 |
| 3/8 | 56 | 4 | 1 |
| 1/2 | 70 | 20 | 4 |
| 5/8 | 56 | 4 | 1 |
| 3/4 | 28 | 3 | 0 |
| 7/8 | 8 | 0 | 0 |
| 1 | 1 | 0 | 0 |

Table 2.3: *Parametrising CA rules space by λ parameter.*

2.5 Syntheses with CA

Different CA models have been developed to address a variety of complex problems not only in computer science but also in other disciplines which heavily rely on computational tools to devise domain specific solutions. The significance of CA for computer science and other disciplines can be summarised as: (1) powerful computational engines, (2) discrete dynamical system simulators, (3) conceptual vehicles for studying pattern formation and complexity and (4) original models of fundamental physics [74].

CA can be considered discrete approximations to partial differential equations and can thus be used as direct models for a variety of natural systems. They can also be considered discrete dynamical systems corresponding to continuous mappings on the *Cantor set*. Finally, they can be viewed as computational systems whose evolution processes information contained in their ICs [75]. Wolfram considered 2D CA to be important tools for comparisons with many experimental results on pattern formation in physical systems [76].

A wide range of CA models have been successfully applied to simulate physical systems [77, 78], chemical systems [79], biological systems [80, 81, 82], ecological systems [83], social dynamics [84], biological pattern formation [85, 86], fluid dynamics [87, 88, 89], reaction-diffusion systems [90], distribution of galaxies [91], pedestrians and crowd [92], cities and urban development [93, 94, 95], brain tumor growth [96], avalanches [97], traffic [98], earthquakes [99, 100], forest fire [101], crystal growth [102, 103], stem cell self-organisation [104] and control of robots [105]. Additionally, they have been used in computer graphics [106], cryptography [107, 108], image processing [109, 110], data compression [111] and many more (see [112, 74, 113, 114] for more CA applications).

2.6 Mechanism of Pattern Formation

The behaviour of a cellular automaton is sensitive to the IC and to L, S, N and f . The behaviour is generally non-linear and sometimes highly complex; no single mathematical analysis can describe, or even estimate, the behaviour of an arbitrary automaton. The vast size of the rule space, and the fact that this rule space is unstructured, mean that knowledge of the behaviour of a particular cellular automaton, or even of a set of automata, gives no insight into the behaviour of any other CA. In the lack of any practical model to predict the behaviour of a cellular automaton, the only feasible method is to run a simulation. In other words, there is no guarantee that for a given automaton rule and a given IC there will be any adequate formula for predicting the developmental sequence of the automaton since CA are computationally irreducible [115]. Fig. 2.7 and Fig. 2.8 illustrate the emergence of complex and interesting patterns by seeding automaton 2.5 with 2.6(a) and 2.6(b) ICs.

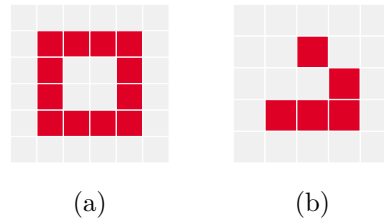


Fig. 2.6. A 12 cell square IC used to seed cellular automaton 2.4 and a 5 cell Glider IC used to seed cellular automaton 2.5.

Cellular Automaton 2.4

$L = 24 \times 24$ (576 cells)

$S = \{0, 1, 2\} \equiv \{\text{grey}, \text{red}, \text{green}\}$

\mathcal{N} : Moore neighbourhood

$f : S^9 \mapsto S$

$$f_{(s_{i,j})}^t = s_{(i,j)}^{t+1} = \left\{ \begin{array}{ll} 0 & \text{if } s_{(i,j)}^t = 2 \quad \text{and } \sigma = 5 - 8 \\ 1 & \text{if } s_{(i,j)}^t = 1,2 \quad \text{and } \sigma = 2,3 \\ 1 & \text{if } s_{(i,j)}^t = 0 \quad \text{and } \sigma = 3 \\ 2 & \text{if } s_{(i,j)}^t = 1,2 \quad \text{and } \sigma = 0 - 8 \\ 0 & \text{otherwise} \end{array} \right\}$$

Table 2.4: Update rule of cellular automaton 2.4.

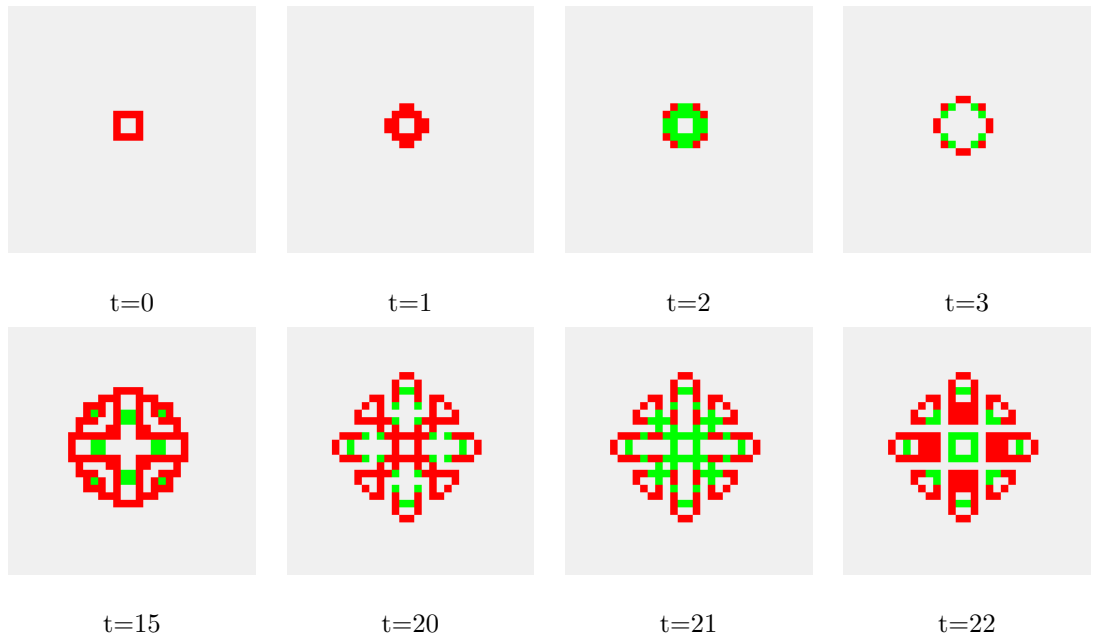


Fig. 2.7. Space-time diagram of the cellular automaton 2.4 with the 12 cell square IC.

Cellular Automaton 2.5

$L = 128 \times 128$ (16384 cells)

$S = \{0, 1, 2\} \equiv \{\text{white}, \text{red}, \text{green}\}$

\mathcal{N} : Moore neighbourhood

$f : S^9 \mapsto S$

$$f_{(i,j)}^t = s_{(i,j)}^{t+1} = \left\{ \begin{array}{ll} 2 & \text{if } s_{(i,j)}^t = 0 \quad \text{and } \sigma = 3 \\ 2 & \text{if } s_{(i,j)}^t = 1,2 \quad \text{and } \sigma = 2,3 \\ 1 & \text{if } s_{(i,j)}^t = 1,2 \quad \text{and } \sigma = 0-8 \\ 0 & \text{otherwise} \end{array} \right\}$$

Table 2.5: Update rule of cellular automaton 2.5.

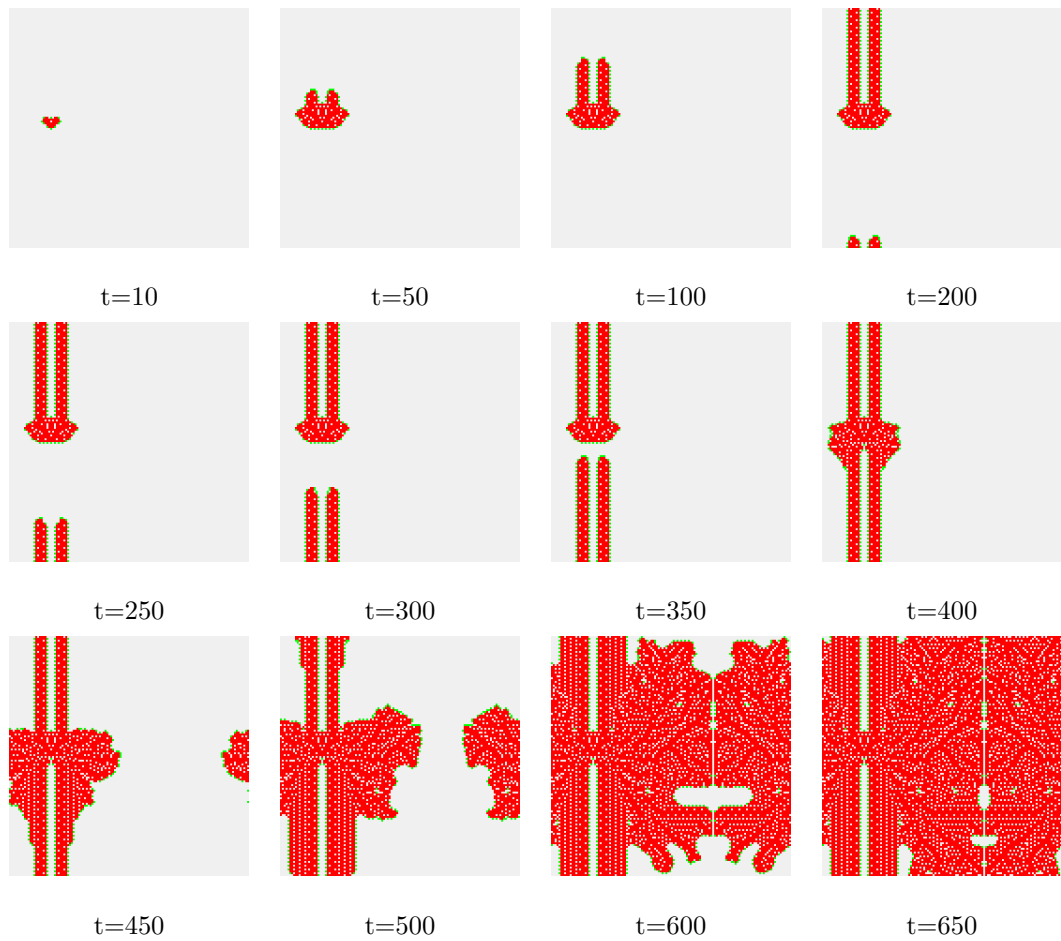


Fig. 2.8. *Space-time diagram of the cellular automaton 2.5 with the Glider IC.*

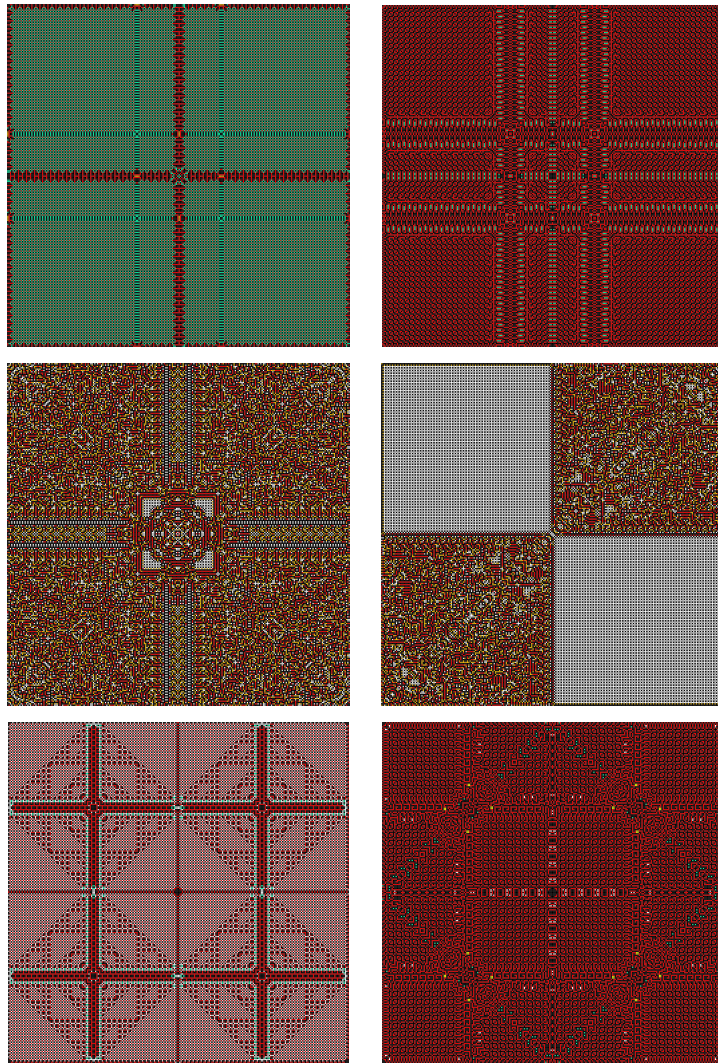


Fig. 2.9. *Samples of multi-state 2D CA patterns generated by the author.*

Fig. 2.9 illustrates some experimental patterns generated by the author to demonstrate the capabilities of CA in exhibiting complex behaviour with visually pleasing qualities.

2.7 Artistic Applications of CA

Some unique characteristics of CA (e.g. automaton as picture element interacting with neighbouring automata using simple rules) make them a suitable framework for generating computer graphics. The significance of a CA-based approach in producing computer art was outlined by Wolfram in his classical studies on CA behaviours collected in “*A New Kind of Science*”.

It seems so easy for nature to produce forms of great beauty. Yet in the past art has mostly just had to be content to imitate such forms. But now, with the discovery that simple programs can capture the essential mechanisms for all sorts of complex behavior in nature, one can imagine just sampling such programs to explore generalizations of the forms we see in nature. Traditional scientific intuition—and early computer art—might lead one to assume that simple programs would always produce pictures too simple and rigid to be of artistic interest. But looking through this book it becomes clear that even a program that may have extremely simple rules will often be able to generate pictures that have striking aesthetic qualities—sometimes reminiscent of nature, but often unlike anything ever seen before [35, p.11].

The dynamics of pattern formation in CA, especially with multi-state CA models has been shown to generate aesthetically pleasing imagery due to the emergence of novel symmetrical patterns [45]. Martin Nowak employed multi-state CA models to study pattern formations in biological systems and generate a sequence of ever-growing “*Persian carpets*” and “*evolutionary kaleidoscope*” patterns that had aesthetic qualities [116]. In addition, combinations of CA with other ALife techniques (e.g. evolutionary computing or L-systems) have been used to explore a set of rules generating patterns with aesthetic qualities [8, 117, 48]. Guy Birkin has used CA for digital art practice and investigating the association of visual complexity with aesthetic perception using CA-generated patterns as test stimuli [118, 119].

A 2D lattice with a periodic boundary provides an endless environment for the growth of patterns and observation of emergent complex behaviour over the time of CA evolution. For some rules the periodic generation of patterns creates an animated sequence of pattern formations over the course of time. This opens up the possibility

of generating animations based on the development of pattern formation where both symmetries and the element of surprise coexist. This capability was observed in [120, p.64], where CA are considered as “self-generating computer graphics movies”.

Because of the neighbourhood relation of cells and the effect of IC, after several time steps the behaviour of CA can become very unpredictable; therefore, from an observer’s point of view the element of surprise becomes intrinsic. Considering the neighbourhood relations of CA cells and the fact that each automaton can act as a pixel, pixels communicate with other pixels to define their spatial location in the next time step. In other words, each pixel is related to another pixel through the exchange of information. This is a very unique method of generating imagery which does not have precedent in human culture and there have not been found any pattern generation technique based on these simple principles [121]. The role of symmetry in art, architecture and its association with aesthetic preferences is a well-known concept [122, 123, 124]. The iterative application of a transition function over IC, especially in multi-state 2D CA can generate complex symmetrical patterns which are extremely challenging to construct using conventional mathematical methods [125].

In the 1950s, Béla Julesz employed a digital computer to create artificial stereo images to study binocular depth perception. The images were composed of black and white square shapes. His work contributed to the idea that 2D patterns can be generated using simple elements (i.e. square shapes) where patterns contain micro-patterns (locally organized) and macro-patterns (globally organized) [126]. In 1963, Ken Knowlton wrote an animation language called *Beflix* (Bell Flicks), the first specialised computer animation language for bitmap movie making, producing images at a resolution of 252×184 in eight shades of grey. The scientific orientation of *Beflix* towards creating graphics and artists’ limited knowledge of programming at the time raised a need to develop special program to facilitate artistic processes with computers. It resulted in the creation of a completely new language, *Explor* (EXplicit Patterns, Local Operations and Randomness) in 1970 for generating 2D patterns, designs and pictures from explicitly provided two-dimensional patterns, local operations and randomness. It aimed not only to provide the computer novice with graphic output; but also a vehicle for depicting the results of simulations in natural (e.g. crystal growth) and hypothetical spaces (e.g. CA), and for the production of a wide variety of designs [127, 128]. Knowlton and Lillian Schwartz used

Explor's CA models to generate “*Pixillation*”, one of the early computer generated animations [26]. They contested in the *Eighth Annual Computer Art Contest* in 1970 with two entries, “*Tapestry I*”, and “*Tapestry II*”, still frames from *Pixillation*. The “*Tapestry I*” won the first prize for new, creative use of the computer as an artist's tool. Their winning entry, “*Tapestry I*” was published on the front cover of the *computers and automation* in August 1970.

Lambert Meertens and Leo Geurts also had an entry in the *Eighth Annual Computer Art Contest* with “*Crystalization*”, an experimental computer graphics with asynchronous updates. Their entries were four drawings intended to generate patterns that combine regularity and irregularity in a natural way using CA [129]. They used majority voting rules (totalistic) with four-cell von Neumann neighbourhood for some of their works and for some others, they used larger neighbourhoods than the immediately adjacent cells. In searching for a contemporary technology for computer art, Joseph Scala noted Knowlton's EXPLOR system, which introduced a new way of generating art using computers. He then created Exploring I, II and III (multi-state CA patterns) using EXPLOR, a line printer, and painted on with acrylic paint in 1975 [130]. He found computers as the electronic interface between human thought and aesthetic expression which would allow human kind to tap into and communicate those cords of humanity necessary for the continuation of human existence with and within our scientific-technological culture [130].

Peter Struycken, the Dutch contemporary digital artist, has created many of his works including “*Computer Structures*” (1969), “*Four Random Drawings for Lien and Ad*” (1972) and FIELDS (1979/1980) with binary and multi-state CA [30, 131]. The SPLASH is a program which allows the exploration of colour patterns. The idea is inspired by throwing a stone into a pond, causing ripples to emanate from the place where the stone hits the water (splashdown). The colour changes are controlled by a number of transitional states between a previously (arbitrarily) established colour pattern serving as an initial state and another previously (arbitrarily) established colour pattern which is to be the final state, or target [131]. The FIELDS uses a square grid with 8-bit colour cells. The transaction function is how the colour of a cell adapts in the direction of the average colour of the surrounding cells. Repeated application of the rule thus ends with a uniformly coloured surface. But before this stable endpoint is reached, the automaton goes through a sequence of configurations of irregular shapes.

Paul Brown, the British contemporary digital artist, also applied various CA rules in his static and kinematic computer art. “*Neighbourhood Count*” (1991), “*Infinite Permutations V1*” (1993-94), “*Infinite Permutations V2*” (1994-95), “*SAND LINES*” (1998), “*My Gasket*”(1998) and “*Chromos*” (199-2000) [132, 31] are some of his CA-based works of art.

While investigating CA at the Institute for Advanced Study in Princeton, Wolfram developed practical applications of computer science, particularly CA for commercial purposes. He designed and published CA postcards with six different automata in full colour. On the back of each card was a statement: “The color of each cell is determined by a simple mathematical rule from the colors of neighboring cells on the line above it.” [133, p.249]. On the bottom of each card there was the statement of the mathematical rule that generated the pattern and then a copyright notice. Some of the cards included hexagonal cellular snowflake developed by Norman Packard. The full-colour formation of a snowflake appeared on Wolfram’s Scientific American article, “Computer Software in Science and Mathematics”, arguing that “The only practical way to generate the pattern is by computer simulation” [134, p.118].

Nature in October 1984 printed seven full-colour pictures of cellular automata on its cover, in which Wolfram published an article entitled “Cellular Automata as Models of Complexity” [135]. Selling postcards of CA patterns initiated a series of ideas about creating wallpaper patterns and murals. Wolfram did not intend to apply CA in a full commercial extent but to bring cellular automata to the world . “One of the things I’ve been meaning to do is to make a bit more of a serious effort to use cellular automata in some kind of computer art ... built a computer-controlled spray-painting machine to produce 14 by 48-foot image to make some huge murals of computer art ... and create a huge cellular automata display which one can put on the side of a building” [133, p.250]. In the spring of 1986, Wolfram received a letter inviting him to an art exhibition in New York City, art based on cellular automata. After attending the exhibition, Wolfram said “It was kind of interesting, actually. I had expected something rather boring, but in fact the pictures were quite nice.” [133, p.250].

Paul Hoke regarded CA-generated patterns as *Cellular Automata Art*. He made a distinction between local and global viewpoints of CA by arguing that the recursive application of a simple rule at the local level can generate complex behaviour at the

global level of a cellular automaton. He experimented with 256-state CA, observing that “the time evolution of 2D CA would have to be displayed as stacks of planes (each of which is an element of the automata), this type of cellular automata is typically shown in an animated fashion; each successive element occupies the screen as it is generated, giving the impression of animation as cells change color.” [136].

John F. Simon Jr created a series of art projects entitled (*Art Appliances*) using CA-based software and LCD panels to exhibit CA pattern formations. *Every Icon* (1996), *ComplexCity* (2000), and *Automata Studies* (2002) are examples of his CA art works [137].

Leo Villareal [138], inspired by Conway’s GoL applied CA to control lightings in architectural installations. He maintains that “central to my work is the element of chance. The goal is to create a rich environment in which emergent behavior can occur without a preconceived outcome. I am an active participant, serving as editor in the process through careful selection of compelling sequences”.

Rafael [139] considers mathematics to be the ultimate abstract art. He generates his artworks by exploring multi-state CA. Robert J. Krawczyk [140] has used different 2D and 3D CA models to generate his artworks and architectural designs.

Erwin Driessen and Maria Verstappen created *Ima Traveler* (1996) and *Breed* (1995-2007) based on CA models in 2D and 3D. The *Ima Traveller* is an interactive CA environment for exploring an infinite universe. The underlying cellular automaton enables the traveller (observer) to make a journey in a real time-space that develops in the direction that the traveller is moving into, so there is no end to the journey of the traveller. The experience is like zooming in an endless universe of infinite size, never reaching any boundaries. The ever-expanding universe starts with a single cell at the centre of the screen. Then the automaton generates new generations of cells based on a cell-division process. The new cells are more or less autonomous cells that are able to define their own colour (hue, brightness and saturation) by interaction with the surrounding cells.

The *Breed* is a 3D automaton for generating sculptures. The underlying principle of the *Breed* is division of cells. The initial cell, a cube, engenders throughout successive stages of cell division to form complex, multi-cellular sculptures. The *Breed*’s morphogenetic rules are guided by an evolutionary algorithm in 3D space determining how the division of a cell occurs, depending on its states and neighbouring cells surrounding [141].

Furthermore, some commercial products benefiting from CA-generated patterns in their designs (e.g. elementary cellular automaton rule 110) are emerging (Fig. 2.10).

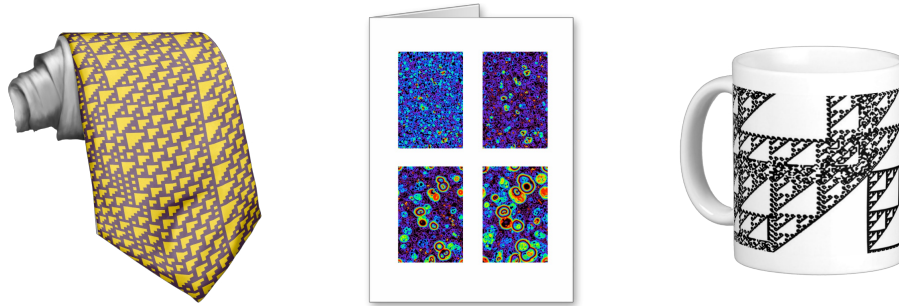


Fig. 2.10. *Samples of commercial products using CA-generated patterns.*

The CA-based artworks reviewed in this chapter are regarded as digital art where the artist utilises the combined generative capabilities of CA models with their own creativity and aesthetic perception to produce digital art. These forms of art works depend on the creativity, aesthetic perception of the artist and generative capabilities of CA models. It is evident that, this method of digital artwork creation lacks the automation for selection/evaluation processes in which the computer evaluates the aesthetic quality of the generated patterns. The automation of the selection process requires computational models which conform to human aesthetic perception.

3. Informational Aesthetics

Our fascination with beautiful objects, whether in its natural or synthetic instances, has contributed to many studies in different bodies of knowledge. Although aesthetics has traditionally been a discipline of philosophy, over the past decades other disciplines have shown interest in addressing questions regarding aesthetic perception with their own scientific theories and tools.

Where traditional aesthetics in philosophy is a purely theoretical subject, modern aesthetics has taken a more practical approach with the emergence of disciplines like *Experimental Aesthetics* [142, 143, 144] *Neuroaesthetics* [145] and *Evolutionary Aesthetics* [146, 147].

Neuroaesthetics, using brain imaging tools, attempts to identify the neural correlates of human aesthetic experience and has so far shown that the experience of visual beauty correlates with activities in a specific region of the brain [148]. Furthermore, neurological theories of aesthetics propose 10 universal laws of art; *peak shift, isolation, grouping, contrast, perceptual problem solving, symmetry, abhorrence of coincidence/generic viewpoint, repetition, rhythm, and orderliness, balance and metaphor* as a framework for understanding aspects of visual art, aesthetics and design independent of cultural boundaries [149].

The evolutionary theory of aesthetic experience evaluates beauty as a promise of a high likelihood of survival and reproductive success in the environments of human evolutionary history, while ugliness is the promise of low survival and reproductive failure [150]. The studies in this field have shown that the perception of beauty is innate [151], although aesthetics judgements may be rather variable across people, cultures and time, the underlying algorithms and constraints should manifest themselves as common universal evolutionary origin [152].

Computational Aesthetics, a fairly new discipline of computer science, aims to

bridge the analytic and synthetic by integrating aspects of computer science, philosophy, psychology, and the fine, applied and performing arts. It seeks to facilitate both the analysis and the augmentation of creative behaviours. Computational Aesthetics also investigates the creation of tools that can enhance the expressive power of the fine and applied arts and furthers our understanding of aesthetic evaluation, perception and meaning [44].

The field addresses evaluation problems of existing works of art and the creation of digital forms of art or objects of design having aesthetic qualities. It is “the research of computational methods that can make applicable aesthetic decisions in a similar fashion as humans can” [42, p.16]. Some major aspects of the discipline are (1) developing computational methods for aesthetic decisions, (2) taking human perception into account, and (3) focusing on aesthetics in form and particularly objects of design, in order to guarantee immediate application [42]. A chronological account covering various research activities that invoke the term *aesthetics* in a computational setting with focus on the problem of making numerical assessments of the aesthetic content of works of art is provided in [153].

There is a sizeable body of literature on various computational approaches to aesthetics. They can be categorized from mathematical, communicative, structural, psychological and neuroscientific perspectives or from their computational approaches (evolutionary, neural, etc.). A thorough review of various models and methodologies from different perspectives are provided in [154, 155, 156].

The review in this chapter mainly focuses on models derived from Birkhoff’s aesthetic measure [51] and informational theories of aesthetics since these models are directly related to this work given the scope of research.

3.1 Aesthetics as Science of Sensation

The 17th and 18th centuries are known as the age of *enlightenment*. It was a time when the influential figures like Descartes (1596-1650) and Leibniz (1646-1716) revolutionised science and philosophy by applying mathematics and reasoning to qualitative subjects.

Descartes's distinction between '*clear and distinct ideas*' and '*obscure and confused ideas*' in human sensory perception [157] influenced Baumgarten (1714-1762), a German philosopher, to establish *aesthetics* as a new science dealing with human sensation and the perception of beauty in nature and art [158], separating it from the classical metaphysical and theological treatment inherited from Plato and Aristotle.

Baumgarten argued that since thought and intellect types of cognition are dealt with logic and reasoning, the perception and sensory types of cognition should be dealt with a new science of sensory perception which he called *aesthetics*, deriving it from the Greek word *aesthanesthai* (to feel or perceive) for 'things perceived by the senses', as opposed to 'things known by the mind' [159].

Aesthetics is currently defined as the theory of perceptibility, appreciation, responsiveness, and enjoyment of the beauty in art and nature. It comprises two aspects: (1) the philosophical or theoretical, dealing with the nature of beauty and art, and (2) the pragmatic or practical, discussing the standards of art appreciation and evaluation [160].

3.1.1 Measuring Sensations

Aesthetic judgements have long been hypothesised to depend on the order and complexity of stimuli. Weber (1795-1878), Fechner (1801-1878) and Wundt (1832-1920) contributed to the foundations of *Experimental Aesthetics* by examining the relations of order and complexity in aesthetic judgements. They studied these relations through experimental studies, drawing quantitative models to measure human sensation and perception across various sensory systems including vision.

Weber studied the minimum amount of changes needed in a stimulus to generate a noticeable change in sensation. From the analysis of empirical data, he proposed a model known as *Weber's law* which states that the sensitivity of the sensory response to the changes in stimuli depends on the *difference threshold* or *just noticeable difference* (JND) of the stimuli (Eq. 3.8)

$$\frac{\Delta I}{I} = k \quad (3.8)$$

where I is the intensity of the standard, ΔI is the increase in the intensity for a JND, and k is a constant (*Weber's constant*). In another words, Weber's Law states that the size of the JND (i.e., ΔI) is a constant proportion of the original stimulus value. He approximated JNDs of light intensity ($k = 0.01$) and sound intensity ($k = 0.15$) in vision and hearing.

Empirical studies on art and aesthetic preferences with the aim of addressing aesthetic problems was initiated by Fechner. He tried to derive the conditions that determine what is aesthetically pleasing (aesthetic preferences) not from a higher ideal of beauty but from below using systematic empirical methods. In his experiments with simple shapes he found that some intermediate degree of stimulus complexity is perceived to be more aesthetically pleasing, while very high degrees of simplicity or complexity are less aesthetically pleasing [142].

Fechner assumed not only that a JND is a constant fraction of stimulus intensity, but also that one JND is perceptually equal to any other JND. He then provided further extension to Weber's law by assuming that (1) two stimuli will be discriminable if they generate a visual response that exceeds some threshold (2) the visual response S to an intensity I is given by Eq. 3.9 [161].

$$S = k \log I \quad (3.9)$$

Wundt postulated that there is a relationship between stimulus complexity and appraisal. He then carried out a number of empirical studies on the aesthetic judgement of human subjects and showed that physiological arousal and subjective stimulus complexity are related and that the relationship is in the form of an inverted-U shape curve [162]. That is to say, aesthetic pleasure is maximal at intermediate degrees of complexity. This relationship is known as the *Wundt Curve* (Fig. 3.11).

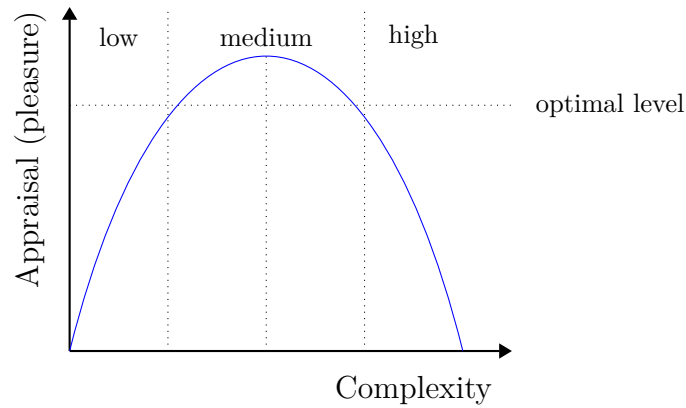


Fig. 3.11. *The inverted-U curve illustrating the relationship between stimuli complexity and appraisal.*

Berlyne, inspired by Wundt, suggested that the aesthetic value and pleasurable-ness of a stimulus starts at a relatively indifferent level, then increases as a function of complexity up to a certain level, after which it decreases and becomes more unpleasant as complexity increases (Fig. 3.12) [52]. For Berlyne, aesthetic preference (“hedonic value”) is determined by the average arousal potential, usually somewhere midway between being arousing/exciting (novel) and dull (very familiar).

This principle explains the general dominance of stimuli or artworks that are not too simple yet not too complex. It also explains a preference for stimuli or artworks that are moderately familiar. This reflects the fact that aesthetic value can be enhanced by an increase in complexity or by an increase in order and the fact that extremely low complexity or order will make a form displeasing [52]. Later experimental studies supported the aesthetic preference in relation to the complexity of visual and auditory stimuli conforming to an inverted-U curve [163, 164, 165].

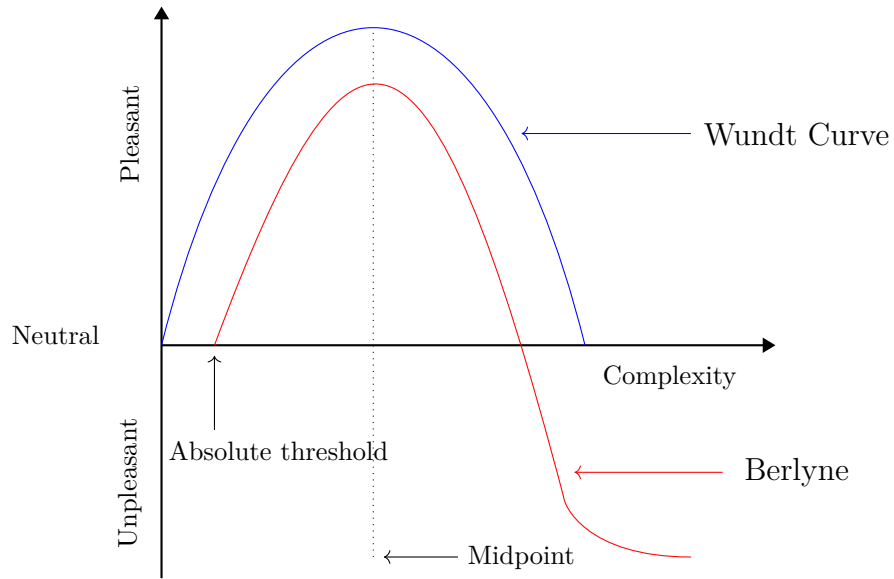


Fig. 3.12. Schematic plot of the relationship between complexity and pleasantness of stimuli adapted from Berlyne.

Stevens suggested a power function to describe the intensity of a sensation based on two assumptions that: (1) the Fechner law is a valid relation, and (2) psychological intensity is appropriately measured in units of JNDs [166](Eq. 3.10). The power function implies that perceived psychological magnitude (Ψ) is a power function of physical magnitude (Φ):

$$\Psi = \Phi^r \quad (3.10)$$

where r is an exponent which is approximated empirically for each sensory modality.

These models are known as psychophysical laws, which explain the relation between the intensity of a stimulus and its perceived sensation based on empirical data. Two conclusions can be drawn from these laws: (1) there is a *non-linear* relation between stimulus intensity and its perceived sensation. The judgements of the magnitude of sensory stimuli are not linearly scaled. Therefore, if a continuum between perceptual and cognitive processes exists, numerical representations should also be scaled on non-linear models [167]; (2) there is a *direct* relation between stimulus intensity and its perceived sensation. In terms of aesthetic perception of visual stimuli, Berlyne, from analysis of empirical data, showed that there is a direct relationship between complexity and aesthetic perception [168].

3.2 Computing Aesthetic Sensation

Birkhoff's *aesthetic measure* is a well-known theory in the field of computational aesthetics. Birkhoff attempted to create "a general mathematical theory of the fine arts, which would do for aesthetics what had been achieved in another philosophical subject, logic, by the symbolisms of Boole, Peano, and Russell" [169, p.127]. He proposed a formula for the aesthetic evaluation of objects and then illustrated its application with the analysis of polygons and vases. He concluded that aesthetic experience can be considered as a process involving three successive phases:

1. A preliminary effort of attention, which is necessary for the act of perception, and which increases in proportion to what we shall call the complexity (C) of the object;
2. The feeling of value or aesthetic measure (M) which rewards this effort; and finally
3. A realization that the object is characterized by a certain harmony, symmetry, or order (O), more or less concealed, which seems necessary to the aesthetic effect.

Birkhoff argued that aesthetic feelings arise primarily because of an unusual degree of harmonious inter relation within the object. More specifically, if we regard M , O , and C as measurable variables, we are led to write:

$$M = \frac{O}{C}. \quad (3.11)$$

This embodies in a basic formula the conjecture that the aesthetic measure is determined by the density of order relations in the aesthetic object [51, 170].

The *aesthetic measure* (M) (Eq. 3.11), influenced by the principle of "unity in variety", is a function of order (O) and complexity (C), with order contributing positively and complexity negatively to the aesthetic value of objects in the same class (e.g. vases, ornaments, polygonal forms, poetry and melodies) [51].

For polygonal form, Birkhoff separated order into five elements of order:

$$O = V + E + R + HV - F \quad (3.12)$$

where V is vertical symmetry, E is equilibrium, R is rotational symmetry, HV is relation to a horizontal-vertical network, and F is unsatisfactory form, involving too small distances from vertices to vertices, angles that are too near 0° or 180° , and other ambiguities. The complexity of polygonal forms is defined as the number of indefinitely extended straight lines that contain all the sides of the polygon.

He then provided measurement of M for set of 90 polygons forms with a maximum aesthetic measure calculated for a square shape (Fig. 3.13). Therefore, the formula favoured simplicity and orderliness as an indicator of the beauty of an object [171].

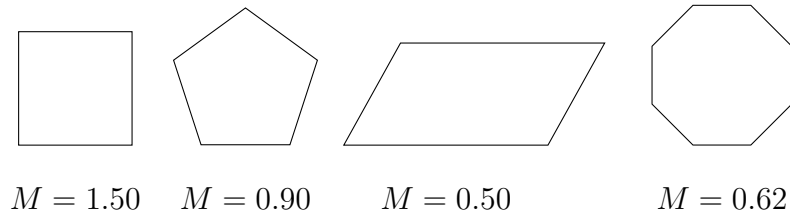


Fig. 3.13. *Aesthetic measures of sample polygonal forms.*

Staudek extended Birkhoff's model by defining a length tolerance as the characteristic network distances (ε) and angle tolerance (ζ) (the relations among the characteristic tangents) and then defined $M(\varepsilon, \zeta)$ as the sum of the partial orders divided by the complexity (Eq. 3.13).

$$M(\varepsilon, \zeta) = \frac{H(\varepsilon) + V(\varepsilon) + P(\varepsilon) + T(\zeta)}{C} \quad (3.13)$$

where $H(\varepsilon)$ is horizontal order, $V(\varepsilon)$ is vertical order, $P(\varepsilon)$ is proportional order, and $T(\zeta)$ is tangent order. The complexity (C) is determined from the number of its characteristic points. Staudek then applied the extended model to the formal aesthetic evaluation of regular geometrical objects, namely Chinese vases [172, 173].

The validity of Birkhoff's model and his approach in measuring order and complexity has been challenged by empirical studies in [174]. Eysenck conducted a series of experiments to test Birkhoff's model with inconclusive results [175, 176] and suggested that: (1) a better expression of a aesthetic evaluation function would be to consider a direct relationship to stimulus complexity rather than an inverse one (Eq. 3.14), (2) the measures of order and complexity should be approximated empirically [177].

$$M = O \times C \quad (3.14)$$

3.2.1 Informational Theories of Aesthetics

Even though the validity of Birkhoff's approach to the relationship and definition of order and complexity has been challenged, the notion of *complexity* and objective methods to quantify it remained a prominent parameter in later proposed aesthetic evaluation models.

Shannon's *information theory* was developed in order to address a reliable communication over an unreliable channel [178]. The notion of *Entropy* is at the core of this theory, providing a measurable quantity of information contained in a message transmitted through a channel with a certain measurable capacity [179]. In this sense, the semantic aspects of a message are irrelevant and *information* is simply a measure of freedom of choice when one selects a message, while the amount of information is defined to be measured by the logarithm of the number of available choices [178]. Let \mathcal{X} be discrete alphabet, X a discrete random variable, $x \in \mathcal{X}$ a particular value of X and $P(x)$ the probability of x . The entropy, $H(X)$, is then:

$$H(X) = - \sum_{x \in \mathcal{X}} P(x) \log_2 P(x). \quad (3.15)$$

The quantity H is the average uncertainty in bits, $\log_2(\frac{1}{p})$ associated with X . Entropy can also be interpreted as the average amount of information needed to describe X . The value of entropy is always non-negative and reaches its maximum for the uniform distribution, $\log_2(|\mathcal{X}|)$:

$$0 \leq H \leq \log_2(|\mathcal{X}|). \quad (3.16)$$

Remark 3.6. We assume that $0 \log_2 0 = 0$.

The lower bound of relation (3.16) corresponds to a deterministic variable (no uncertainty), while the upper bound corresponds to a maximum uncertainty associated with a random variable. Another interpretation of entropy is as a measure of *order* and *complexity*. A low entropy implies low uncertainty, so the message is highly predictable, ordered and less complex. By contrast, a high entropy implies high uncertainty, less predictability, highly disordered and highly complex. These interpretations of entropy provided a quantitative means to measure human sensory perception including measures of order and complexity of objects in relation to their aesthetic value.

In a series of studies in the late 1950s influenced by information theory and the development of computers, it was argued that human psychological and cognitive processes (e.g. human sensory perception) are information-processing models, rather than organisms, that are simply conditioned to respond to external stimulus; these processes are then simulated by developing programs with a computer [180].

Franke put forward an *aesthetic perception* model by making a distinction between the amount of information being stored and the rate of information flowing through a channel as *information flow* measured in *bits/sec* [181]. Staudek’s multi-criteria approach (informational and structural) as *exact aesthetics*, an extension of Birkhoff’s measure, applied information flow I' by defining it as a measure assessing principal information transmission qualities in time [173].

Moles [182], Bense [183, 184, 185] and Arnheim [143, 186, 187] were pioneers in the application of entropy to quantify order and complexity in Birkhoff’s formula by adapting statistical measure of information in aesthetic objects.

Moles made a distinction between value judgements and scientific aesthetics where information measure is a tool for scientific aesthetics. He argued that the human mind cannot absorb more than $16 - 20$ *bits/sec* of information. In order for a message to be perfectly understood, it should carry information in this range. Beyond these limits, either the mind rejects the message because of too much information or it loses interest due to too little information [182].

Bense combined Birkhoff’s model, information theory and Chomsky’s generative grammar for the aesthetic analysis of the English language. He argued that aesthetic objects are “vehicles of aesthetical information” where statistical information can quantify the aesthetical information of objects. From the analysis of art objects on a micro-aesthetic level, the macro-aesthetic values of aesthetic objects are quantifiable [183]:

$$M_B = \frac{H_{max} - H}{H_{max}} = 1 - H \quad (3.17)$$

where H quantifies the entropy of the selection process from a determined repertoire of elements and H_{max} is the maximum entropy of a predefined repertoire of elements [185]. He also drew a line between the generation process and evaluation of artworks [188]. Bense’s informational aesthetics is founded on these basic assumptions: (1) Objects are material carriers of aesthetic state, and such aesthetic

states are independent of subjective observers, (2) A particular kind of information is conveyed by the aesthetic state of the object (or process) as *aesthetic information*, and (3) an objective measure of aesthetic objects is related with the degree of order and complexity in an object [189]. Berlyne also adopted an information-theoretic approach in his psychological experiments to determine humans' perceptual curiosity of visual stimuli, demonstrating a direct relationship between complexity and aesthetic perception [168].

Gunzenhäuser suggested viewing order as the relative redundancy (R) and complexity as the average statistical information (H) in Birkhoff's formula to form an informational model of aesthetics (Eq. 3.18) [190]:

$$M_G = \frac{R}{H} = \frac{1 - \frac{H}{H_{max}}}{H} = \frac{1}{H} - \frac{1}{H_{max}}. \quad (3.18)$$

Machado and Cardoso [191] proposed a model based on Birkhoff's approach revolving around the ratio of *image complexity* to *processing complexity*, arguing that images with high visual complexity are processed easily, so they have the highest aesthetic value. Adapting Bense's informational aesthetics to different approaches of the concepts of order and complexity in an image in [192], three measures based on Kolmogorov complexity, Shannon entropy (for RGB channels) and Zurek's physical entropy were introduced. The measures were then applied to analyse the aesthetic values of several paintings (Mondrian, Pollock, and van Gogh).

Leder [193] proposed an information-processing stage model of aesthetic processing, derived from an analysis of the appreciation of modern art. According to the model, aesthetic experiences involve five stages: perception, explicit classification, implicit classification, cognitive mastering, and evaluation. The model also differentiates between aesthetic emotions and aesthetic judgements as two distinct types of outputs.

Although informational theories of aesthetics have all considered that the human observer and the artist play a crucial role in the process of artistic appreciation and creation, they incorrectly invoke information theory in a situation where the "symbols" that constitute aesthetic stimuli (and natural images more generally) are unknown. Indeed, the "true" entropy of an image is a perceptual quantity, and cannot therefore be characterized with only image statistics [194].

4. Quantifying Spatial Complexity

Despite the dominance of entropy as a measure of order and complexity in computational aesthetics, it fails to reflect on the structural characteristics of 2D patterns. The main reason for this drawback is that it measures the distribution of symbols, not their arrangements.

This fact was noted by Arnheim, who stated that “entropy theory is indeed a first attempt to deal with global form; but it has not been dealing with structure. All it says is that a large sum of elements may have properties not found in a smaller sample of them” [195, p.18].

Fig. 4.14 illustrates the measurements of entropy for CA-generated 2D patterns with various structural characteristics. Fig. 4.14(a) and 4.14(b) generated by a cellular automaton. Fig. 4.14(a) is a fully symmetrical pattern, Fig. 4.14(b) is a pattern with local structures and Fig. 4.14(c) is a fairly structureless random pattern.

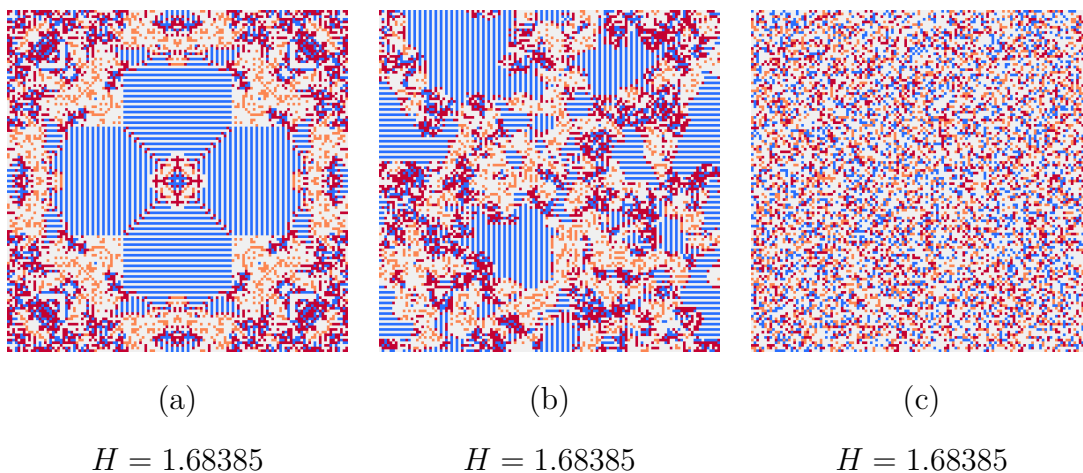


Fig. 4.14. *The measurements of H for structurally different patterns.*

The comparison of the structural characteristics of these patterns with their corresponding entropy values shows that despite their structural differences, all of the patterns have the same entropy value. This clearly demonstrates the failure of entropy to discriminate structurally different 2D patterns. In other words, entropy is invariant to the spatial arrangement of the composing elements of 2D patterns. This is in contrast to our intuitive perception of the complexity of patterns. For the purpose of measuring the complexity of CA behaviour, particularly with multi-state structures, it would be problematic if only entropy measure was applied.

4.1 Conceptual Model

Considering our intuitive perception of complexity and the structural characteristics of 2D patterns, a complexity measure must be bounded by two extreme points of complete order and disorder. It is reasonable to assume that *regular structures*, *irregular structures* and *structureless* patterns lie between these extremes, as illustrated in Fig. 4.15.

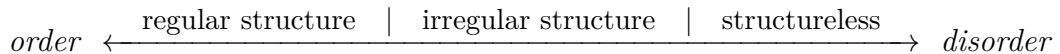


Fig. 4.15. *The spectrum of spatial complexity.*

A complete regular structure is a pattern of high symmetry, while an irregular structure is a pattern with some structure, though not as regular as a fully symmetrical pattern; finally a structureless pattern is a random arrangement of elements [125].

4.2 Spatial Complexity Measure

Although Shannon further provided definitions of joint and conditional entropies in the framework of information theory [178, p.52], its applications in measuring structural complexity of dynamical systems remained unrecognised until studies in [54, 55, 56, 196] showed its merits.

A measure introduced in [54, 55, 56], known as *information gain*, has been proposed as a means of characterising the complexity of dynamical systems and of 2D

patterns. It measures the amount of information gained in bits when specifying the value, x , of a random variable X given knowledge of the value, y , of another random variable Y ,

$$G_{x,y} = -\log_2 P(x|y). \quad (4.19)$$

$P(x|y)$ is the conditional probability of a state x conditioned on the state y . The *mean information gain* (MIG), $\overline{G}_{X,Y}$, is the average amount of information gain from the description of all possible states of Y :

$$\overline{G}_{X,Y} = \sum_{x,y} P(x,y)G_{x,y} = -\sum_{x,y} P(x,y) \log_2 P(x|y) \quad (4.20)$$

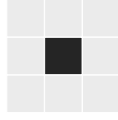
where $P(x,y)$ is the joint probability, $\text{prob}(X = x, Y = y)$. \overline{G} is also known as the conditional entropy, $H(X|Y)$ [179]. Conditional entropy is the reduction in uncertainty of the joint distribution of X and Y given knowledge of Y , $H(X|Y) = H(X,Y) - H(Y)$. The lower and upper bounds of $\overline{G}_{X,Y}$ are

$$0 \leq \overline{G}_{X,Y} \leq \log_2 |\mathcal{X}|. \quad (4.21)$$

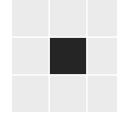
Fig. 4.16 shows details of the calculations of $\overline{G}_{r,s}$ for a 2D pattern composed of two different cells $S = \{\text{white}, \text{black}\}$, so the set of all possible 2-tuples are $\{ww, wb, bb, bw\}$. Considering the mean information gain from Eq. 4.2 and given the relative position matrix M in Eq. 4.23, the calculations can be performed as follows:

In *white – white*, case G measures the homogeneity and spatial configurations where $P(w, s_{(i,j+1)})$ is the joint probability that a cell is white and has a neighbouring cell at its $(i, j + 1)$ position, $P(w|w_{(i,j+1)})$ is the conditional probability of a cell is white given that it has a white neighbouring cell at its $(i, j + 1)$ position, $P(w, w_{(i,j+1)})$ is the joint probability that a cell is white and has a neighbouring cell at its $(i, j + 1)$ position, $G(w, w_{(i,j+1)})$ is information gain in *bits* from specifying a white cell where it has a white neighbouring cell at its $(i, j + 1)$ position.

The same calculations are performed for the rest of the cases; *black – black*, *white – black* and *black – white*.



(a)



(b)

white – white

$$P(w, s_{(i,j+1)}) = \frac{5}{6}$$

$$P(w|w_{(i,j+1)}) = \frac{4}{5}$$

$$P(w, w_{(i,j+1)}) = \frac{5}{6} \times \frac{4}{5} = \frac{2}{3}$$

$$G(w, w_{(i,j+1)}) = \frac{2}{3} \log_2 P\left(\frac{4}{5}\right)$$

$$G(w, w_{(i,j+1)}) = 0.2146 \text{ bits}$$

white – black

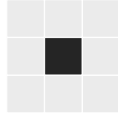
$$P(w, s_{(i,j+1)}) = \frac{5}{6}$$

$$P(w|b_{(i,j+1)}) = \frac{1}{5}$$

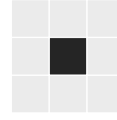
$$P(w, b_{(i,j+1)}) = \frac{5}{6} \times \frac{1}{5} = \frac{1}{6}$$

$$G(w, b_{(i,j+1)}) = \frac{1}{6} \log_2 P\left(\frac{1}{5}\right)$$

$$G(w, b_{(i,j+1)}) = 0.3869 \text{ bits}$$



(b)



(c)

black – black

$$P(b, s_{(i,j+1)}) = \frac{1}{6}$$

$$P(b|b_{(i,j+1)}) = \frac{1}{1}$$

$$P(b, b_{(i,j+1)}) = \frac{1}{6} \times \frac{1}{1} = \frac{1}{6}$$

$$G(b, b_{(i,j+1)}) = \frac{1}{6} \log_2 P(1)$$

$$G(b, b_{(i,j+1)}) = 0 \text{ bits}$$

black – white

$$P(b, s_{(i,j+1)}) = \frac{1}{6}$$

$$P(b|w_{(i,j+1)}) = \frac{0}{1}$$

$$P(b, w_{(i,j+1)}) = \frac{1}{6} \times 0$$

$$G(b, w_{(i,j+1)}) = 0 \text{ bits}$$

$$\overline{G}(S, S_{(i,j+1)}) = G(w, w_{(i,j+1)}) + G(w, b_{(i,j+1)}) + G(b, b_{(i,j+1)}) + G(b, w_{(i,j+1)})$$

$$\overline{G}(S, S_{(i,j+1)}) = 0.2146 + 0.3869 = 0.6015 \text{ bits}$$

Fig. 4.16. Calculations of $\overline{G}_{r,s}$ for a 2D pattern composed of black and white cells.

Definition 4.4. A spatial complexity measure G , of a cellular automaton configuration is the sum of the mean information gains of cells having homogeneous/heterogeneous neighbouring cells over a lattice.

For a cellular automaton configuration, \overline{G} can be calculated by considering the distribution of cell states over pairs of cells r, s ,

$$\overline{G}_{r,s} = - \sum_{s_r, s_s} P(s_r, s_s) \log_2 P(s_r, s_s) \quad (4.22)$$

where s_r, s_s are the states at r and s , respectively. Since $|\mathcal{S}|= N$, $\overline{G}_{r,s}$ is a value in $[0, N]$.

The vertical, horizontal, primary diagonal (\setminus) and secondary diagonal ($/$) neighbouring pairs provide eight $\overline{G}s$; $\overline{G}_{(i,j),(i-1,j+1)}$, $\overline{G}_{(i,j),(i,j+1)}$, $\overline{G}_{(i,j),(i+1,j+1)}$, $\overline{G}_{(i,j),(i-1,j)}$, $\overline{G}_{(i,j),(i+1,j)}$, $\overline{G}_{(i,j),(i-1,j-1)}$, $\overline{G}_{(i,j),(i,j-1)}$ and $\overline{G}_{(i,j),(i+1,j-1)}$. The relative positions for non-edge cells are given by matrix M :

$$M = \begin{bmatrix} (i-1,j+1) & (i,j+1) & (i+1,j+1) \\ (i-1,j) & (i,j) & (i+1,j) \\ (i-1,j-1) & (i,j-1) & (i+1,j-1) \end{bmatrix}. \quad (4.23)$$

Correlations between cells on opposing lattice edges are not considered. The result of this edge condition is that $G_{i+1,j}$ is not necessarily equal to $\overline{G}_{i-1,j}$.

In addition, the differences between the horizontal (vertical) and two diagonal mean information rates reveal left/right (up/down), primary and secondary orientation of 2D patterns. So the sequence of generated configurations by a multi-state 2D cellular automaton can be analysed using the differences between the vertical ($i, j \pm 1$), horizontal ($i \pm 1, j$), primary diagonal (P_d) and secondary diagonal (S_d) mean information gains by means of:

$$\Delta \overline{G}_{i,j \pm 1} (\Delta \overline{G}_V) = |\overline{G}_{i,j+1} - \overline{G}_{i,j-1}|, \quad (4.24a)$$

$$\Delta \overline{G}_{i \pm 1, j} (\Delta \overline{G}_H) = |\overline{G}_{i-1, j} - \overline{G}_{i+1, j}|, \quad (4.24b)$$

$$\Delta \overline{G}_{P_d} = |\overline{G}_{i-1, j+1} - \overline{G}_{i+1, j-1}|, \quad (4.24c)$$

$$\Delta \overline{G}_{S_d} = |\overline{G}_{i+1, j+1} - \overline{G}_{i-1, j-1}|. \quad (4.24d)$$

4.3 Kolmogorov Complexity of 2D Patterns

From an information theory perspective, the object X is a random variable drawn according to a probability mass function $P(x)$. If X is random, then the descriptive complexity of the event $X = x$ is $\log \frac{1}{P(x)}$, because $\lceil \log \frac{1}{P(x)} \rceil$ is the number of bits required to describe x . Thus, the descriptive complexity of an object depends on the probability distribution [179].

Kolmogorov attributed the algorithmic (descriptive) complexity of an object to the minimum length of a program such that a universal computer (universal turing machine) can generate a specific sequence [57]. Thus, the Kolmogorov complexity of an object is independent of the probability distribution. Kolmogorov complexity is related to entropy ($H(X)$), in that the expected value of $K(x)$ for a random sequence is approximately the entropy of the source distribution for the process generating the sequence. However, Kolmogorov complexity differs from entropy in that it relates to the specific string being considered rather than the source distribution [197, 179]. Kolmogorov complexity can be described as follows, where φ represents a universal computer, p represents a program, and x represents a string:

$$K_{\varphi}(x) = \left\{ \min_{\varphi(p)=x} l(p) \right\} \quad (4.25)$$

Random strings have rather high Kolmogorov complexity - on the order of their length, as patterns cannot be discerned to reduce the size of a program generating such a string. On the other hand, strings with a high degree of structure have fairly low complexity. Universal computers can be equated through programs of constant length, thus a mapping can be made between universal computers of different types. The Kolmogorov complexity of a given string on two computers differs by known or determinable constants. The Kolmogorov complexity $K(y|x)$ of a string y , given string x as input is described by the equation below:

$$K_{\varphi}(y|x) = \left\{ \begin{array}{l} \min_{\varphi(p,y)=y} l(p) \\ \infty, \text{ if there is no } p \text{ such that } \varphi(p, x) = y \end{array} \right\} \quad (4.26)$$

where $l(p)$ represents program length p and φ is a particular universal computer under consideration. Thus, knowledge or input of a string x may reduce the com-

plexity or program size necessary to produce a new string y . The major difficulty with Kolmogorov complexity is that it is uncomputable. Any program that produces a given string is an upper bound on the Kolmogorov complexity for this string, but it is not possible to compute the lower bound.

Lempel and Ziv defined a measure of complexity for finite sequences rooted in the ability to produce strings from simple copy operations [198]. This method, known as *LZ78* universal compression algorithm, harnesses this principle to yield a universal compression algorithm that can approach the entropy of an infinite sequence produced by an ergodic source. As such, *LZ78* compression has been used as an estimator for K . Kolmogorov complexity is the ultimate compression bound for a given finite string and, thus, a natural choice for the estimation of complexity in the class of universal compression techniques. In order to estimate the K value of 2D configurations generated by multi-state 2D CA, we generate linear strings of configurations by means of six different templates illustrated in Fig. 4.17.

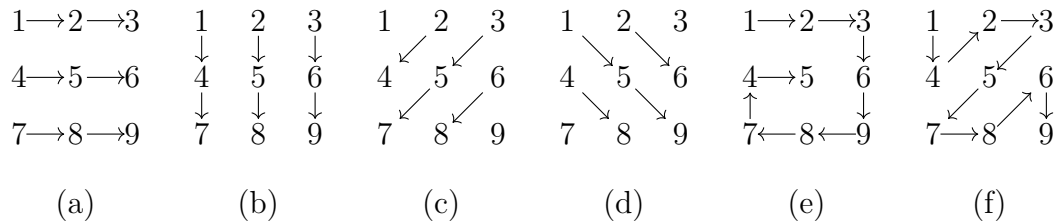
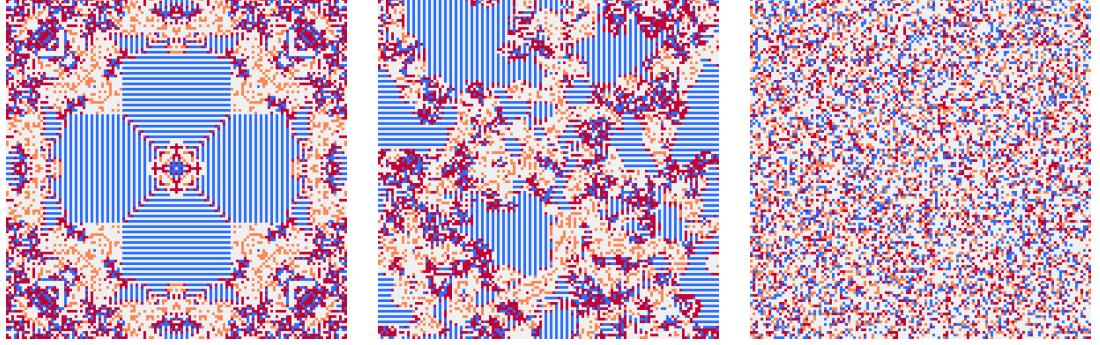


Fig. 4.17. Six different templates applied for the estimation of K in 2D plane.

1. A horizontal string $S_h = \{1, 2, 3, 4, 5, 6, 7, 8, 9\}$ (Fig. 4.17(a))
2. A vertical string $S_v = \{1, 4, 7, 2, 5, 8, 3, 6, 9\}$ (Fig. 4.17(b))
3. A diagonal string $S_d = \{1, 2, 4, 3, 5, 7, 6, 8, 9\}$ (Fig. 4.17(c))
4. A reverse diagonal string $S_{rd} = \{3, 2, 6, 1, 5, 9, 4, 8, 7\}$ (Fig. 4.17(d))
5. A spiral string $S_s = \{1, 2, 3, 6, 9, 8, 7, 4, 5\}$ (Fig. 4.17(e))
6. A continuous spiral string $S_{cs} = \{1, 4, 2, 3, 5, 7, 8, 6, 9\}$ (Fig. 4.17(f))

Then, using the *LZ78* compression algorithm, the upper bound of K is estimated as the lowest value among the six different templates. The comparison of the measurements of H , \overline{G}_s , $\Delta\overline{G}_s$ and K for structurally different patterns is illustrated in Fig. 4.18. It is evident from the measurements, K is able to discriminate the complexity of patterns; however, it fails to discriminate the spatial orientations.

Fig. 4.18 demonstrates the merits of \bar{G} in discriminating structurally different patterns for the sample patterns in Fig. 4.18. As can be observed, the measures of H are identical for structurally different patterns; however, $\bar{G}s$ and $\Delta\bar{G}s$ reflect both the complexity of patterns and the spatial distribution of their constituting elements ($\mu Gs_{(a)} = 1.51946 > \mu Gs_{(b)} = 1.55110 > \mu Gs_{(c)} = 1.68396$).



| (a) | (b) | (c) |
|-------------------------------|---------------------------------|---------------------------------|
| $H = 1.68385$ | $H = 1.68385$ | $H = 1.68385$ |
| $\bar{G}_{i,j+1} = 1.10365$ | $\bar{G}_{i,j+1} = 1.10486$ | $\bar{G}_{i,j+1} = 1.10941$ |
| $\bar{G}_{i,j-1} = 1.10365$ | $\bar{G}_{i,j-1} = 1.10410$ | $\bar{G}_{i,j-1} = 1.10956$ |
| $\Delta\bar{G}_V = 0$ | $\Delta\bar{G}_V = 0.00076$ | $\Delta\bar{G}_V = 0.00015$ |
| $\bar{G}_{i-1,j} = 1.10365$ | $\bar{G}_{i-1,j} = 1.10548$ | $\bar{G}_{i-1,j} = 1.10845$ |
| $\bar{G}_{i+1,j} = 1.10365$ | $\bar{G}_{i+1,j} = 1.10512$ | $\bar{G}_{i+1,j} = 1.11022$ |
| $\Delta\bar{G}_H = 0$ | $\Delta\bar{G}_H = 0.00036$ | $\Delta\bar{G}_H = 0.00177$ |
| $\bar{G}_{i-1,j+1} = 0.75235$ | $\bar{G}_{i-1,j+1} = 0.70165$ | $\bar{G}_{i-1,j+1} = 1.11006$ |
| $\bar{G}_{i+1,j-1} = 0.75235$ | $\bar{G}_{i+1,j-1} = 0.70123$ | $\bar{G}_{i+1,j-1} = 1.10843$ |
| $\Delta\bar{G}_{P_d} = 0$ | $\Delta\bar{G}_{P_d} = 0.00042$ | $\Delta\bar{G}_{P_d} = 0.00163$ |
| $\bar{G}_{i+1,j+1} = 0.75235$ | $\bar{G}_{i+1,j+1} = 0.69028$ | $\bar{G}_{i+1,j+1} = 1.10821$ |
| $\bar{G}_{i-1,j-1} = 0.75235$ | $\bar{G}_{i-1,j-1} = 0.68917$ | $\bar{G}_{i-1,j-1} = 1.11014$ |
| $\Delta\bar{G}_{S_d} = 0$ | $\Delta\bar{G}_{S_d} = 0.00111$ | $\Delta\bar{G}_{S_d} = 0.00193$ |
| $\mu Gs = 1.51946$ | $\mu Gs = 1.55110$ | $\mu Gs = 1.68396$ |
| $K = 0.08425$ | $K = 0.08281$ | $K = 0.11460$ |

Fig. 4.18. The measurements of H , $\bar{G}s$, $\Delta\bar{G}s$ and K for structurally different patterns.

4.4 Experiments and Results

A set of experiments was designed to examine the effectiveness of \overline{G} and K in discriminating the particular configurations that are generated by a multi-state 2D cellular automaton. The experimental rule (Table 4.6) maps four states, represented by *white*, *red*, *blue* and *orange*; the quiescent state is *white*.

| Cellular Automaton 4.6 | |
|---|--|
| $L = 65 \times 65$ (4225 cells) | |
| $S = \{0, 1, 2, 3\} \equiv \{\text{white}, \text{red}, \text{blue}, \text{orange}\}$ | |
| \mathcal{N} : Moore neighbourhood | |
| $f : S^9 \mapsto S$ | |
| $f(s_{i,j})(t) = s_{i,j}(t+1) = \left\{ \begin{array}{ll} 3 & \text{if } s_{i,j}^{(t+1)} = 0 \quad \text{and } \sigma = 1 \\ 2 & \text{if } s_{i,j}^{(t+1)} = 1-3 \quad \text{and } \sigma = 2 \\ 1 & \text{if } s_{i,j}^{(t+1)} = 1-3 \quad \text{and } \sigma = 3 \\ 0 & \text{otherwise} \end{array} \right\}$ | |

Table 4.6: Update rule of cellular automaton 4.6.

The experiments were conducted with four different ICs:

1. All cells are quiescent except for a single cell (Fig. 4.19(a))
2. A right oriented 5-cell (Fig. 4.19(b))
3. A left oriented 5-cell (Fig. 4.19(c))
4. A random configuration with 2112 *white* quiescent cells covering $\approx 50\%$ of the lattice, 749 *red*, 682 *blue* and 682 *orange* cells (Fig. 4.19(d))

The experimental rule was iterated synchronously for 200 successive time steps. Then the sequence of configurations were analysed using Eq. 4.24a, 4.24b, 4.24c, 4.24d and K . Fig. 4.20, 4.22, 4.24 and 4.30 illustrate a sample of time steps starting from the four different ICs (Appendix A illustrates the full space-time diagrams).

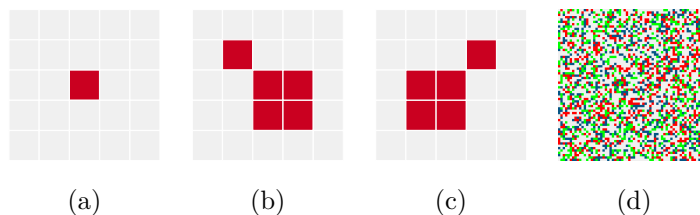


Fig. 4.19. Four different ICs used to seed cellular automaton 4.6.

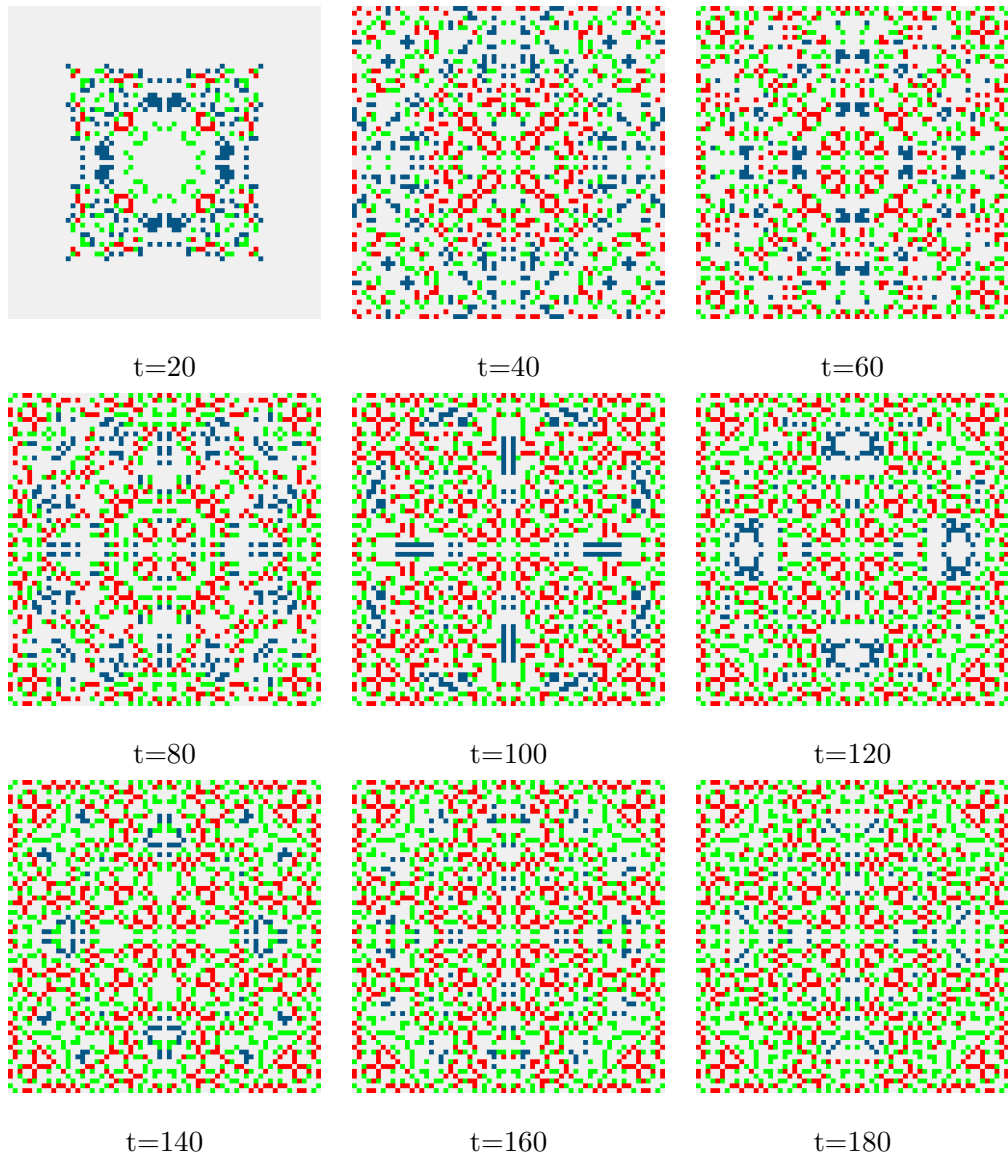


Fig. 4.20. The space-time diagram of cellular automaton 4.6 for a sample of time steps starting from the single cell IC (4.19(a)).

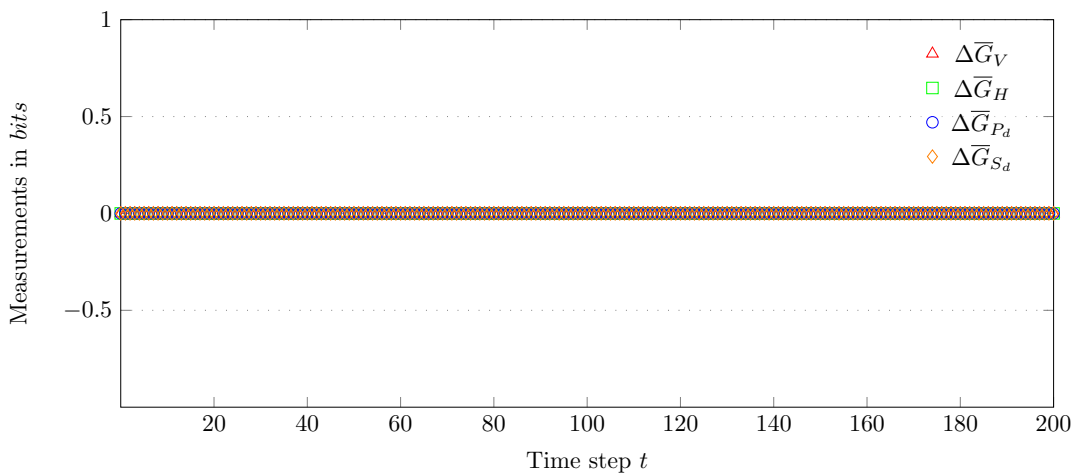


Fig. 4.21. The measurements of $\Delta\bar{G}$ s for 4.19(a) (single cell) IC.

The behaviour of a cellular automaton from the single cell IC is a sequence of symmetrical patterns (Fig. 4.20). This fact is reflected on the measurements of $\Delta\bar{G}s$ (Fig. 4.21), where they are constant for all 200 time steps ($\Delta\bar{G}_V = \Delta\bar{G}_H = \Delta\bar{G}_{P_d} = \Delta\bar{G}_{S_d} = 0$). This is an indicator of the development of complete symmetrical patterns in four directions for each of the 200 configurations generated by experimental cellular automaton 4.6. However, the measurement of entropy starts from $H_0^{4.19(a)} = 0.00319$ and reaches $H_{200}^{4.19(a)} = 1.35548$ by the end of the runs (Fig. 4.26).

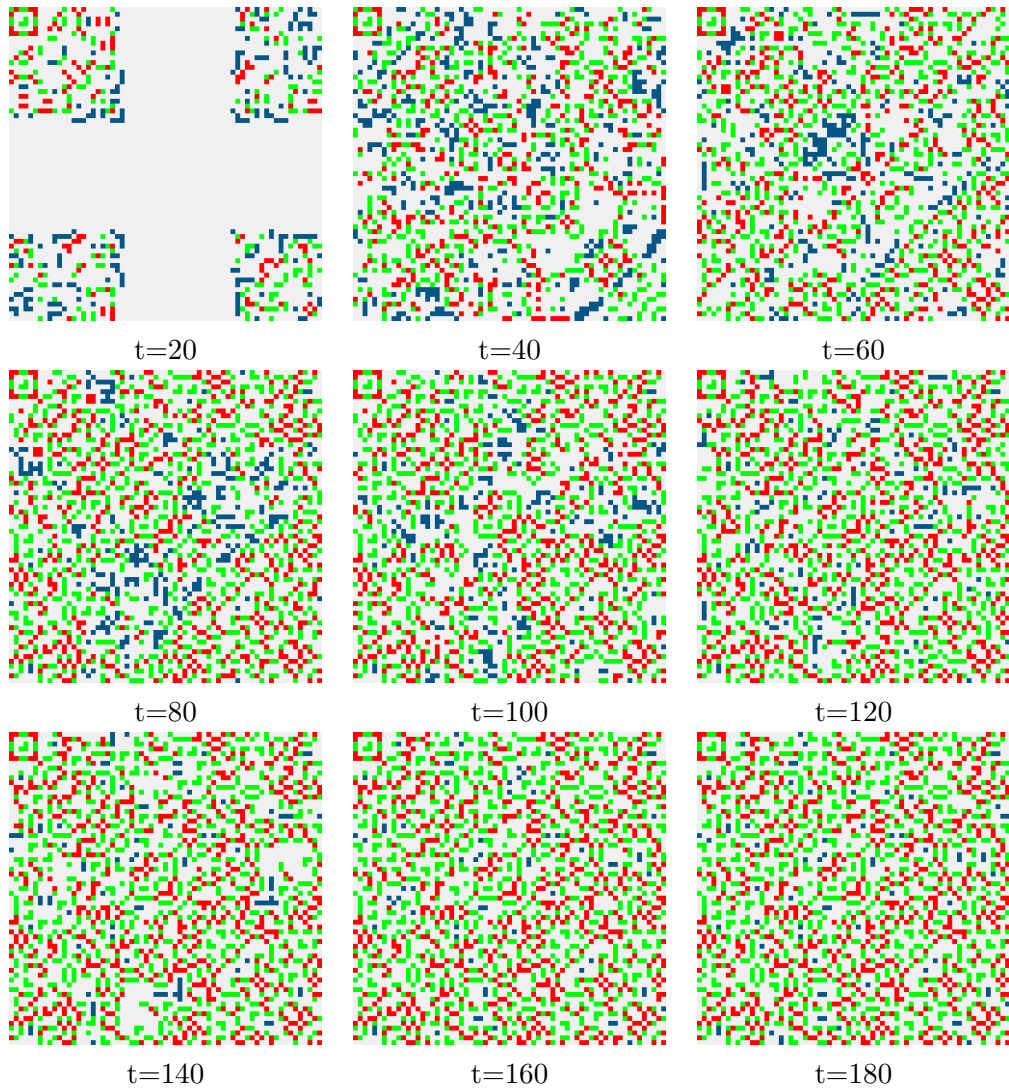


Fig. 4.22. The space-time diagram of the cellular automaton 4.6 for a sample of time steps starting from 4.19(b) IC.

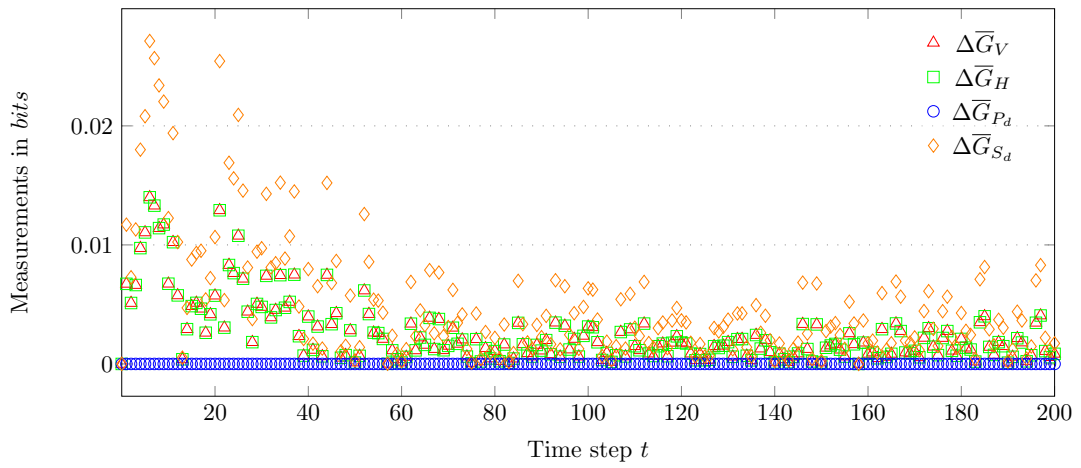


Fig. 4.23. The measurements of $\Delta \bar{G}$ s for 4.19(b) IC.

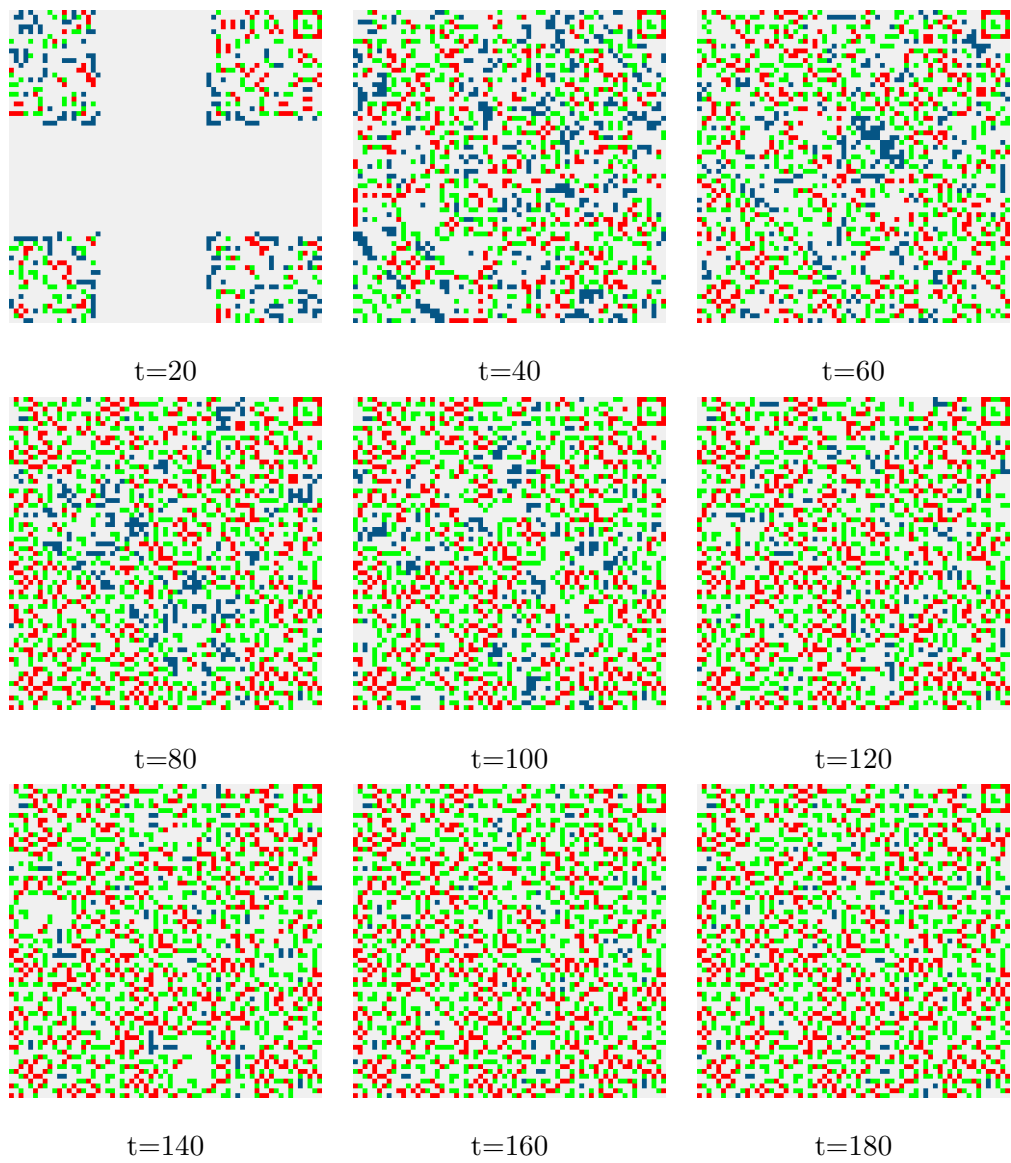


Fig. 4.24. The space-time diagram of the cellular automaton 4.6 for a sample of time steps starting from 4.19(c) IC.

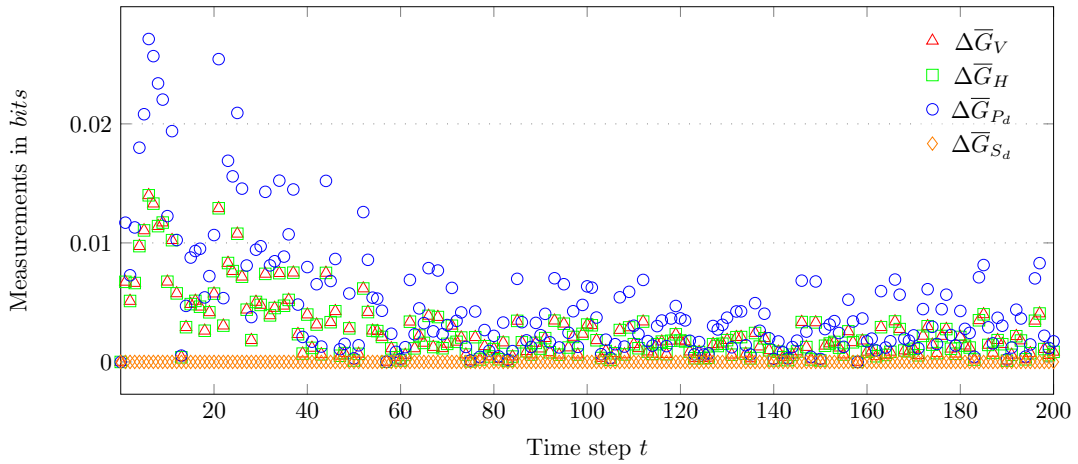


Fig. 4.25. The measurements of $\Delta\bar{G}s$ for 4.19(c) IC.

The two 5-cell ICs (4.19(b) and 4.19(c)) generate sequences of symmetrical patterns with different orientations (Fig. 4.22 and Fig. 4.24). The measurements of H for these two sequences of structurally different but symmetrical configurations are identical from $t = 0$ to $t = 200$, where $H_0^{4.19(b)} = H_0^{4.19(c)} = 0.01321$ and $H_{200}^{4.19(b)} = H_{200}^{4.19(c)} = 1.42028$ (Fig. 4.26). On the other hand, the measurements of $\Delta\bar{G}s$, particularly $\Delta\bar{G}_{P_d}$ and $\Delta\bar{G}_{S_d}$, reflect the differences in the orientations of the symmetrical configurations (Fig. 4.27 and Fig. 4.28). This is further illustrated in Fig. 4.29, where the measures of H , $\bar{G}s$ and $\Delta\bar{G}s$ are compared for two configurations generated at $t = 40$ from two different 4.19(b) and 4.19(c) ICs.

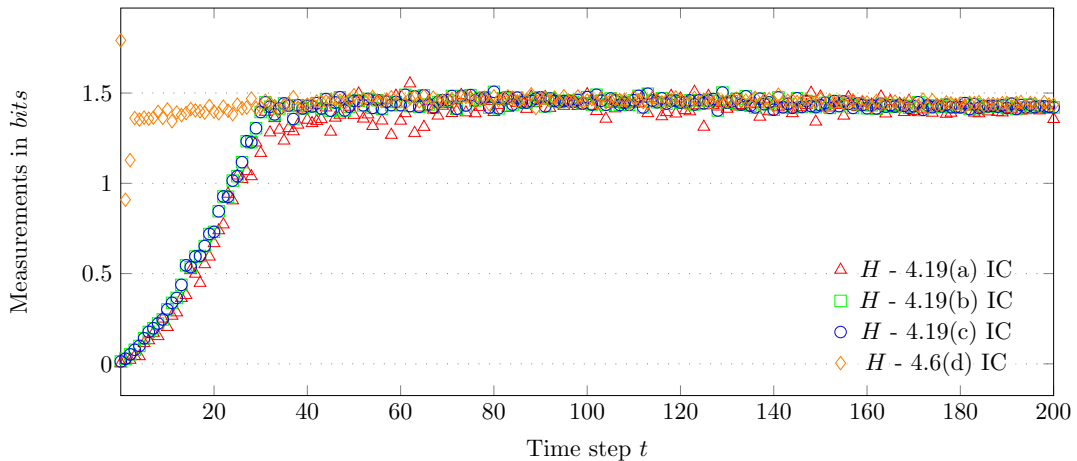


Fig. 4.26. The measurements of H for 4.19(a), 4.19(b), 4.19(c) and 4.19(d) ICs.

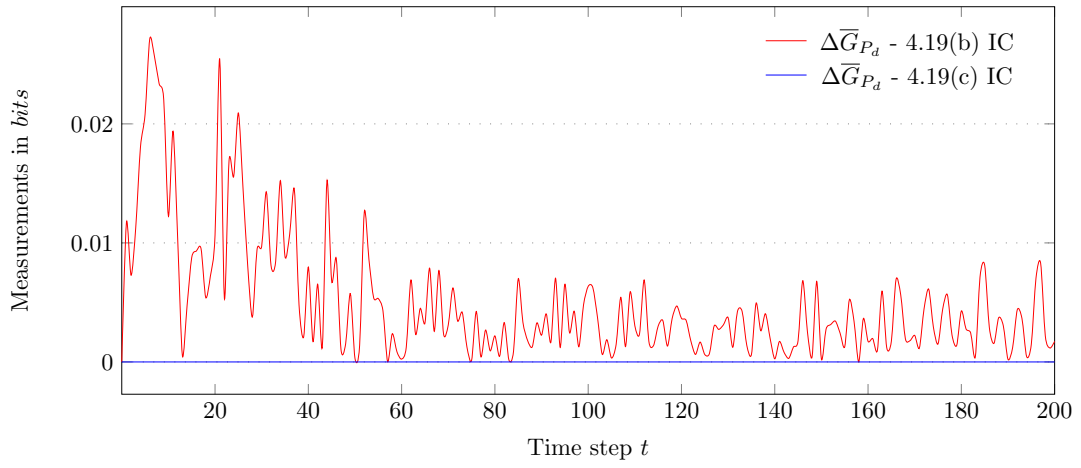


Fig. 4.27. Comparison of the measurement of $\Delta \bar{G}_{P_d}$ for 4.19(a) and 4.19(b) ICs.

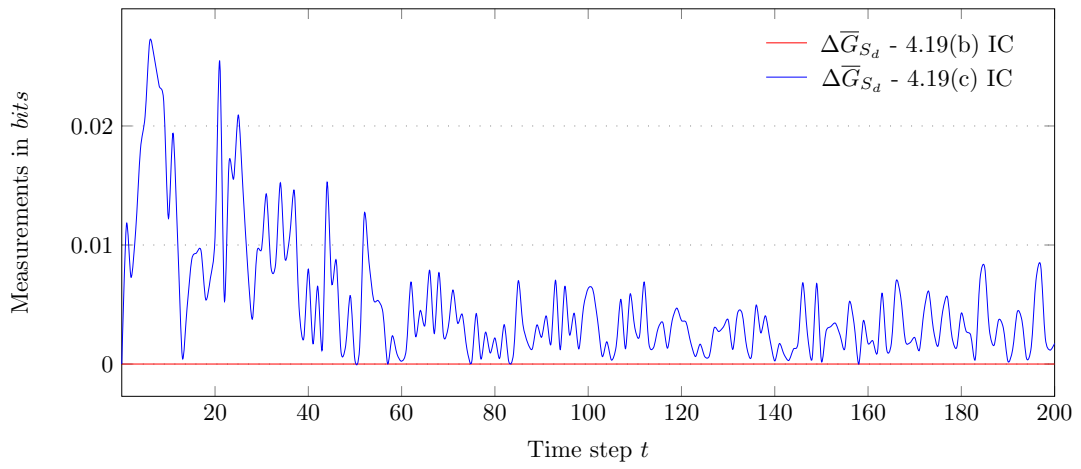
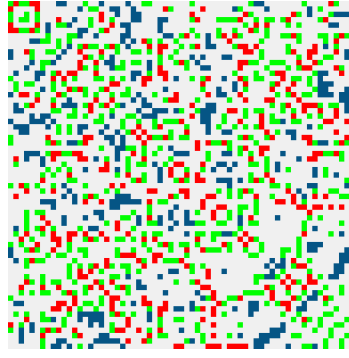
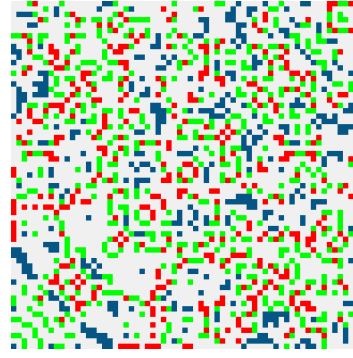


Fig. 4.28. Comparison of the measurement of $\Delta \bar{G}_{S_d}$ for 4.19(a) and 4.19(b) ICs.



(a)

$$\begin{aligned}
 H &= 1.42929 \\
 \bar{G}_{\uparrow} &= 1.36140 \\
 \bar{G}_{\downarrow} &= 1.36538 \\
 \Delta\bar{G}_V &= 0.00398 \\
 \bar{G}_{\leftarrow} &= 1.36140 \\
 \bar{G}_{\rightarrow} &= 1.36538 \\
 \Delta\bar{G}_H &= 0.00398 \\
 \bar{G}_{\swarrow} &= 1.36634 \\
 \bar{G}_{\searrow} &= 1.37431 \\
 \Delta\bar{G}_{P_d} &= 0.00797 \\
 \bar{G}_{\swarrow} &= 1.37148 \\
 \bar{G}_{\nearrow} &= 1.37148 \\
 \Delta\bar{G}_{S_d} &= 0 \\
 K &= 0.15929
 \end{aligned}$$



(b)

$$\begin{aligned}
 H &= 1.42929 \\
 \bar{G}_{\uparrow} &= 1.36140 \\
 \bar{G}_{\downarrow} &= 1.36538 \\
 \Delta\bar{G}_V &= 0.00398 \\
 \bar{G}_{\leftarrow} &= 1.36538 \\
 \bar{G}_{\rightarrow} &= 1.36140 \\
 \Delta\bar{G}_H &= 0.00398 \\
 \bar{G}_{\swarrow} &= 1.37148 \\
 \bar{G}_{\searrow} &= 1.37148 \\
 \Delta\bar{G}_{P_d} &= 0 \\
 \bar{G}_{\swarrow} &= 1.37431 \\
 \bar{G}_{\nearrow} &= 1.36634 \\
 \Delta\bar{G}_{S_d} &= 0.00797 \\
 K &= 0.16118
 \end{aligned}$$

Fig. 4.29. The comparison of H , $\bar{G}s$, $\Delta\bar{G}s$ and K for cellular automaton 4.6 conformations at $t = 40$ for 4.19(b) and 4.19(c) ICs.

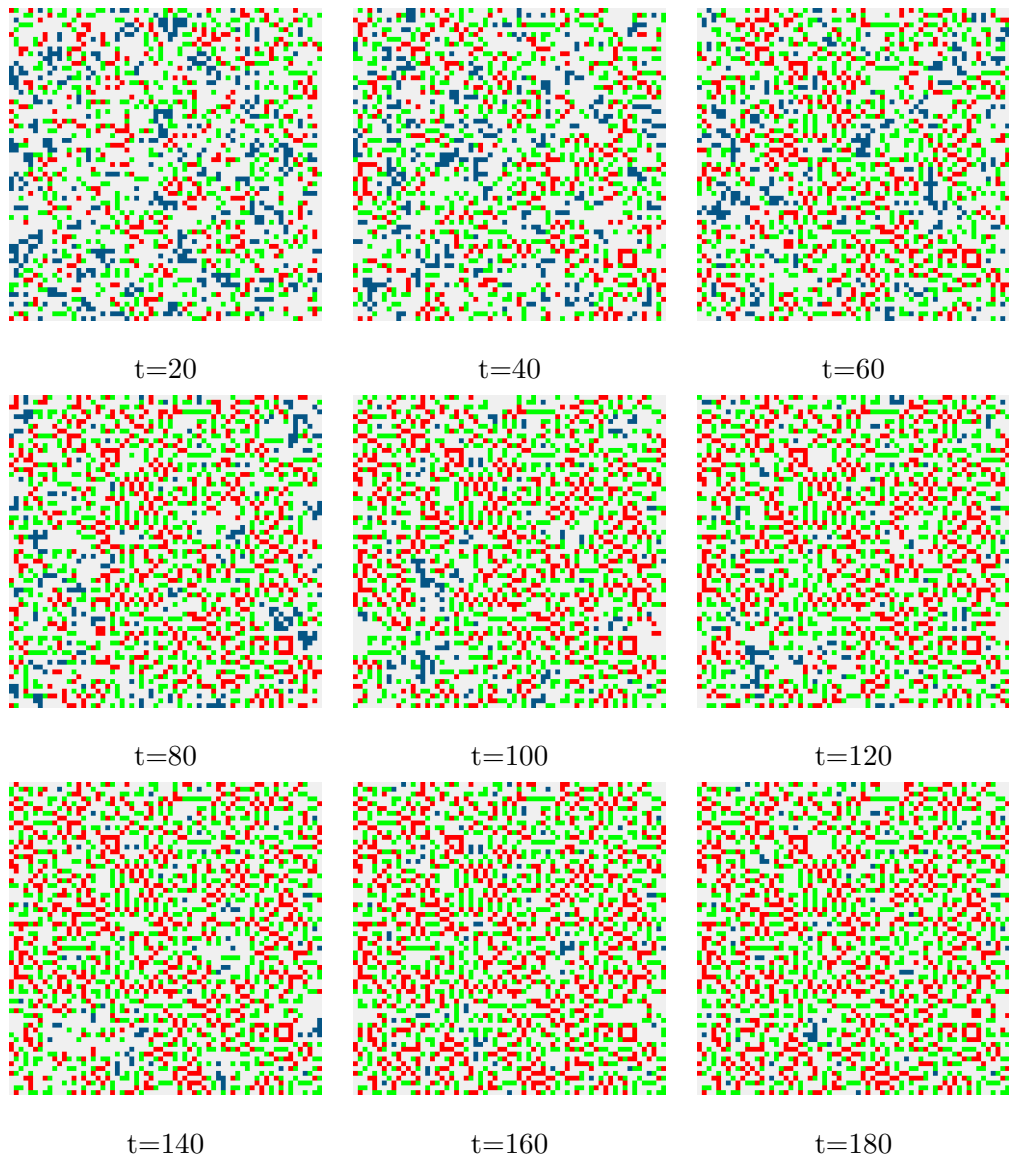


Fig. 4.30. The space-time diagram of the cellular automaton 4.6 for a sample of time steps for the random IC (4.19(d)) .

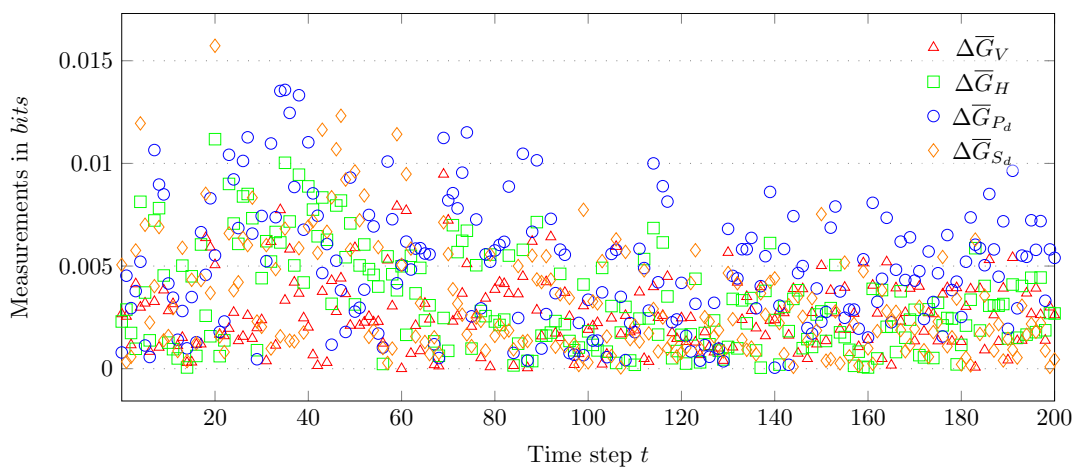


Fig. 4.31. The measurements of $\Delta\bar{G}$ s for 4.19(d) IC.

The development of configurations from the random IC results in a sequence of irregular structures (Fig. 4.30). The formation of patterns with local structures has reduced the values of $\Delta\overline{G}s$ until a stable oscillating pattern is attained (Fig. 4.31). This is an indicator of the development of irregular structures. However, the patterns are not random since the maximum four-state value of $\log_2(4) = 2$ (Eq. 4.21). The measurement of H for $H_0^{4.19(d)} = 1.79195$ and for $H_{200}^{4.19(d)} = 1.43572$ also reflects the reduction of entropy, indicating the formation of less random patterns compared to IC at $t = 0$.

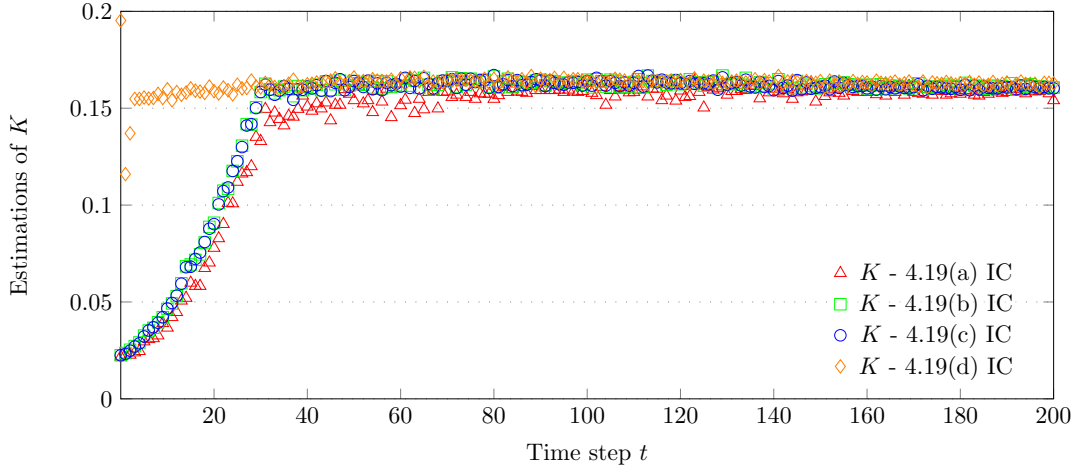


Fig. 4.32. *The estimations of K for 4.19(a), 4.19(b), 4.19(c) and 4.19(d) ICs.*

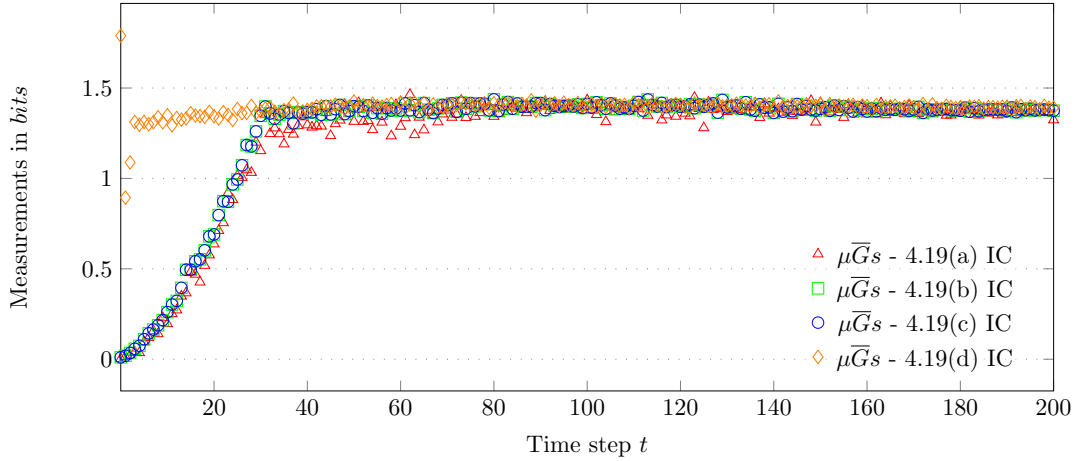


Fig. 4.33. *The measurements of $\mu\overline{G}s$ for 4.19(a), 4.19(b), 4.19(c) and 4.19(d) ICs.*

In addition, the relationship between K and $\overline{G}s$ are examined using the Pearson correlation coefficient (r) test. Table 4.7 shows the calculations of r for different directional $\overline{G}s$. Since the values of r are ≈ 0.99 , there is a strong positive correlation between K and $\overline{G}s$.

| | | | |
|----------------------------------|------------------------------------|------------------------------------|-------------------------------------|
| $r_{K\bar{G}_\uparrow} = 0.9985$ | $r_{K\bar{G}_\downarrow} = 0.9985$ | $r_{K\bar{G}_\leftarrow} = 0.9985$ | $r_{K\bar{G}_\rightarrow} = 0.9985$ |
| $r_{K\bar{G}_\nwarrow} = 0.9975$ | $r_{K\bar{G}_\searrow} = 0.9975$ | $r_{K\bar{G}_\nearrow} = 0.9975$ | $r_{K\bar{G}_\swarrow} = 0.9975$ |

Calculations of r for 4.19(a) IC.

| | | | |
|----------------------------------|------------------------------------|------------------------------------|-------------------------------------|
| $r_{K\bar{G}_\uparrow} = 0.9996$ | $r_{K\bar{G}_\downarrow} = 0.9995$ | $r_{K\bar{G}_\leftarrow} = 0.9996$ | $r_{K\bar{G}_\rightarrow} = 0.9995$ |
| $r_{K\bar{G}_\nwarrow} = 0.9996$ | $r_{K\bar{G}_\searrow} = 0.9996$ | $r_{K\bar{G}_\nearrow} = 0.9994$ | $r_{K\bar{G}_\swarrow} = 0.9995$ |

Calculations of r for 4.19(b) IC.

| | | | |
|----------------------------------|------------------------------------|------------------------------------|-------------------------------------|
| $r_{K\bar{G}_\uparrow} = 0.9996$ | $r_{K\bar{G}_\downarrow} = 0.9995$ | $r_{K\bar{G}_\leftarrow} = 0.9995$ | $r_{K\bar{G}_\rightarrow} = 0.9996$ |
| $r_{K\bar{G}_\nwarrow} = 0.9995$ | $r_{K\bar{G}_\searrow} = 0.9996$ | $r_{K\bar{G}_\nearrow} = 0.9996$ | $r_{K\bar{G}_\swarrow} = 0.9996$ |

Calculations of r for 4.19(c) IC.

| | | | |
|----------------------------------|------------------------------------|------------------------------------|-------------------------------------|
| $r_{K\bar{G}_\uparrow} = 0.9854$ | $r_{K\bar{G}_\downarrow} = 0.9842$ | $r_{K\bar{G}_\leftarrow} = 0.9874$ | $r_{K\bar{G}_\rightarrow} = 0.9838$ |
| $r_{K\bar{G}_\nwarrow} = 0.9885$ | $r_{K\bar{G}_\searrow} = 0.9879$ | $r_{K\bar{G}_\nearrow} = 0.9794$ | $r_{K\bar{G}_\swarrow} = 0.9831$ |

Calculations of r for 4.19(d) IC.

Table 4.7: *Calculations of r for different ICs.*

These experiments demonstrate that a cellular automaton rule seeded with different ICs leads to the formation of patterns with structurally diverse characteristics. The gradient of the mean information rate along lattice axes is able to detect the structural characteristics of patterns generated by this particular multi-state 2D cellular automaton. From the comparison of H with $\Delta\bar{G}s$ in the set of experiments, it is clear that entropy fails to discriminate between the diversity of patterns that can be generated by various CA.

The structured but asymmetrical patterns emerging from the random IC are clearly distinguished from the symmetrical patterns, including their orientation. It is evident from the results of the experiments, the measures of H are identical for structurally different patterns; however, the measure of $\bar{G}s$ and $\Delta\bar{G}s$ reflect not only the complexity of patterns but their spatial arrangements (i.e. orientation of symmetries) as well.

4.5 Summary

Entropy, one of the most commonly applied measures of complexity, is based on the probability distribution of symbols, not their arrangements. Despite the dominance of entropy as a measure of order and complexity, it fails to reflect the structural characteristics of 2D patterns and of CA configurations.

However, spatial complexity measure takes into account conditional and joint probabilities between pairs of cells and, since it is based on correlations between cells, holds promise for patterns discrimination. Kolmogorov's algorithmic complexity is another measure of complexity which can be used to estimate the complexity of 2D configurations generated by a cellular automaton.

In this chapter, a set of experiments with a cellular automaton were conducted using four different initial conditions, leading to the formation of patterns with structurally diverse characteristics. The potential of spatial complexity measure and Kolmogorov complexity for distinguishing multi-state 2D CA patterns is demonstrated. The measures appear to be particularly good at distinguishing different types of random patterns from non-random patterns. Furthermore, spatial complexity measure is also able to discriminate the orientation of symmetries.

5. Experiments and Results

This chapter details two experiments and their results on the correlation between three measures, namely spatial complexity measure ($\mu(G)s$), Kolmogorov complexity (K) and entropy (H), and human aesthetic judgement. For the first experiment, 252 experimental stimuli patterns were adopted from an empirical study of human aesthetic judgements of 2D symmetrical and asymmetrical patterns reported in [199]. The main reason for this adoption is that the patterns have been ranked based on their aesthetic judgements by humans thus making it possible to investigate the relationship between human aesthetic judgement and the measurements of $\mu(G)s$, K and H . For the second experiment, a set of 2D patterns with various structural properties were generated by seeding CA, then a survey was designed and used to compare their aesthetic values with the measurements of $\mu(G)s$, K and H .

5.1 Objectives

The purpose of experimentations in this chapter is to investigate the relationship between human aesthetic judgement and the measurements of $\mu(G)s$, K and H , with the purpose of evaluating the following set of hypotheses:

H1: *The measurement of $\mu(G)s$ for a 2D pattern is linearly related with human aesthetic judgement.*

H2: *The estimation of K for a 2D pattern is linearly related with human aesthetic judgement.*

H3: *The measurement of H for a 2D pattern is linearly related with human aesthetic judgement.*

Thus $\mu(G)s$, K and H are the independent variables for the present experimentations.

5.2 Experiment I

This section starts by summarising the research and results reported by Jacobsen and Höfel [199]. The details in the subsequent sections of *Method*, *Material*, *Procedure* and *Results* are directly adopted from [199]. An extended study is provided, where the 250 experimental stimuli were adopted from their empirical study of human aesthetic judgements of symmetrical and asymmetrical patterns to evaluate the effectiveness of $\mu(G)s$, K and H .

5.2.1 Method

Fifty-five young adults (15 males and 45 females) participated in the experiment for course credit or partial fulfilment of course requirements. All were first or second-year psychology students at the University of Leipzig. None of them had received professional training in the fine arts or participated in a similar experiment before. All participants reported normal or corrected-to-normal visual acuity.

5.2.2 Material

A set of 252 stimuli were constructed. Each consisted of a solid black circle (6.4 cm in diameter) showing a centred, quadratic, rhombic cut-out (4 cm) and an arrangement of 86 to 88 basic graphic elements (small black triangles). These were positioned within the rhombus according to a grid and resulted in a graphic pattern. The basic elements were arranged such that geometric figures like triangles, squares, rhombuses, and horizontal, vertical, or oblique bars of different sizes were created. Using this collection of basic elements, the overall luminance was identical for all stimuli. Half of the patterns (130) were symmetrical, that is a maximum of two mirroring operations giving four possible symmetry axes were permitted. The other half of the stimuli were not symmetrical. Stimulus complexity was manipulated by varying the number of elements composing a pattern. Fig. 5.34 depicts a sample of constructed stimuli patterns.

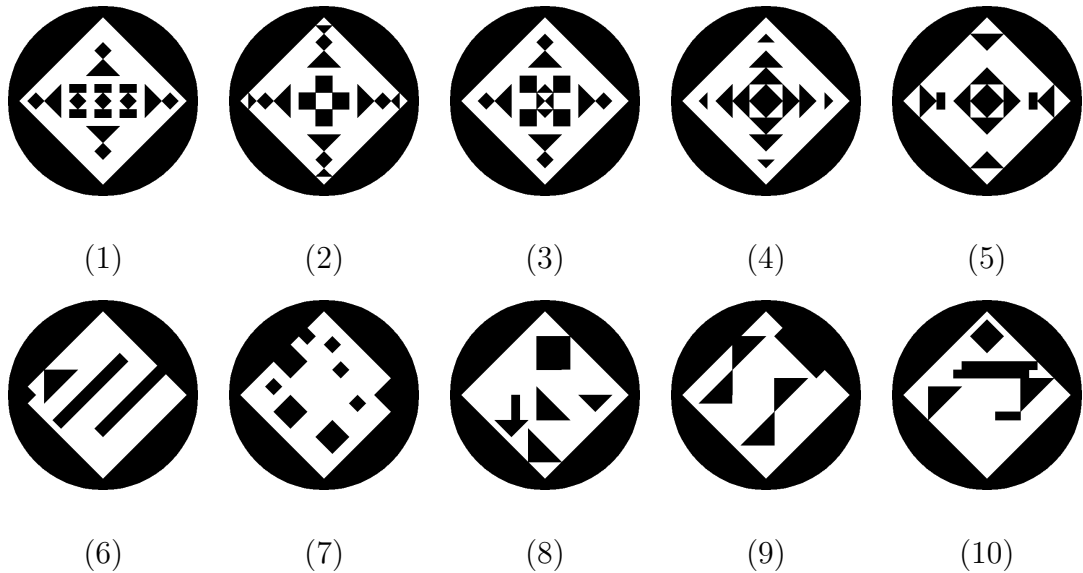


Fig. 5.34. *Samples of stimuli patterns adopted from Jacobsen and Höfel.*

5.2.3 Procedure

Participants responded to 252 stimulus patterns in individualised randomised order. They were instructed to judge each pattern according to the pattern’s aesthetic value. They were instructed to use the words “beautiful” and “not beautiful” for their aesthetic judgements. They were also instructed to anchor their judgement to the present stimuli set and not to take any irrelevant objects or classes of objects, like paintings, works of design, or any other works of art, into consideration for their aesthetic judgements of beauty. Participants were told to take their time and spread the patterns out in front of them so that they could have a good overall impression of the stimulus set before they made their judgements. They were instructed to create three bins:

1. one of at least 75 “beautiful” patterns,
2. one of at least 75 “not beautiful” patterns,
3. a third possible category of “indifferent” patterns.

The last bin could form the largest one (up to 102 stimuli) but could also contain no elements, if that was preferred. This procedure was chosen to give participants some freedom of choice while still limiting them to using the three bins. The post-experimental interviews indicated that participants had no difficulties in distinguishing aesthetic and non-aesthetic patterns.

5.2.4 Results

Symmetry was the most important stimulus feature predicting participants' aesthetic judgements. In general, participants showed agreement that the symmetrical patterns were more beautiful than the asymmetrical ones. In summary, the judgement analysis supported the hypothesis that symmetry and complexity are important factors in aesthetic judgements.

5.2.5 Procedure for the Extended Study

All the 252 stimuli patterns were 453×453 pixels ($S = \{white, black\}$) and the black circular background was replaced by a square in order to reduce aliasing errors. The patterns were ordered from the highest to the lowest mean aesthetic ratings. For example, Fig. 5.34(1) had the highest mean aesthetic rating, 74.73 (ranked 1st), Fig. 5.34(2) had a mean aesthetic rating of 73.73 (ranked 2nd) . . . , and Fig. 5.34(10) was left with the lowest mean aesthetic rating, 28.58 (ranked 252nd).

The mean aesthetic ratings of stimuli patterns with their ranking are plotted in Fig. 5.35. The spatial complexity, $\mu(G)s$, K and H , were then calculated. A sample of calculations are detailed in Fig. 5.36.

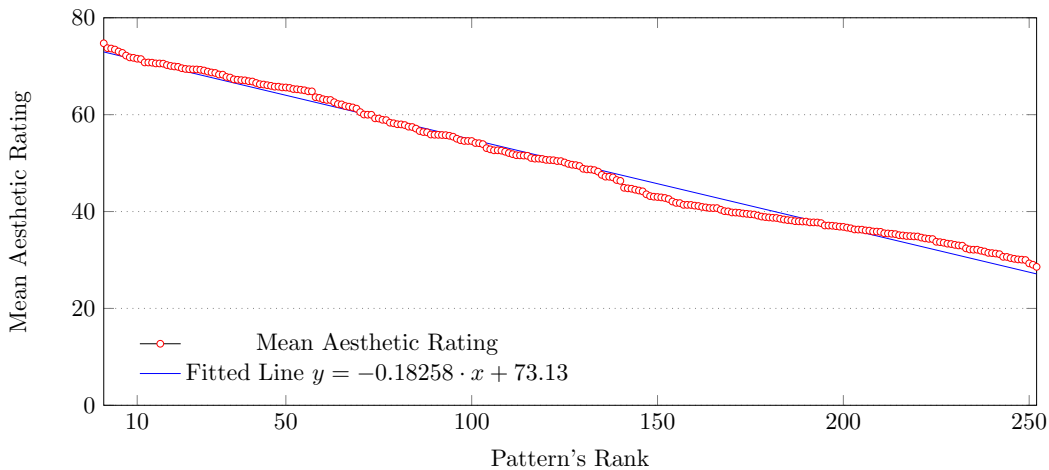
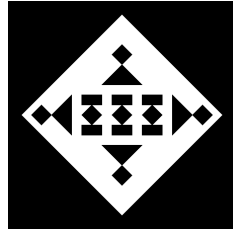


Fig. 5.35. Mean aesthetic judgements of stimuli patterns and their ranking.



(1)

$$Rank = 1$$

$$Rating = 74.73$$

$$H = 0.88290$$

$$\bar{G}\uparrow = 0.08771$$

$$\bar{G}\downarrow = 0.08771$$

$$\Delta\bar{G}_V = 0$$

$$\bar{G}\leftarrow = 0.08096$$

$$\bar{G}\rightarrow = 0.08096$$

$$\Delta\bar{G}_H = 0$$

$$\bar{G}\swarrow = 0.10003$$

$$\bar{G}\searrow = 0.10003$$

$$\Delta\bar{G}_{P_d} = 0$$

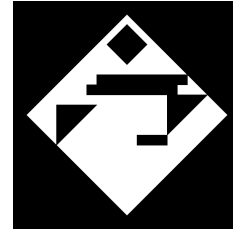
$$\bar{G}_{\swarrow} = 0.10003$$

$$\bar{G}_{\nearrow} = 0.10003$$

$$\Delta\bar{G}_{S_d} = 0$$

$$\mu Gs = 0.09218$$

$$K = 0.01138$$



(2)

$$Rank = 252$$

$$Rating = 28.58$$

$$H = 0.87780$$

$$\bar{G}\uparrow = 0.07002$$

$$\bar{G}\downarrow = 0.07002$$

$$\Delta\bar{G}_V = 0$$

$$\bar{G}\leftarrow = 0.05791$$

$$\bar{G}\rightarrow = 0.05791$$

$$\Delta\bar{G}_H = 0$$

$$\bar{G}\swarrow = 0.07349$$

$$\bar{G}\searrow = 0.07349$$

$$\Delta\bar{G}_{P_d} = 0$$

$$\bar{G}_{\swarrow} = 0.08426$$

$$\bar{G}_{\nearrow} = 0.08426$$

$$\Delta\bar{G}_{S_d} = 0$$

$$\mu Gs = 0.07142$$

$$K = 0.00952$$

Fig. 5.36. A sample of the calculations of spatial complexity, $\mu(G)s$, K and H for two stimuli patterns.

5.2.6 Results and Analysis

Two sets of calculations were performed. The first set of calculations was the measurement of $\mu(G)s$, K and H for stimuli patterns ordered based on their ranking. The results of these calculations are plotted in Fig. 5.37. The second set of calculations was the measurement of $\mu(G)s$, K and H for stimuli patterns ordered based on their ratings. The results of these calculations are plotted in Fig. 5.38. Then the relationship between the independent variables of $\mu(G)s$, K , H and the patterns' ranking and mean aesthetic ratings were examined using the Pearson correlation

coefficient (r) test. Table 5.8 summarises the results of the correlation test between $\mu(G)s$, K , H and pattern ranking and their mean aesthetic ratings.

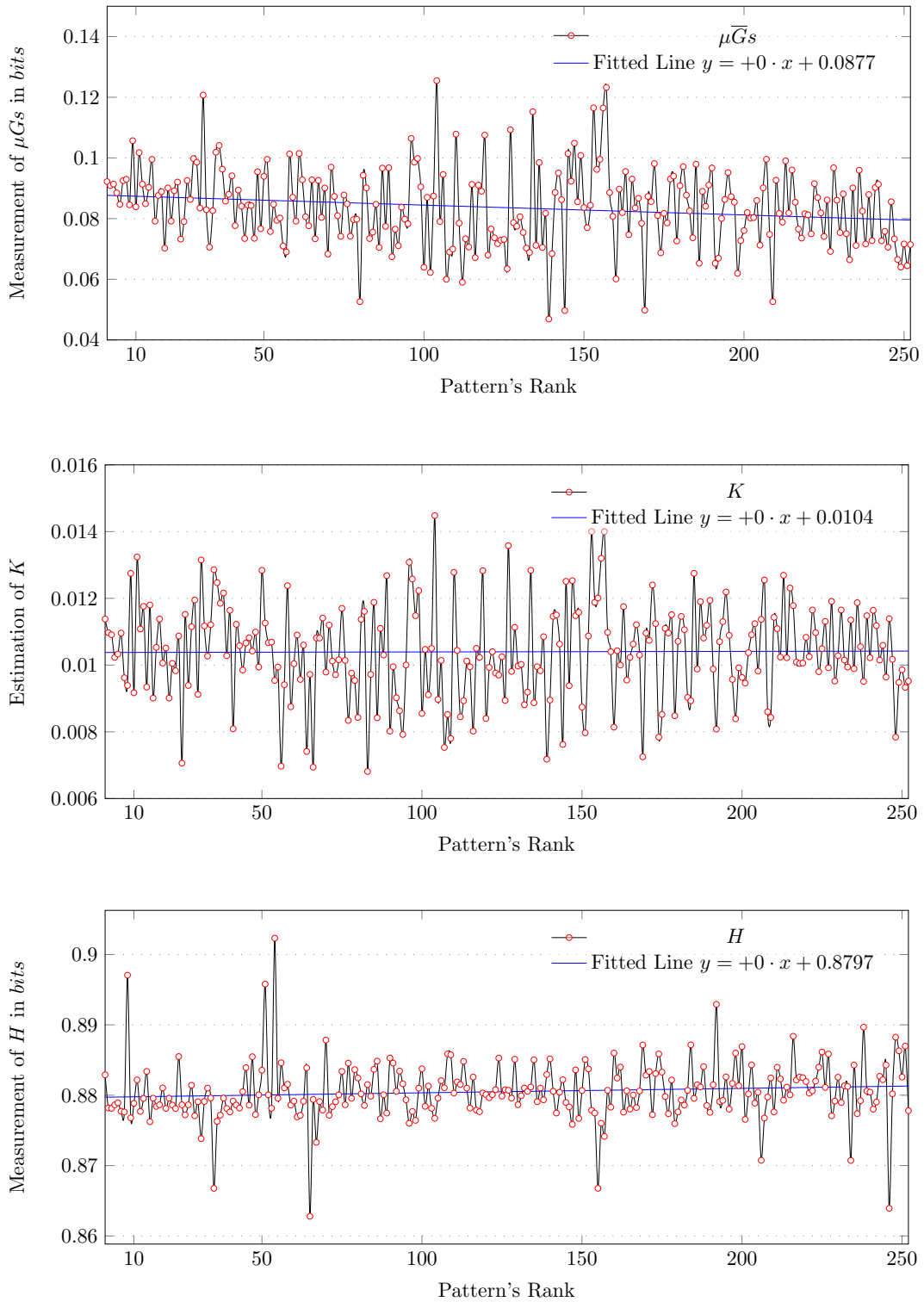


Fig. 5.37. The measurement of $\mu(G)s$, K and H for stimuli patterns ordered based on their ranking.

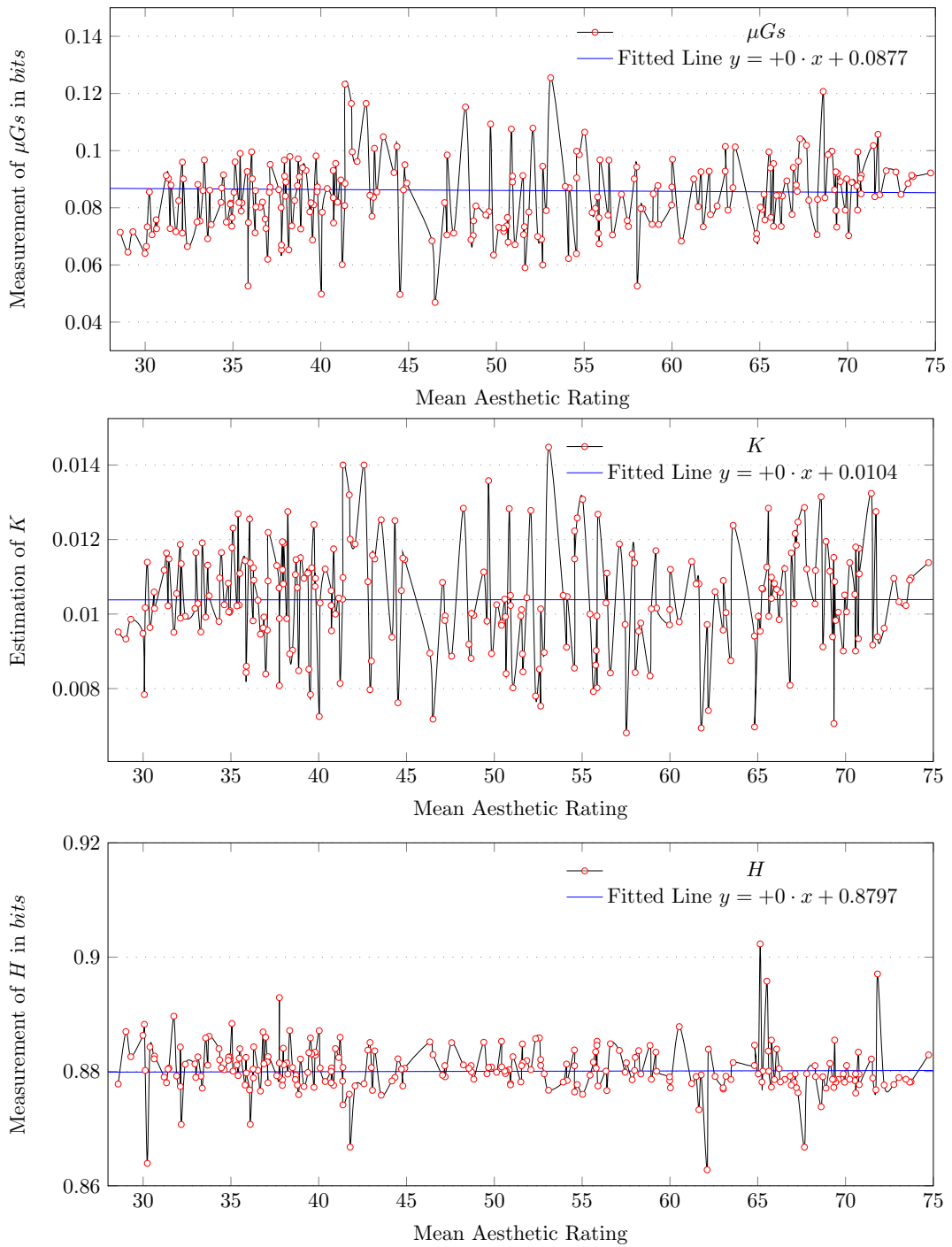


Fig. 5.38. The measurement of $\mu(G)s$, K and H for stimuli patterns ordered based on their ranking.

| | μGs | K | H |
|-------------------------------|----------|---------|---------|
| <i>Patterns Ranks</i> | -0.1846 | 0.0085 | 0.1086 |
| <i>Mean Aesthetic Ratings</i> | 0.1724 | -0.0105 | -0.1023 |

Table 5.8: *The results of Pearson correlation coefficient test between μGs , K , H and pattern ranking along with mean aesthetic ratings of the 252 stimuli patterns.*

The results of the calculations are as follows:

The value of r for μGs is -0.1846 with $y = 0.0877$ for pattern ranks. This indicates *a negative linear correlation*; also, the relationship between μGs and pattern ranks is *only weak*,

The value of r for K is 0.0085 with $y = 0.0104$ for patterns ranks. This indicates *a positive linear correlation* and the relationship between K and pattern ranks is *weak*,

The value of r for H is 0.1086 with $y = 0.8797$ for patterns ranks. This indicates *a positive linear correlation*, and the relationship between H and pattern ranks is *weak*,

The value of r for μGs is 0.1724 with $y = 0.0877$ for pattern ratings. This indicates *a positive linear correlation*, and the relationship between μGs and pattern ratings is *weak*,

The value of r for K is -0.0105 with $y = 0.0104$ for patterns ratings. This indicates *a negative linear correlation*, and the relationship between K and pattern ratings is *only weak*,

The value of r for H is -0.1023 with $y = 0.8797$ for patterns ranks. This indicates *a negative linear correlation*, and the relationship between H and pattern ratings is *only weak*.

Considering the values of r for the Pearson correlation coefficient test and regression analysis, it is evident that there are *no statistically significant correlations* between μGs , K , H and patterns' ratings and ranking. Therefore, all the hypotheses (**H1**, **H2** and **H3**) are rejected for the experiment conducted with the adopted 252 stimulus patterns. These results indicate that the measurement of $\mu(G)s$, K and H do not conform to the aesthetic ranking of the 252 stimuli.

Given that the measures are primarily developed for CA environment and for CA-generated patterns, there are intrinsic relationship between the cells, update rule and neighbouring cells; the measures fail to distinguish the complexity of 252 stimuli in relation to their aesthetic rankings. In other words, the measures do not accurately measuring the complexity of non-CA generated patterns.

5.3 Experiment II

5.3.1 Method

An online survey was conducted using SurveyMonkey, a web-based survey platform where registered users are paid for participating in the surveys. A total of 100 participants aged between 18 and 60 in the USA participated in the survey.

5.3.2 Material

For this experiment, 10 patterns with various structural characteristics reflecting the spectrum of spatial complexity (4.15) were generated by seeding 3-state CA with different ICs. Fig. 5.40 illustrates the generated experimental patterns. The patterns fall in three categories, namely regular structures (Fig. 5.40(1),(2),(3),(4),(5)), irregular structures (Fig. 5.40(6),(7),(8),(9)), and structureless patterns (Fig. 5.40(10)). Grey scale colours were used for the colour assignments of the CA states to eliminate possible individual colour preferences in aesthetic judgements ($S = \{0, 1, 2\} \equiv \{\blacksquare, \blacksquare, \blacksquare\}$). The size of lattice for all the patterns was $L = 65 \times 65$ (4225 cells) with an image size of 651×651 pixels.

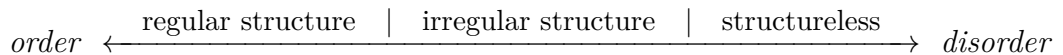


Fig. 5.39. *The spectrum of spatial complexity considered for the generation of 10 experimental patterns .*

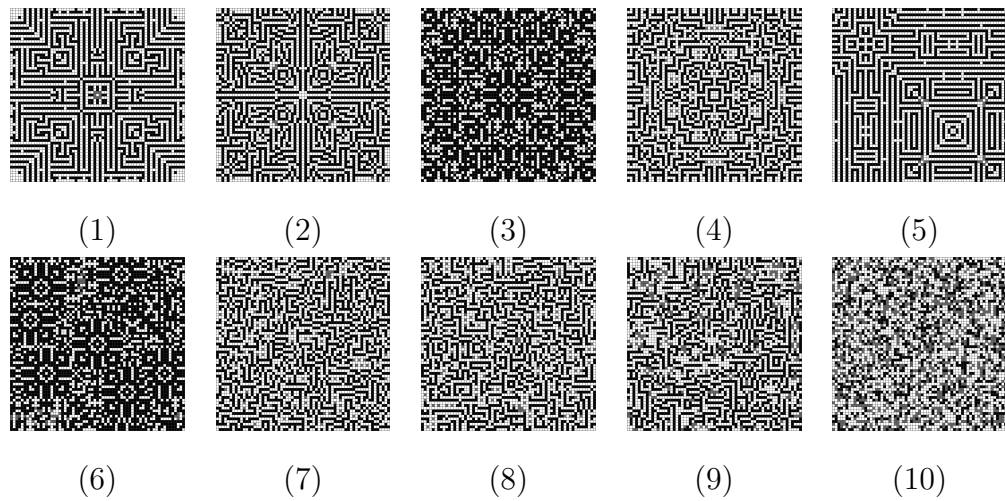
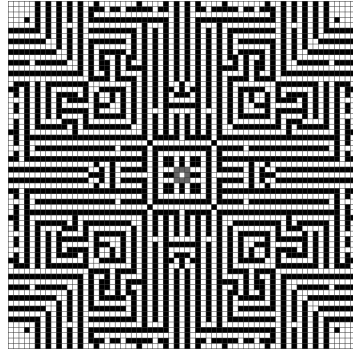


Fig. 5.40. *Generated patterns with various structural characteristics reflecting the spectrum of spatial complexity 4.15.*

The spatial complexity measure, $\mu(G)_s$, K and H , were then calculated for all the patterns. Fig. 5.41, 5.42, 5.43, 5.44, 5.45 show the details of these calculations and Fig. 5.46 shows the measurements of $\mu(G)_s$, K and H for the generated patterns.



(1)

$$H = 1.01633$$

$$\overline{G}_{\uparrow} = 1.00948$$

$$\overline{G}_{\downarrow} = 1.00948$$

$$\Delta\overline{G}_V = 0$$

$$\overline{G}_{\leftarrow} = 1.00948$$

$$\overline{G}_{\rightarrow} = 1.00948$$

$$\Delta\overline{G}_H = 0$$

$$\overline{G}_{\swarrow} = 0.58810$$

$$\overline{G}_{\searrow} = 0.58810$$

$$\Delta\overline{G}_{P_d} = 0$$

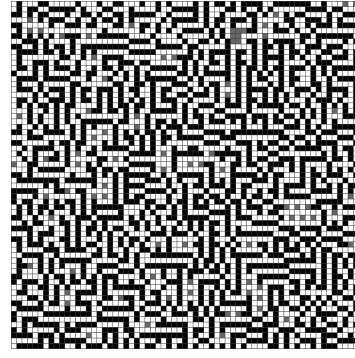
$$\overline{G}_{\swarrow} = 0.58810$$

$$\overline{G}_{\nearrow} = 0.58810$$

$$\Delta\overline{G}_{S_d} = 0$$

$$\mu Gs = 0.79879$$

$$K = 0.09420$$



(2)

$$H = 1.11255$$

$$\overline{G}_{\uparrow} = 1.09434$$

$$\overline{G}_{\downarrow} = 1.09240$$

$$\Delta\overline{G}_V = 0.00194$$

$$\overline{G}_{\leftarrow} = 1.08993$$

$$\overline{G}_{\rightarrow} = 1.09054$$

$$\Delta\overline{G}_H = 0.00061$$

$$\overline{G}_{\swarrow} = 1.02205$$

$$\overline{G}_{\searrow} = 1.02062$$

$$\Delta\overline{G}_{P_d} = 0.00135$$

$$\overline{G}_{\swarrow} = 1.01699$$

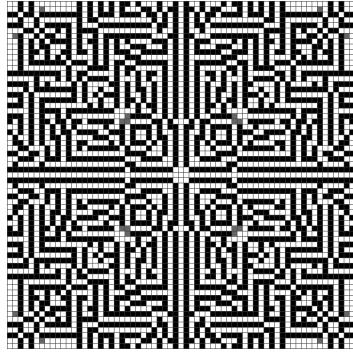
$$\overline{G}_{\nearrow} = 1.01564$$

$$\Delta\overline{G}_{S_d} = 0.00143$$

$$\mu Gs = 1.05530$$

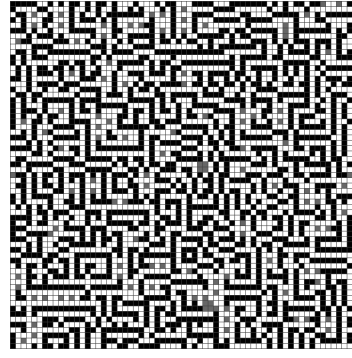
$$K = 0.13538$$

Fig. 5.41. The measurements of spatial complexity measure, $\mu(G)s$, K and H for the generated patterns with various structural characteristics.



(3)

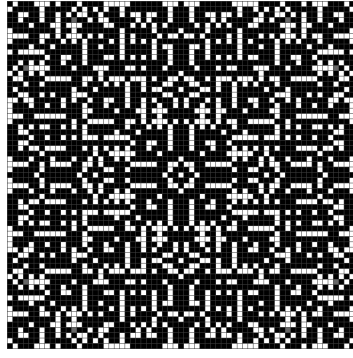
$$\begin{aligned}
 H &= 1.03815 \\
 \overline{G}_{\uparrow} &= 1.02822 \\
 \overline{G}_{\downarrow} &= 1.02822 \\
 \Delta \overline{G}_V &= 0 \\
 \overline{G}_{\leftarrow} &= 1.02822 \\
 \overline{G}_{\rightarrow} &= 1.02822 \\
 \Delta \overline{G}_H &= 0 \\
 \overline{G}_{\swarrow} &= 0.86511 \\
 \overline{G}_{\searrow} &= 0.86511 \\
 \Delta \overline{G}_{P_d} &= 0 \\
 \overline{G}_{\swarrow} &= 0.86511 \\
 \overline{G}_{\nearrow} &= 0.86511 \\
 \Delta \overline{G}_{S_d} &= 0 \\
 \mu Gs &= 0.94666 \\
 K &= 0.12142
 \end{aligned}$$



(4)

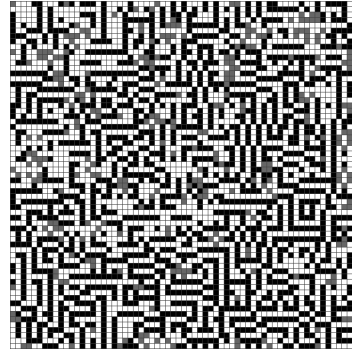
$$\begin{aligned}
 H &= 1.14569 \\
 \overline{G}_{\uparrow} &= 1.12644 \\
 \overline{G}_{\downarrow} &= 1.12366 \\
 \Delta \overline{G}_V &= 0.00278 \\
 \overline{G}_{\leftarrow} &= 1.12442 \\
 \overline{G}_{\rightarrow} &= 1.12413 \\
 \Delta \overline{G}_H &= 0.00029 \\
 \overline{G}_{\swarrow} &= 1.03548 \\
 \overline{G}_{\searrow} &= 1.03244 \\
 \Delta \overline{G}_{P_d} &= 0.00304 \\
 \overline{G}_{\swarrow} &= 1.02297 \\
 \overline{G}_{\nearrow} &= 1.02558 \\
 \Delta \overline{G}_{S_d} &= 0.00261 \\
 \mu Gs &= 1.07690 \\
 K &= 0.13538
 \end{aligned}$$

Fig. 5.42. The measurements of spatial complexity measure, $\mu(G)s$, K and H for the generated patterns with various structural characteristics.



(5)

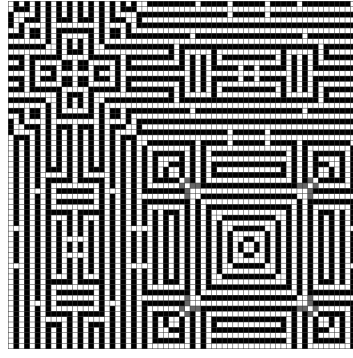
$$\begin{aligned}
 H &= 0.92648 \\
 \overline{G}_{\uparrow} &= 0.92483 \\
 \overline{G}_{\downarrow} &= 0.92483 \\
 \Delta \overline{G}_V &= 0 \\
 \overline{G}_{\leftarrow} &= 0.92483 \\
 \overline{G}_{\rightarrow} &= 0.92483 \\
 \Delta \overline{G}_H &= 0 \\
 \overline{G}_{\swarrow} &= 0.90643 \\
 \overline{G}_{\searrow} &= 0.90643 \\
 \Delta \overline{G}_{P_d} &= 0 \\
 \overline{G}_{\swarrow} &= 0.90643 \\
 \overline{G}_{\nearrow} &= 0.90643 \\
 \Delta \overline{G}_{S_d} &= 0 \\
 \mu G_s &= 0.91563 \\
 K &= 0.12331
 \end{aligned}$$



(6)

$$\begin{aligned}
 H &= 1.29257 \\
 \overline{G}_{\uparrow} &= 1.26551 \\
 \overline{G}_{\downarrow} &= 1.26833 \\
 \Delta \overline{G}_V &= 0.00282 \\
 \overline{G}_{\leftarrow} &= 1.26517 \\
 \overline{G}_{\rightarrow} &= 1.26762 \\
 \Delta \overline{G}_H &= 0.00245 \\
 \overline{G}_{\swarrow} &= 1.18740 \\
 \overline{G}_{\searrow} &= 1.19340 \\
 \Delta \overline{G}_{P_d} &= 0.00600 \\
 \overline{G}_{\swarrow} &= 1.19600 \\
 \overline{G}_{\nearrow} &= 1.19562 \\
 \Delta \overline{G}_{S_d} &= 0.00038 \\
 \mu G_s &= 1.22990 \\
 K &= 0.14888
 \end{aligned}$$

Fig. 5.43. The measurements of spatial complexity measure, $\mu(G)_s$, K and H for the generated patterns with various structural characteristics.



(7)

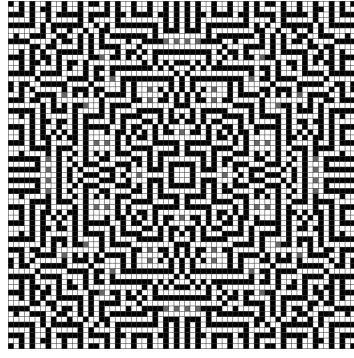
$$\begin{aligned}
 H &= 1.04381 \\
 \bar{G}_{\uparrow} &= 1.04021 \\
 \bar{G}_{\downarrow} &= 1.03945 \\
 \Delta\bar{G}_V &= 0.00076 \\
 \bar{G}_{\leftarrow} &= 1.03945 \\
 \bar{G}_{\rightarrow} &= 1.04029 \\
 \Delta\bar{G}_H &= 0.00084 \\
 \bar{G}_{\swarrow} &= 0.49065 \\
 \bar{G}_{\searrow} &= 0.49073 \\
 \Delta\bar{G}_{P_d} &= 0.00008 \\
 \bar{G}_{\swarrow} &= 0.49055 \\
 \bar{G}_{\nearrow} &= 0.49217 \\
 \Delta\bar{G}_{S_d} &= 0.00162 \\
 \mu Gs &= 0.76544 \\
 K &= 0.08260
 \end{aligned}$$



(8)

$$\begin{aligned}
 H &= 0.97108 \\
 \bar{G}_{\uparrow} &= 0.96149 \\
 \bar{G}_{\downarrow} &= 0.96415 \\
 \Delta\bar{G}_V &= 0.00266 \\
 \bar{G}_{\leftarrow} &= 0.95605 \\
 \bar{G}_{\rightarrow} &= 0.95589 \\
 \Delta\bar{G}_H &= 0.00016 \\
 \bar{G}_{\swarrow} &= 0.95349 \\
 \bar{G}_{\searrow} &= 0.95574 \\
 \Delta\bar{G}_{P_d} &= 0.00225 \\
 \bar{G}_{\swarrow} &= 0.95974 \\
 \bar{G}_{\nearrow} &= 0.95691 \\
 \Delta\bar{G}_{S_d} &= 0.00283 \\
 \mu Gs &= 0.95793 \\
 K &= 0.12521
 \end{aligned}$$

Fig. 5.44. The measurements of spatial complexity measure, $\mu(G)s$, K and H for the generated patterns with various structural characteristics.



(9)

$$\begin{aligned}
 H &= 1.07796 \\
 \overline{G}_{\uparrow} &= 1.06625 \\
 \overline{G}_{\downarrow} &= 1.06625 \\
 \Delta \overline{G}_V &= 0 \\
 \overline{G}_{\leftarrow} &= 1.06625 \\
 \overline{G}_{\rightarrow} &= 1.06625 \\
 \Delta \overline{G}_H &= 0 \\
 \overline{G}_{\swarrow} &= 0.93292 \\
 \overline{G}_{\searrow} &= 0.93292 \\
 \Delta \overline{G}_{P_d} &= 0 \\
 \overline{G}_{\swarrow} &= 0.93292 \\
 \overline{G}_{\nearrow} &= 0.93292 \\
 \Delta \overline{G}_{S_d} &= 0 \\
 \mu G_s &= 0.99959 \\
 K &= 0.12663
 \end{aligned}$$



(10)

$$\begin{aligned}
 H &= 1.49686 \\
 \overline{G}_{\uparrow} &= 1.49746 \\
 \overline{G}_{\downarrow} &= 1.49641 \\
 \Delta \overline{G}_V &= 0.00105 \\
 \overline{G}_{\leftarrow} &= 1.49454 \\
 \overline{G}_{\rightarrow} &= 1.49560 \\
 \Delta \overline{G}_H &= 0.00106 \\
 \overline{G}_{\swarrow} &= 1.49703 \\
 \overline{G}_{\searrow} &= 1.49728 \\
 \Delta \overline{G}_{P_d} &= 0.00025 \\
 \overline{G}_{\swarrow} &= 1.49602 \\
 \overline{G}_{\nearrow} &= 1.49841 \\
 \Delta \overline{G}_{S_d} &= 0.00239 \\
 \mu G_s &= 1.49659 \\
 K &= 0.17373
 \end{aligned}$$

Fig. 5.45. The measurements of spatial complexity measure, $\mu(G)s$, K and H for the generated patterns with various structural characteristics.

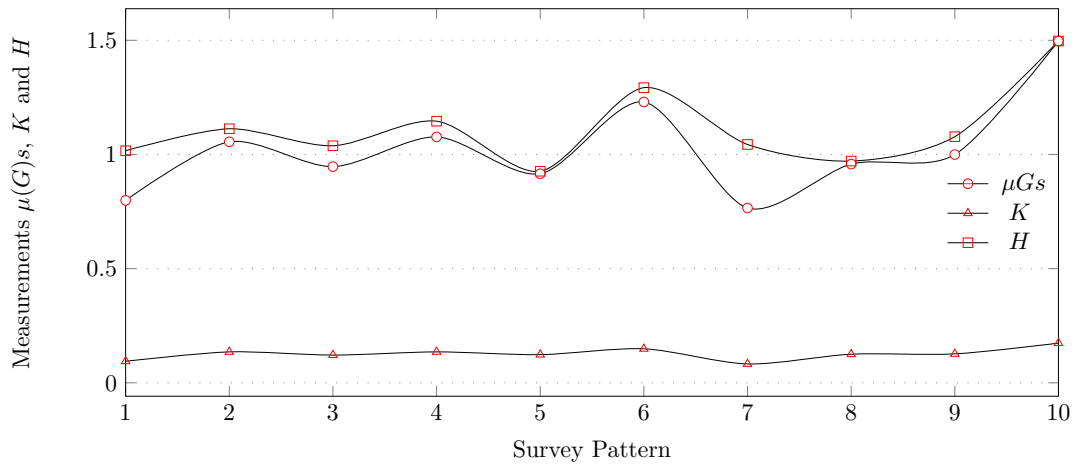


Fig. 5.46. The plot of $\mu(G)s$, K and H for the generated survey patterns.

5.3.3 Procedure

An online survey was designed with the 10 generated patterns ordered according to Fig. 5.47. A five-point Likert scale [200] was used to obtain quantitative measurements of the aesthetic judgements of respondents. The patterns were presented one at a time to the 100 participants with the following instructions:

The following 10 images have been generated by computers.

Please rate them in terms of their aesthetic appeal.

The participants were asked to rate how well they agreed with the following statement:

This image is aesthetically pleasing (beautiful).

The five-point Likert scale consisted of “Strongly Disagree (SD)”, “Disagree (D)”, “Neutral (N)”, “Agree (A)” and “Strongly Agree (SA)” rates.

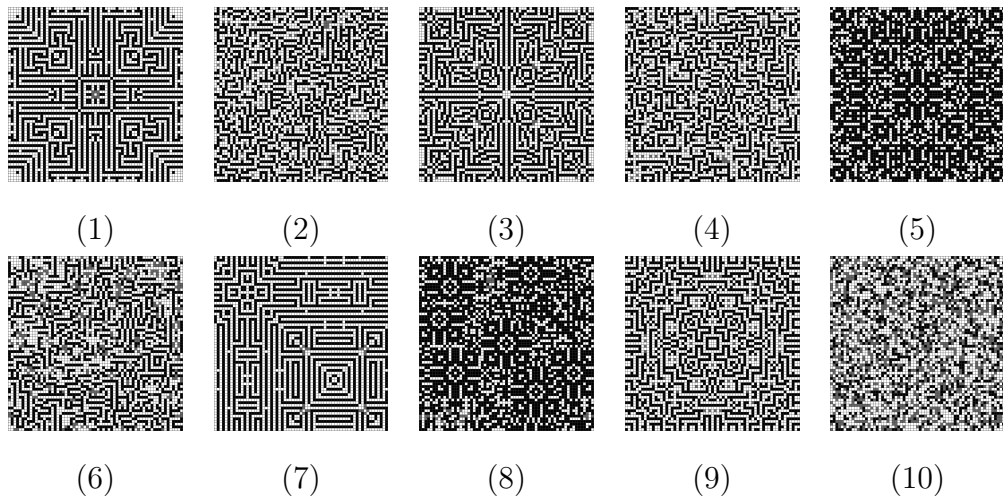


Fig. 5.47. The order of patterns used in the survey.

5.3.4 Results and Analysis

The online survey yielded 68 valid responses consisted of 25 males and 43 females with an age group distribution illustrated in table 5.9 and table 5.10 summarises the results of the survey.

| Age Group | | | | Gender | | |
|-----------|---------|---------|----|--------|--------|-------|
| 18 - 29 | 30 - 44 | 45 - 59 | 60 | Male | Female | Total |
| 17 | 16 | 26 | 9 | 25 | 43 | 68 |

Table 5.9: *The distribution of age groups and genders for 68 collected valid responses.*

| Pattern | SD | D | N | A | SA | Total |
|---------|----|----|----|----|----|-------|
| 1 | 7 | 21 | 17 | 17 | 6 | 68 |
| 2 | 23 | 35 | 10 | 0 | 0 | 68 |
| 3 | 4 | 14 | 19 | 26 | 5 | 68 |
| 4 | 22 | 37 | 8 | 1 | 0 | 68 |
| 5 | 19 | 5 | 20 | 20 | 4 | 68 |
| 6 | 25 | 33 | 8 | 2 | 0 | 68 |
| 7 | 5 | 24 | 20 | 13 | 6 | 68 |
| 8 | 7 | 30 | 19 | 11 | 1 | 68 |
| 9 | 4 | 9 | 20 | 26 | 9 | 68 |
| 10 | 30 | 22 | 13 | 3 | 0 | 68 |

Table 5.10: *The results of survey.*

Since Likert scale data are ordinal data (i.e. they only show that a rating is higher/lower than another and not the distance between the scales), the data must be aggregated across the collected data to ensure an accurate estimation of each scale's value for the patterns. In order to get an aggregated score (AScore) of the ratings, each of the scales were assigned a weight according to table 5.11.

| Scale | SD | D | N | A | SA |
|--------|----|---|---|---|----|
| Weight | 1 | 2 | 3 | 4 | 5 |

Table 5.11: *Assigned weight to each scale.*

The following formula was used to calculate the aggregated score of the five-point Likert scale for the survey:

$$AScore = \frac{1}{5} \sum N.W, \quad (5.27)$$

where N is the total number of ratings for each scale and W is the assigned weight to each scale. The highest possible aggregated score for a five-point Likert scale is $5 \times N$, while the lowest possible score is $1 \times N$. For example, given the total number of participants' responses to the statement of the survey from Table 5.10, assigned weight to each scale from table 5.11 and Eq. 5.27, the following calculation was performed to obtain the aggregated score for pattern one:

$$AScore \text{ for pattern one} = \frac{1}{5} \{(7 * 1) + (21 * 2) + (17 * 3) + (17 * 4) + (6 * 5)\} = 39.6.$$

Fig. 5.49 shows the individual aggregated scores for each of the 10 patterns and Fig. 5.48 illustrates the total ratings and the plot of the aggregated scores for the patterns. Fig. 5.50 shows the survey pattern arranged based on aesthetic judgement from the most aesthetically appealing (Fig. 5.50(1)) to the least aesthetically appealing (Fig. 5.50(10)).

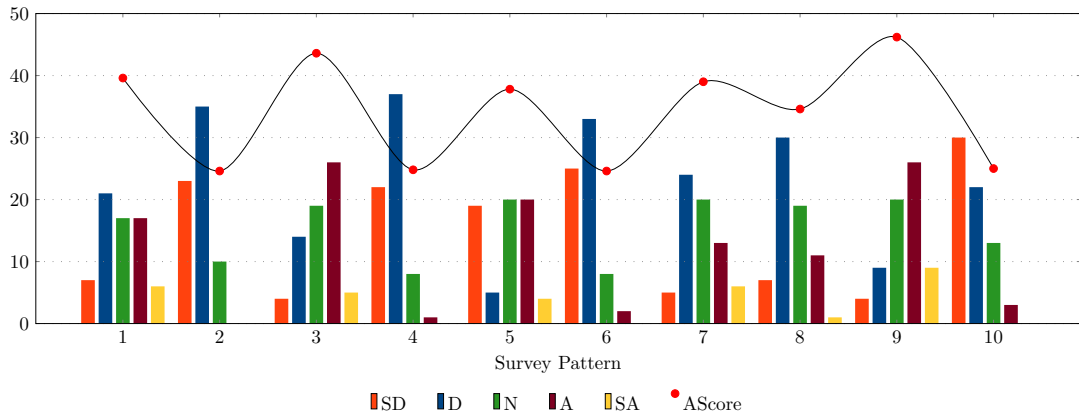


Fig. 5.48. The total ratings and the aggregated scores for the patterns.

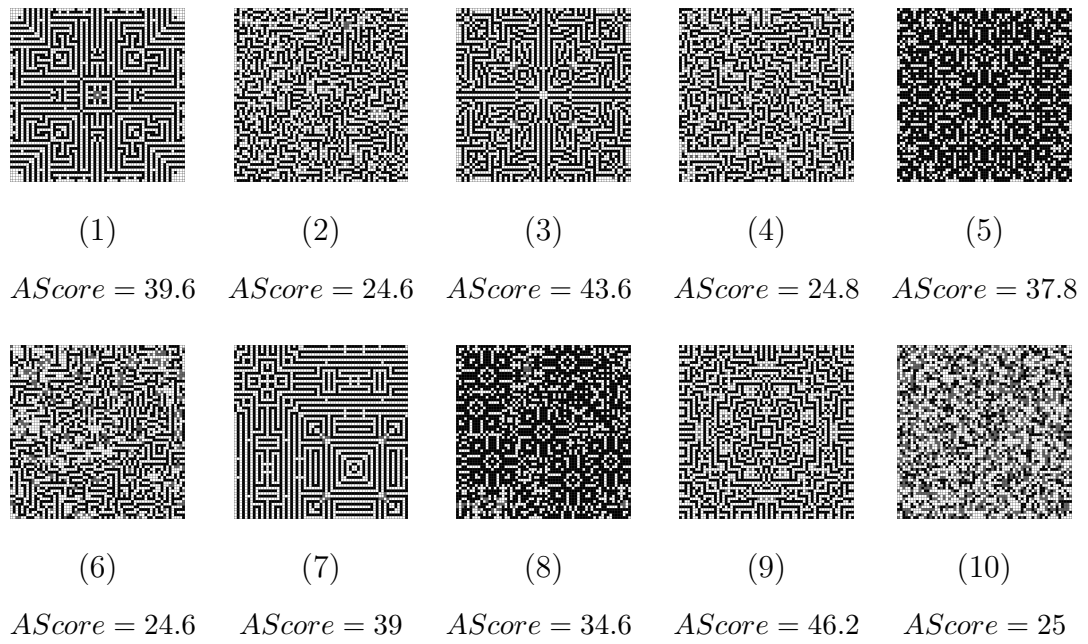


Fig. 5.49. *The aggregated scores of survey patterns.*

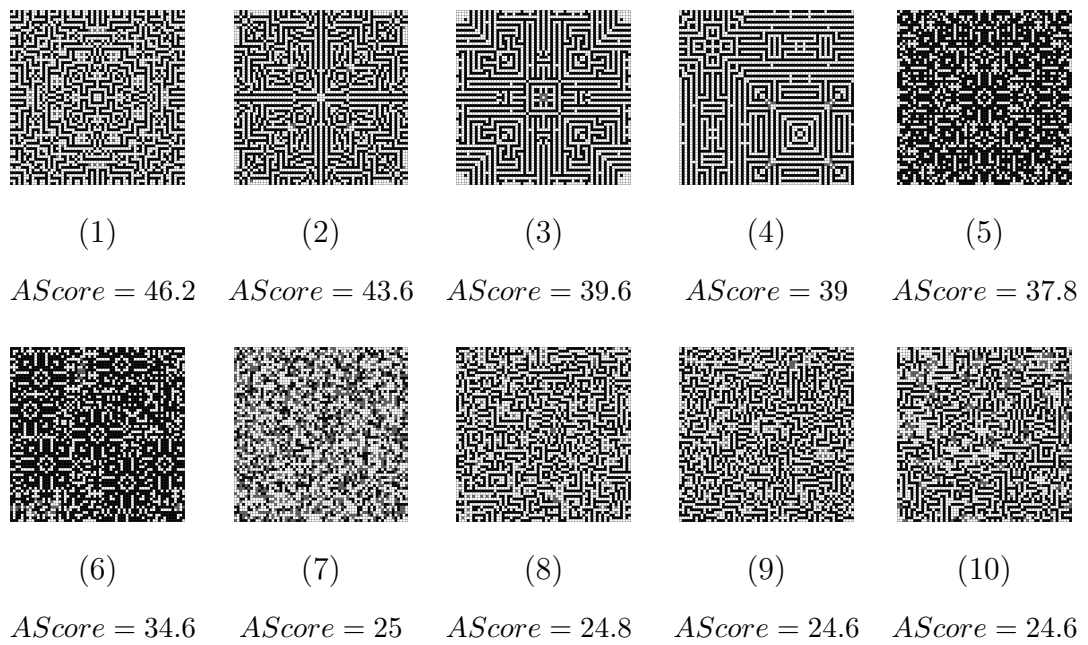


Fig. 5.50. *The arrangement of patterns in descending order of their aggregated scores.*

Due to the ordinal nature of data, a non-parametric Spearman rank correlation (r_s) [201] was applied for the analysis of data with a significance level of $\alpha = 0.05$. Table 5.12 shows the results of the rank correlation test between the aggregated scores and the measurements of μGs , K and H .

| | μGs | K | H |
|----------|----------|---------|---------|
| $AScore$ | -0.6383 | -0.6859 | -0.5288 |
| p | 0.04702 | 0.02852 | 0.11599 |

Table 5.12: *The results of Spearman rank correlation test (r_s) between μGs , K , H and the aggregated scores of survey patterns.*

The value of r_s for μGs is -0.6383 and the 2-tailed $p = 0.04702 < 0.05$. Thus, there is a *negative linear correlation* between μGs and the aggregated scores and the association between the two variables is *statistically significant*. The value of r_s for K is -0.6859 and the 2-tailed value of $p = 0.02852 < 0.05$. Therefore, there is a *negative linear correlation* between K and the aggregated scores and the association between the two variables is *statistically significant*. The value of r_s for H is -0.5288 and the 2-tailed value of $p = 0.11599 > 0.05$. As such, the association between the two variables is *not statistically significant*. Considering the values of r_s for the Spearman rank correlation and regression analysis, the following conclusions can be drawn:

There is a statistically significant relationship between the measurement of $\mu(G)s$ for CA-generated patterns and human aesthetic judgement and the direction of the relationship is negative.

There is a statistically significant relationship between the estimation of K for CA-generated patterns and human aesthetic judgement and the direction of the relationship is negative.

There is no statistically significant relationship between the measurement of H for CA-generated patterns and human aesthetic judgement.

Therefore, hypotheses **H1** and **H2** are accepted and hypothesis **H3** is rejected for the experiment conducted with CA-generated patterns.

5.4 Discussions

One of the major challenges in computational notions of aesthetics and generative art is the development of a quantitative model which conforms to human intuitive perceptions of aesthetic. As discussed in Chapters 3 and 4, informational theories of aesthetics based on the measurements of entropy have failed to discriminate structurally different patterns in a 2D plane. Consequently, spatial complexity (G) and Kolmogorov complexity (K) were suggested for quantifying the spatial complexity of 2D patterns.

The main purpose of the experimentations in this chapter was to examine the relationship between the measurements of G and K and human aesthetic judgement. Since entropy (H) has emerged as a dominant measure of order and complexity in computational notions of aesthetics, we compared its relation with human aesthetic judgement as well. Three hypotheses were evaluated by conducting two sets of experimentations (I and II).

The first experiment, in which 252 symmetrical and asymmetrical stimulus patterns were adopted from an empirical study of human aesthetic judgement reported in [199], showed that there were *no statistically significant correlation* between μGs , K , and H and the 252 symmetrical and asymmetrical stimulus patterns. The current results of experiment I are in contrast to our previous study in [202], which showed *a strong positive correlation* between μGs and mean aesthetic judgements. The main reason for this discrepancy is the number of available stimulus patterns (12 patterns) for the measurements of μGs at the time of previous experimentation.

For the second experiment, a set of CA-generated patterns with various structural properties reflecting the spectrum of spatial complexity (section 4.1), was used to examine the relationship between the measurements of $\mu(G)s$, K and H and human aesthetic judgement. The results of the survey showed that there is a statistically significant negative linear relationship between the measurement of $\mu(G)s$ and K for CA-generated pattern and human aesthetic judgement. On the other hand, the results of experiment II failed to show any statistically significant relationship between the measurement of H and human aesthetic judgement for CA-generated patterns.

6. Conclusion

This chapter summarises the work of the thesis in relation to the objective of investigating computational notions of aesthetics in the framework of multi-state 2D CA. The broad aim of this thesis was to address aesthetic problems within the framework of 2D CA by investigating the possibility of formulating a complexity measure for aesthetic evaluation of CA-generated patterns.

A review of the findings is presented where we summarise the avenues that have been provisionally investigated as exploratory steps for further research in the broad domain of informational theories of aesthetics and quantifying spatial complexity utilising several measures, including spatial complexity measure and Kolmogorov complexity. Additionally, possibilities for future research and applications are also presented.

This thesis lays the foundation of the work by providing a literature review into the various aspects of generating interesting imagery with 2D CA, cellular automata art, and informational theories of aesthetics. This is then followed by several experiments demonstrating the aims of the thesis.

The concept of cellular automaton, one of the early biologically inspired systems, has contributed to the creation of many forms of computer art. The popularity of the GoL drew the attention of the wider community of digital artists and designers to the unexplored potential of CA in generating rich digital content from the iteration of simple deterministic rules. The machinery of CA is based on the local interaction of each automaton with its immediate neighbourhood automata according to a set of rules. The interaction of automata at a local level generates the emergent behaviour, sometimes with attractive complexity, at the global level. The main characteristics of CA that make them particularly interesting to digital artists are their ability to generate visually appealing and very complex patterns on the basis

of very simple rules. Also, the lattice of CA represents each automaton as picture element interacting with neighbouring automata making them a suitable framework for generating computer graphics with unique characteristics.

Chapter 2 covered the historical development of automata devices and CA. Formal definitions provided with an analysis of CA behaviour followed by a review of some applications. Chapter 3 covered a review of historical background on experimental aesthetics, the association of the order and complexity of stimuli with aesthetic judgements, the computational models derived from Birkhoff's aesthetic measure and informational theories of aesthetics.

In Chapter 4 by comparing the structural characteristics of CA patterns with their corresponding entropy values, we showed that despite their structural differences, all of the patterns had the same entropy value. In other words, entropy was invariant to the spatial arrangement of the composing elements of 2D patterns.

Although Shannon's entropy is dominant in computational notions of aesthetics, it failed to accurately discriminate structurally different patterns in two dimensions. The failing of entropy, as a measure of order and complexity, to reflect the structural characteristics of 2D patterns, is caused by its inclination to measure the distribution of symbols and not their arrangements. Therefore, it was possible to generate radically different patterns (structurally different 2D patterns) with the same entropy.

This observation was in contrast to our intuitive perception of the complexity of patterns. Therefore, taking into account our intuitive perception of complexity and the structural characteristics of 2D CA patterns, we proposed a conceptual model as *spectrum of spatial complexity* (4.15). Then we argued that a complexity measure must be bounded by two extreme points of complete *order* and *disorder*. Also, we assumed that *regular structures*, *irregular structures* and *structureless* patterns lie between these extremes. The conceptual model facilitated the mapping of the complexity of 2D patterns based on their structural characteristics between the two extremes of order and disorder.

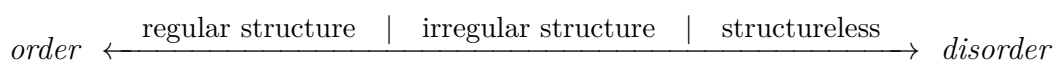


Fig. 6.51. *The spectrum of spatial complexity.*

For the purpose of measuring the complexity of CA behaviour, particularly with multi-state structures, we developed the *spatial complexity measure* and extended

the algorithmic information theory of Kolmogorov for estimating the complexity of patterns in 2D plane.

The spatial complexity measure based on *information gain* and has been proposed as a means of characterising the complexity of dynamical systems and of 2D patterns [54, 55, 56]. We defined spatial complexity measure as the following:

A spatial complexity measure of a cellular automaton configuration is the sum of the mean information gains of cells having homogeneous/heterogeneous neighbouring cells over a lattice.

Kolmogorov attributed the algorithmic complexity of an object to the minimum length of a program such that a universal computer can generate a specific sequence [57]. Kolmogorov complexity is related to entropy ($H(X)$), in that the expected value of $K(x)$ for a random sequence is approximately the entropy of the source distribution for the process generating the sequence. However, Kolmogorov complexity differs from entropy in that it relates to the specific string being considered rather than the source distribution [197, 179]. Random strings have rather high Kolmogorov complexity - on the order of their length, as patterns cannot be discerned to reduce the size of a program generating such a string. On the other hand, strings with a high degree of structure have fairly low complexity. The main difficulty with Kolmogorov complexity is that it is uncomputable. Any program that produces a given string is an upper bound on the Kolmogorov complexity for this string, but it is not possible to compute the lower bound.

Lempel and Ziv defined a measure of complexity for finite sequences rooted in the ability to produce strings from simple copy operations [198]. This method, known as *LZ78* universal compression algorithm, harnesses this principle to yield a universal compression algorithm that can approach the entropy of an infinite sequence produced by an ergodic source. As such, *LZ78* compression has been used as an estimator for K . In order to estimate the K value of 2D configurations generated by multi-state 2D CA, we generated linear strings of configurations by means of six different templates (Fig. 4.17). Then, using the *LZ78* compression algorithm, the upper bound of K was estimated as the lowest value among the six different templates.

A set of experiments was conducted to examine the effectiveness of the models in discriminating the particular configurations that were generated by a multi-state

2D cellular automaton. The results of experiments exhibited the potential of spatial complexity measure in discriminating symmetries and the orientation of CA generated patterns, making more accurate measurements of complexity in relation to aesthetic evaluation functions. Furthermore, it was observed that K is able to discriminate the complexity of patterns; however, it failed to discriminate the spatial orientations. In addition, the experiments showed a strong positive correlation between Kolmogorov complexity and spatial complexity measures.

In Chapter 5, details of two experiments and their results on the correlation between three measures, namely spatial complexity measure ($\mu(G)s$), Kolmogorov complexity (K) and entropy (H), and human aesthetic judgement were reported.

In the first experiment, 252 experimental stimulus patterns were adopted from an empirical study of human aesthetic judgement of 2D symmetrical and asymmetrical patterns ranked based on their aesthetic judgements. This paved the way for an exploration of any possible relationship between human aesthetic judgement and the measurements of $\mu(G)s$, K and H . The benchmark of 252 experimental stimulus patterns, established symmetry as the most important stimulus feature predicting participants' aesthetic judgements.

Participants exhibited a general agreement that the symmetrical patterns were more beautiful than the asymmetrical ones. Therefore, the judgement analysis supported the hypothesis that symmetry and complexity are important factors in aesthetic judgements. Using the same set of experimental stimulus patterns, this time fed into the aforementioned measurements, it is demonstrated that there are no statistically significant correlations between $\mu(G)s$, K , and H and the 252 symmetrical and asymmetrical stimulus patterns. Given that the measures were primarily developed for CA-generated patterns, the measures failed to distinguish the complexity of 252 stimuli in relation to their aesthetic rankings.

For the second experiment, a set of CA-generated patterns with various structural properties reflecting the spectrum of spatial complexity, was used to examine the relationship between the measurements of $\mu(G)s$, K and H and human aesthetic judgement. The experiment furthers the above mentioned analysis by using an online survey designed and used to compare the aesthetic values of a set of 2D patterns with various structural properties generated by seeding CA with the measurements of $\mu(G)s$, K and H .

There is a statistically significant relationship between the measurement of $\mu(G)s$ for CA-generated patterns and human aesthetic judgement and the direction of the relationship is negative.

There is a statistically significant relationship between the estimation of K for CA-generated patterns and human aesthetic judgement and the direction of the relationship is negative.

There is no statistically significant relationship between the measurement of H for CA-generated patterns and human aesthetic judgement.

The result of this experiment highlighted the presence of a statistically significant negative linear relationship between the measurement of $\mu(G)s$ and K for CA-generated pattern and human aesthetic judgement. On the other hand, the result of second experiment failed to show statistically significant relationship between the measurement of H and human aesthetic judgement for CA-generated patterns.

The implications of these findings is that both spatial complexity measure and Kolmogorov complexity are conforming to the human aesthetic judgement but with an inverse direction. It contradicts the assumption of this thesis where we considered direct relationship between stimulus complexity and aesthetic preference. However, it confirms the validity of theories which consider *inverse* relationship between stimulus complexity and aesthetic preference (i.e. Birkhoff's aesthetic).

Furthermore, considering the general hypotheses of this thesis (section 1.4), we can accept both of the hypotheses and draw the following conclusions:

1. The aesthetic value of a cellular automaton pattern depends on the sum of mean information gains of cells having homogeneous/heterogeneous neighbouring cells over the lattice of a cellular automaton.
2. The aesthetic value of a cellular automaton pattern depends on the estimation of the Kolmogorov complexity of a cellular automaton pattern.

In addition, the proposed models of complexity were able to meet the following criteria:

The measure uses only information available within the framework of 2D CA, such as the number of cells and their states, size of lattice and neighbourhood

template. This constraint considers the generated patterns of CA to be internal objects of CA environment.

The measure reflects on the structural characteristics of CA patterns (i.e. homogeneity/heterogeneity of cells and their spatial distribution over the lattice of CA).

These results could potentially provide researchers with a direction for future aesthetics analysis of CA-generated patterns using $\mu(G)s$ and K , both of which exhibited a noticeable relationship with human aesthetic judgement. The proposed models can be applied for the aesthetic evaluation of other types of imageries with applications in the area of image processing, image aesthetic enhancement, multimedia content creation, computer generated aesthetics and art.

6.1 Further Directions

The following are identified amongst possible future research topics:

The work of this thesis was limited to 2D models of CA with square cells. Other models, such as 3D CA or CA with different primitive cells (e.g. hexagonal cells) can be explored for the generation of patterns and evaluation of their aesthetic qualities with proposed models of complexities.

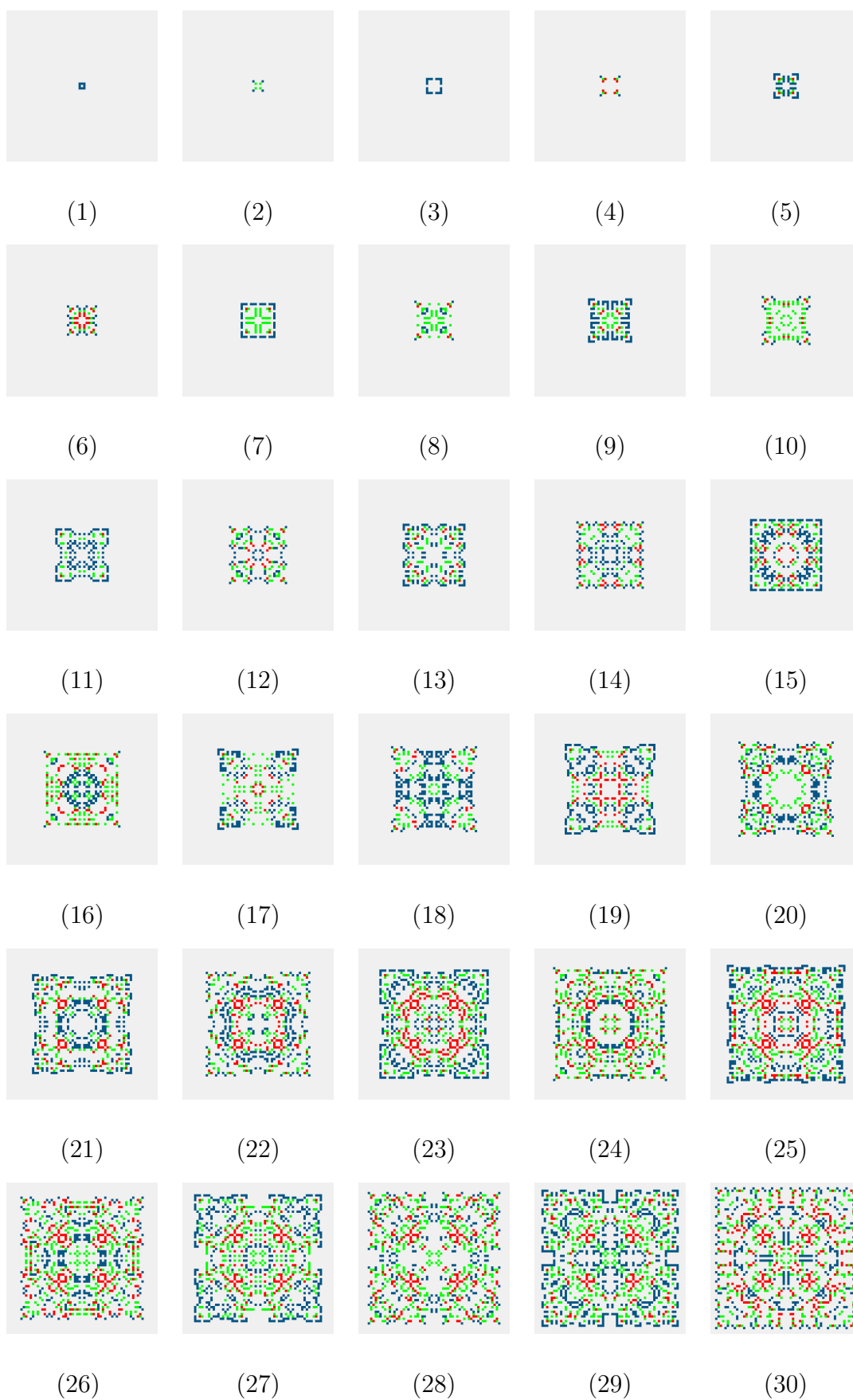
The generated experimental stimuli were limited to grey scale colours to isolate colour preferences in aesthetic judgements. Colour preference theories can be utilised to evaluate the aesthetic qualities of polychromatic CA-generated patterns.

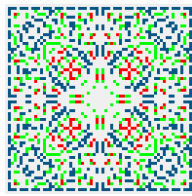
The models of CA which were used in this thesis were limited to 8-cell neighbourhoods. Other neighbourhood templates (e.g. 4, 5, 9 cells) with asynchronous and stochastic updates can be used for the generation of pattern and then evaluated for their aesthetic values using spatial complexity measure and Kolmogorov complexity measure.

The automation of aesthetic evaluation and selection processes in a way which is capable of making aesthetic judgements conforming to human aesthetic perception is fundamental to computational notions of aesthetics. And the ultimate goal of computational aesthetics is to close the loop of generation and evaluation where both processes are functions of computational methods. Since the spatial complexity and Kolmogorov complexity measures conformed to some degree to human aesthetic judgement, these models have the potential to be integrated with generative tools to partially “replace humans” in the process of generation and in the evaluation of computational aesthetics.

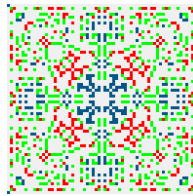
Appendices

A Space-Time Diagrams of Cellular Automaton 4.6

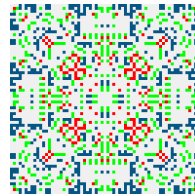




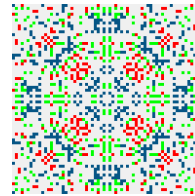
(31)



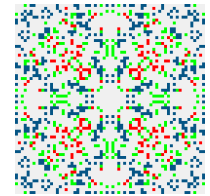
(32)



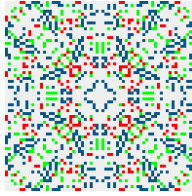
(33)



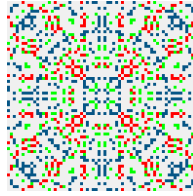
(34)



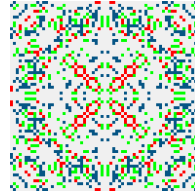
(35)



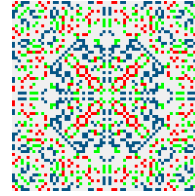
(36)



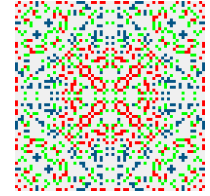
(37)



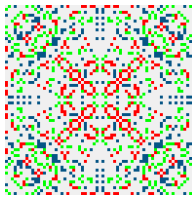
(38)



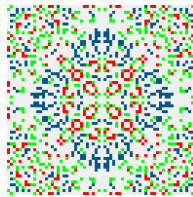
(39)



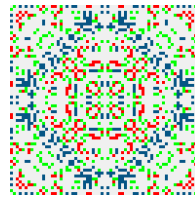
(40)



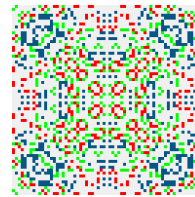
(41)



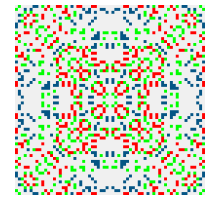
(42)



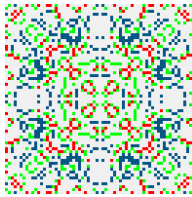
(43)



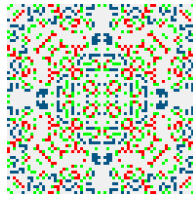
(44)



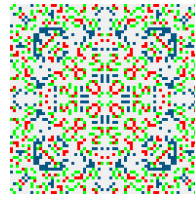
(45)



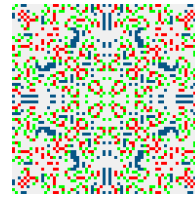
(46)



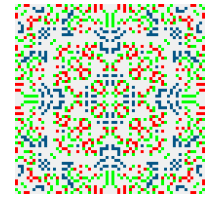
(47)



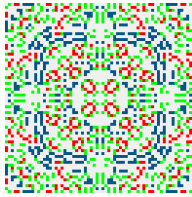
(48)



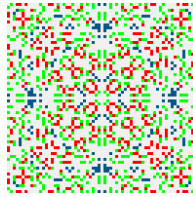
(49)



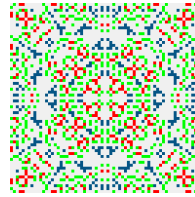
(50)



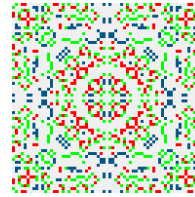
(51)



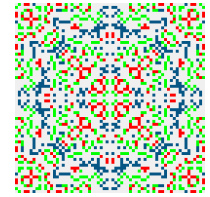
(52)



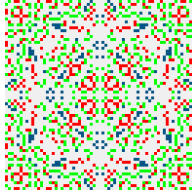
(53)



(54)



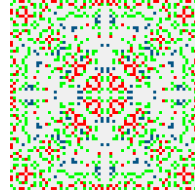
(55)



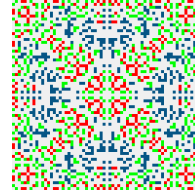
(56)



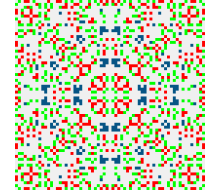
(57)



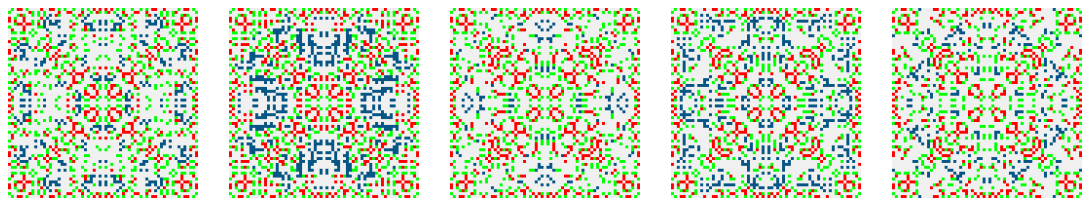
(58)



(59)



(60)



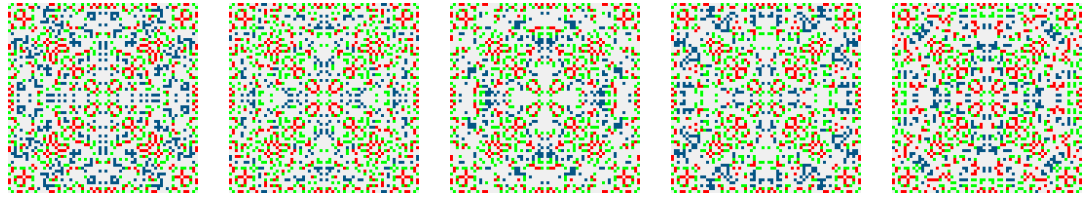
(61)

(62)

(63)

(64)

(65)



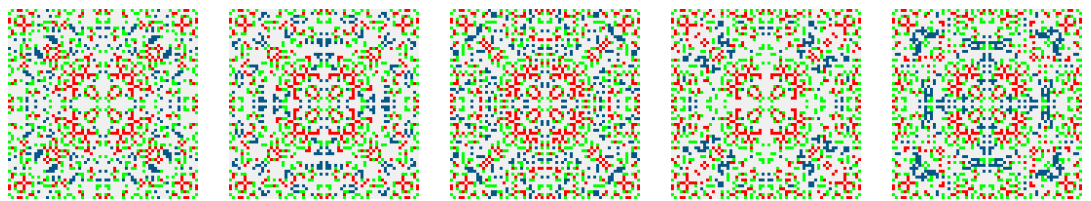
(66)

(67)

(68)

(69)

(70)



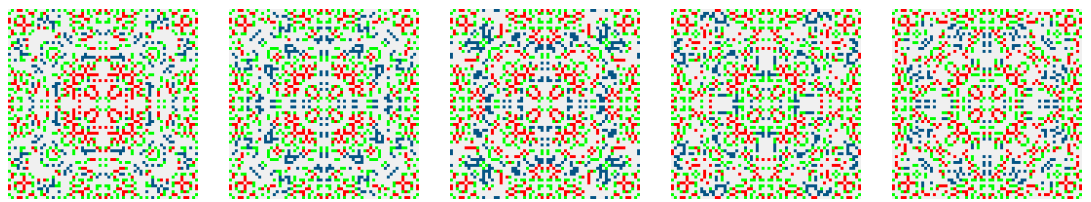
(71)

(72)

(73)

(74)

(75)



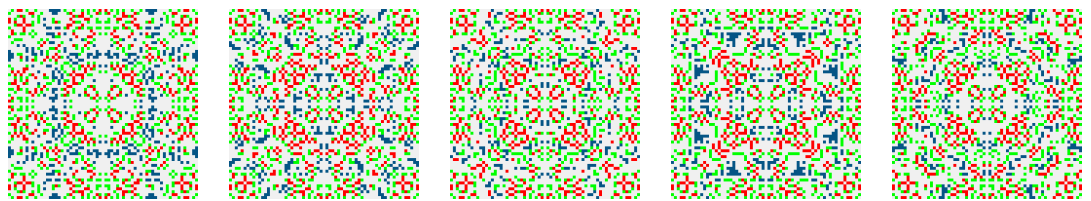
(76)

(77)

(78)

(79)

(80)



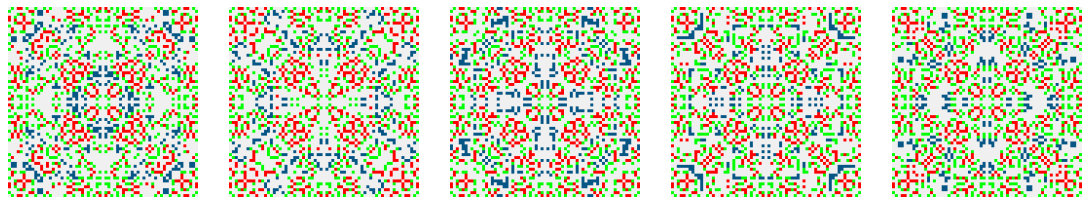
(81)

(82)

(83)

(84)

(85)



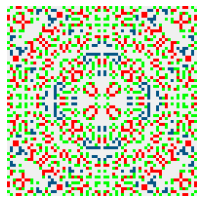
(86)

(87)

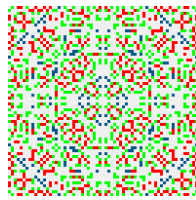
(88)

(89)

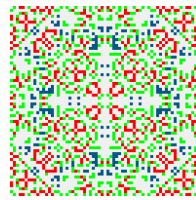
(90)



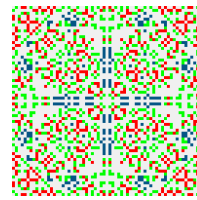
(91)



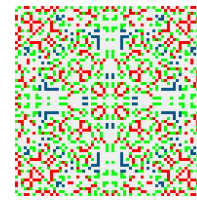
(92)



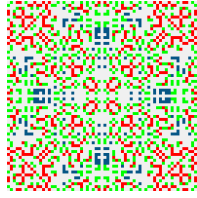
(93)



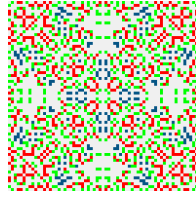
(94)



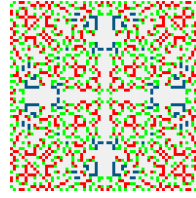
(95)



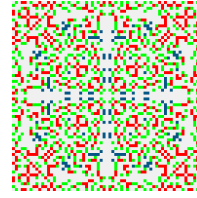
(96)



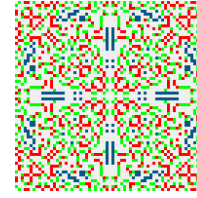
(97)



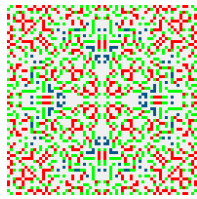
(98)



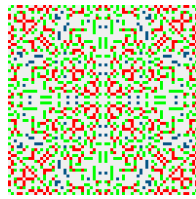
(99)



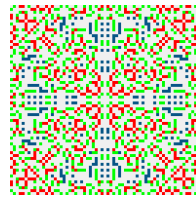
(100)



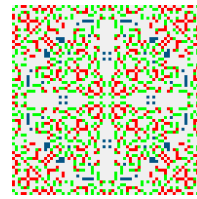
(101)



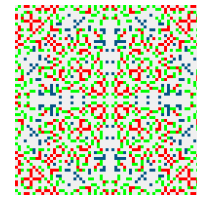
(102)



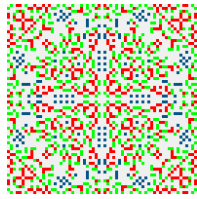
(103)



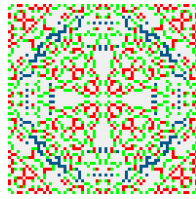
(104)



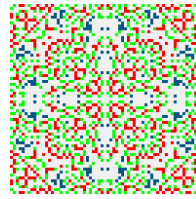
(105)



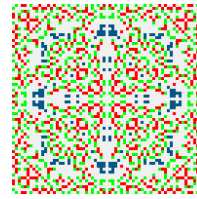
(106)



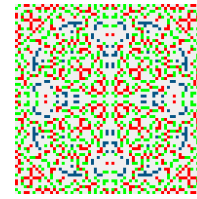
(107)



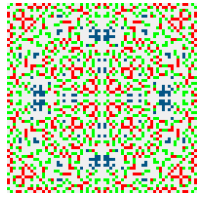
(108)



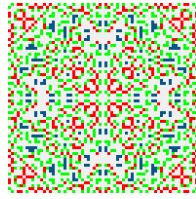
(109)



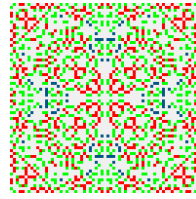
(110)



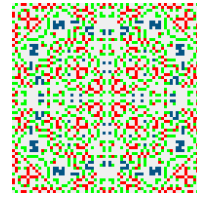
(111)



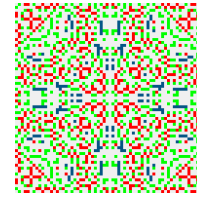
(112)



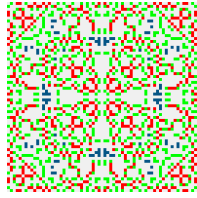
(113)



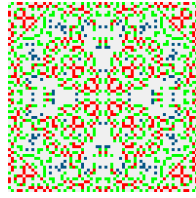
(114)



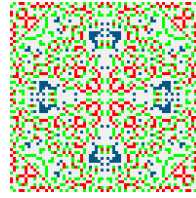
(115)



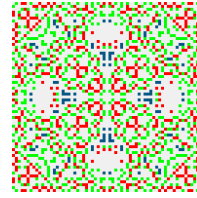
(116)



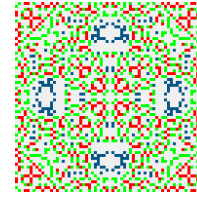
(117)



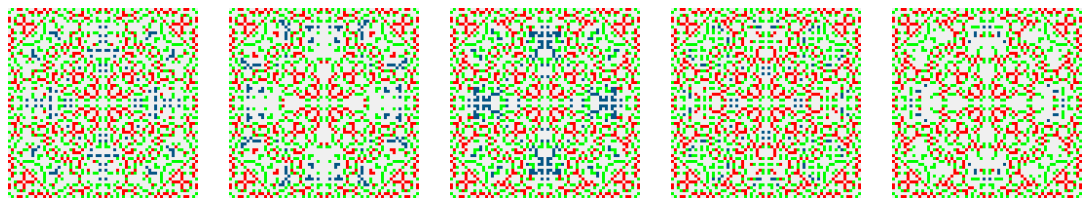
(118)



(119)



(120)



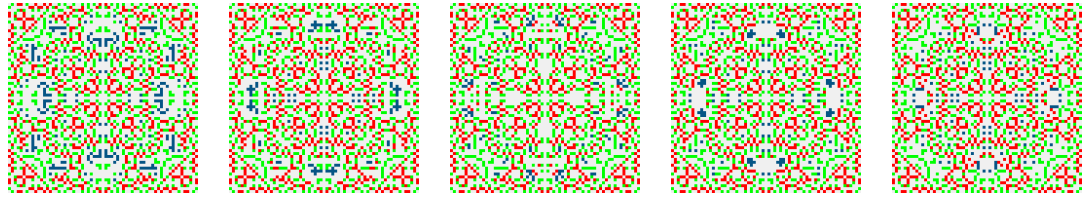
(121)

(122)

(123)

(124)

(125)



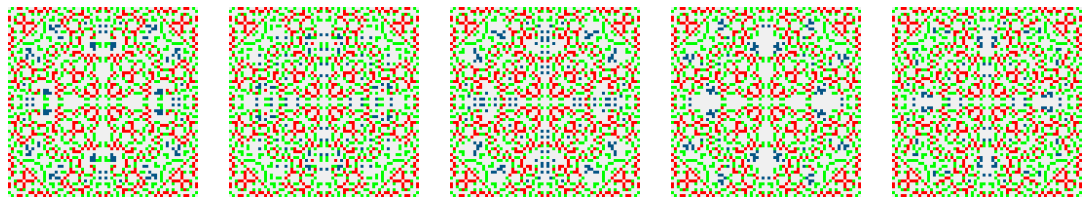
(126)

(127)

(128)

(129)

(130)



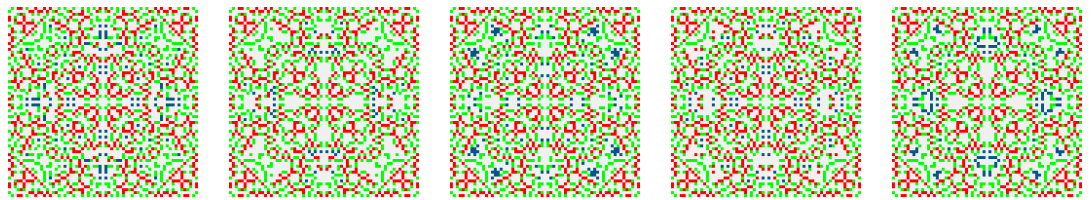
(131)

(132)

(133)

(134)

(135)



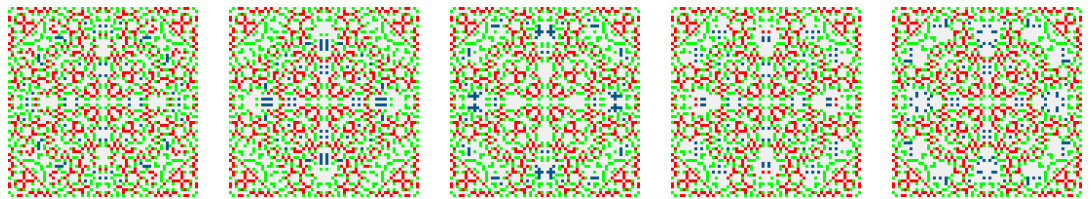
(136)

(137)

(138)

(139)

(140)



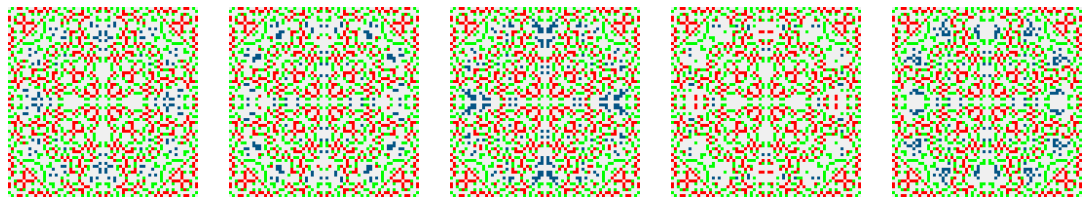
(141)

(142)

(143)

(144)

(145)



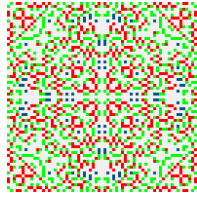
(146)

(147)

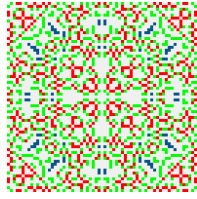
(148)

(149)

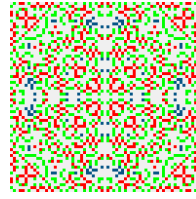
(150)



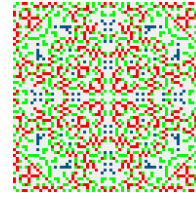
(151)



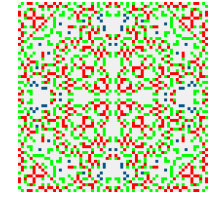
(152)



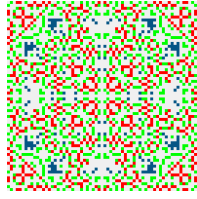
(153)



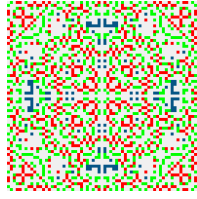
(154)



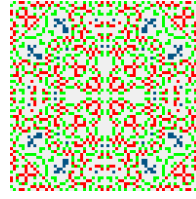
(155)



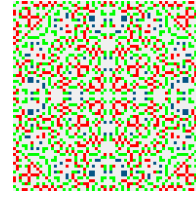
(156)



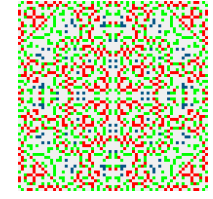
(157)



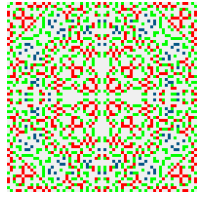
(158)



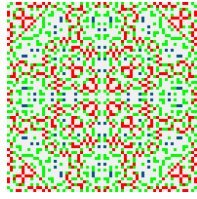
(159)



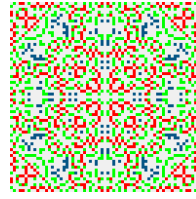
(160)



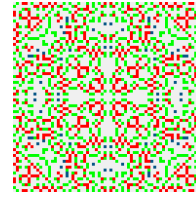
(161)



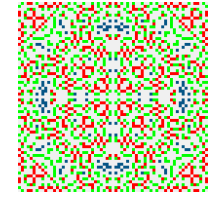
(162)



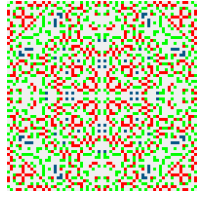
(163)



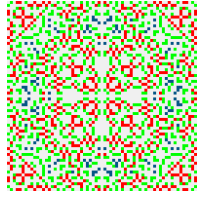
(164)



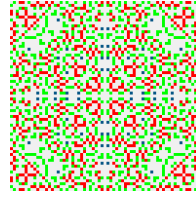
(165)



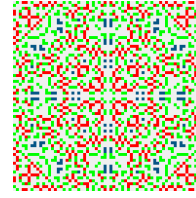
(166)



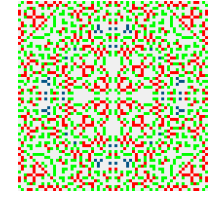
(167)



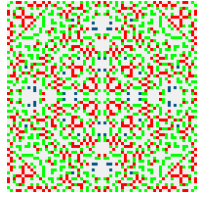
(168)



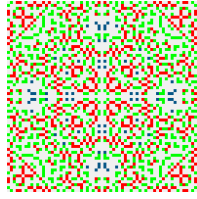
(169)



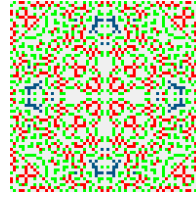
(170)



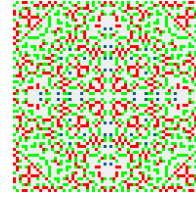
(171)



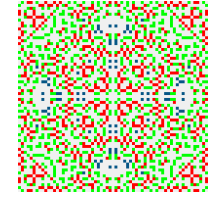
(172)



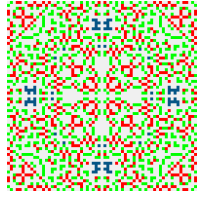
(173)



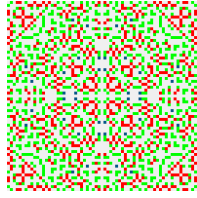
(174)



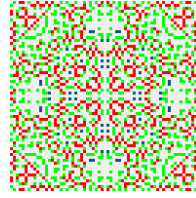
(175)



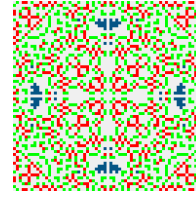
(176)



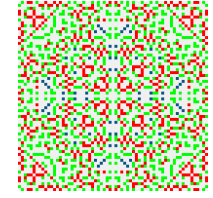
(177)



(178)



(179)



(180)

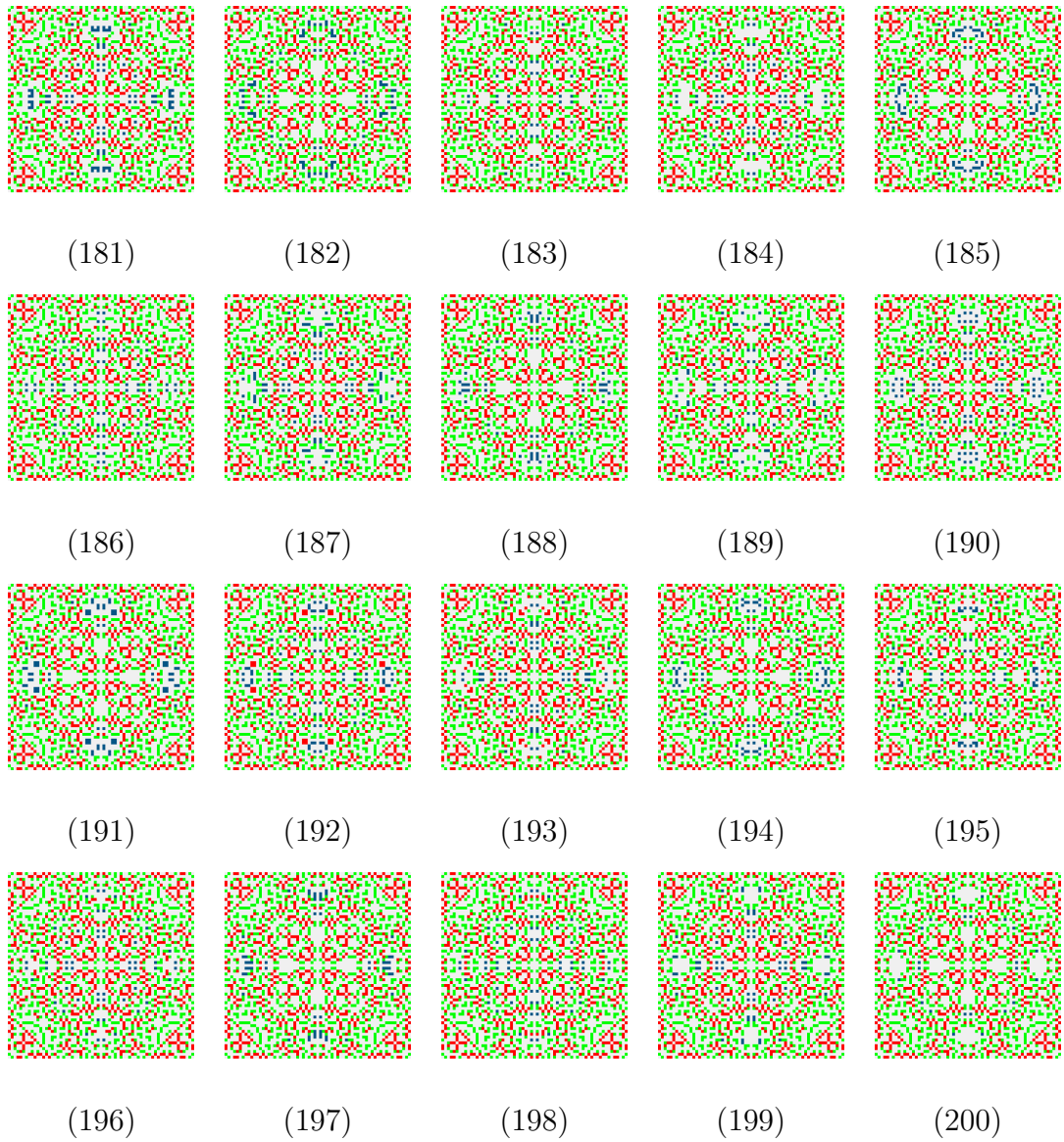
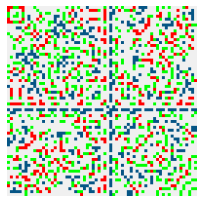
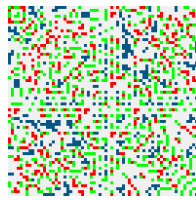


Fig. A.1. *The space-time diagram of cellular automaton 4.6 for 200 time steps starting from the single cell IC (4.19(a)).*

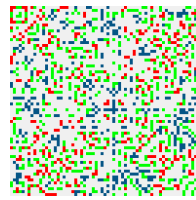




(31)



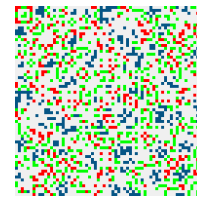
(32)



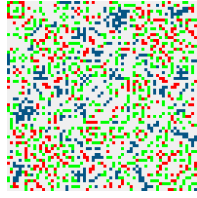
(33)



(34)



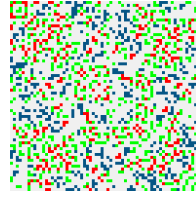
(35)



(36)



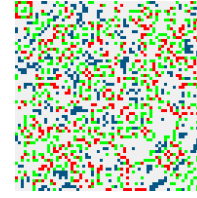
(37)



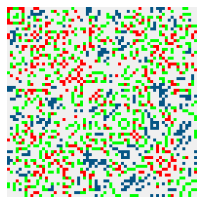
(38)



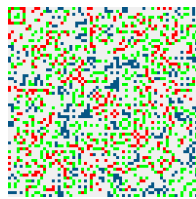
(39)



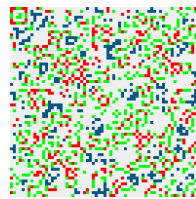
(40)



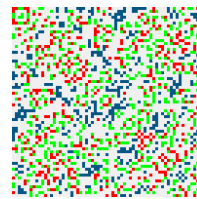
(41)



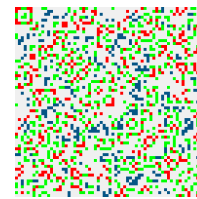
(42)



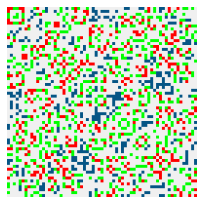
(43)



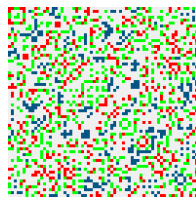
(44)



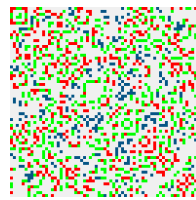
(45)



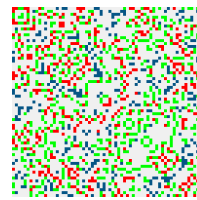
(46)



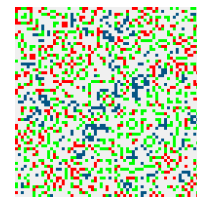
(47)



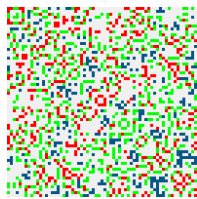
(48)



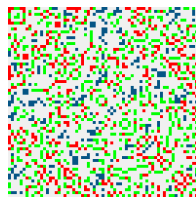
(49)



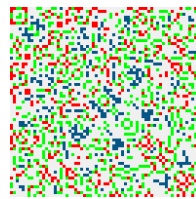
(50)



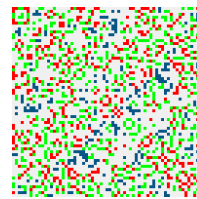
(51)



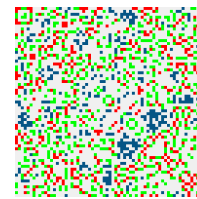
(52)



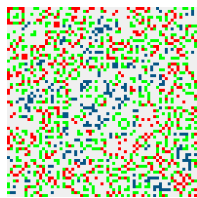
(53)



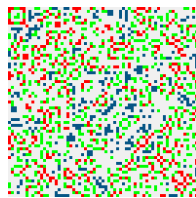
(54)



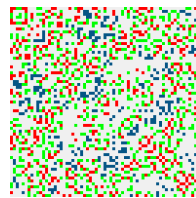
(55)



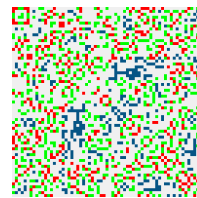
(56)



(57)



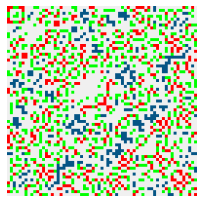
(58)



(59)



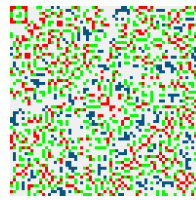
(60)



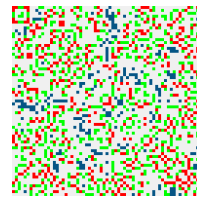
(61)



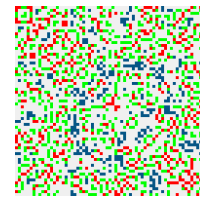
(62)



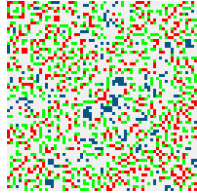
(63)



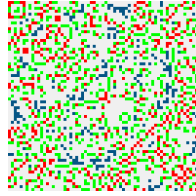
(64)



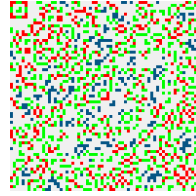
(65)



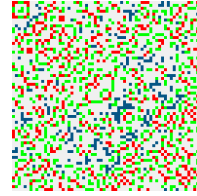
(66)



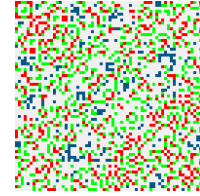
(67)



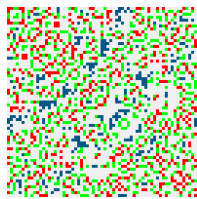
(68)



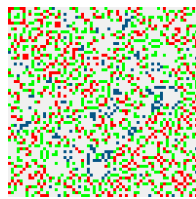
(69)



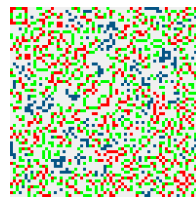
(70)



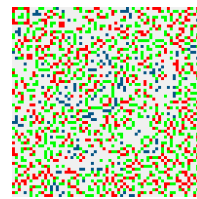
(71)



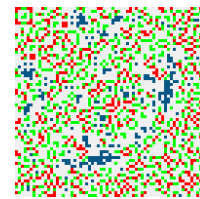
(72)



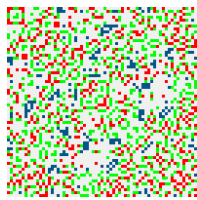
(73)



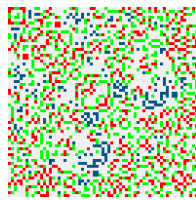
(74)



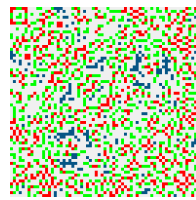
(75)



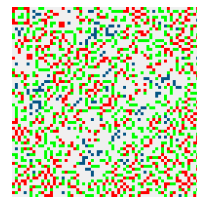
(76)



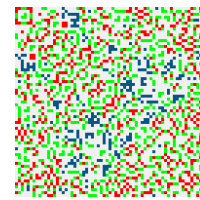
(77)



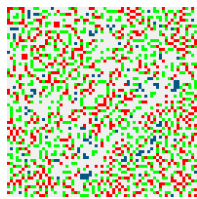
(78)



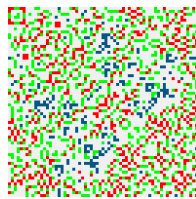
(79)



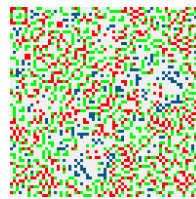
(80)



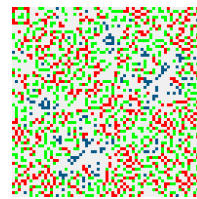
(81)



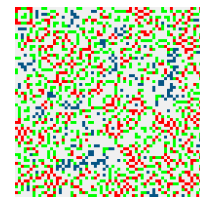
(82)



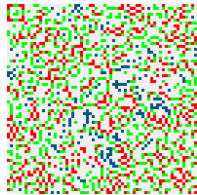
(83)



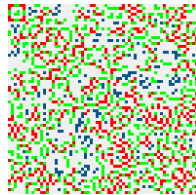
(84)



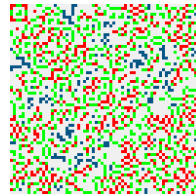
(85)



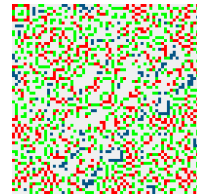
(86)



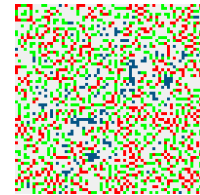
(87)



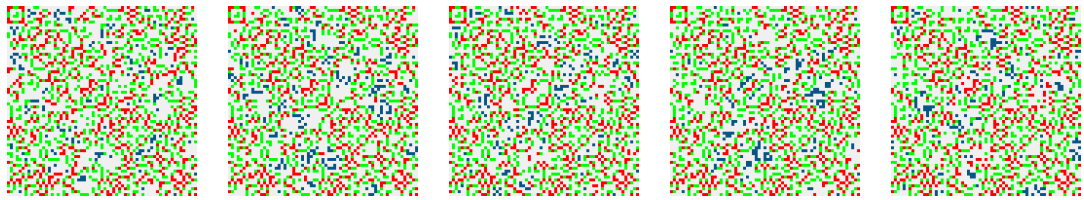
(88)



(89)



(90)



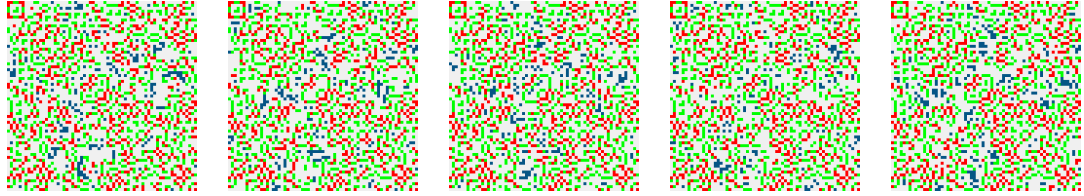
(91)

(92)

(93)

(94)

(95)



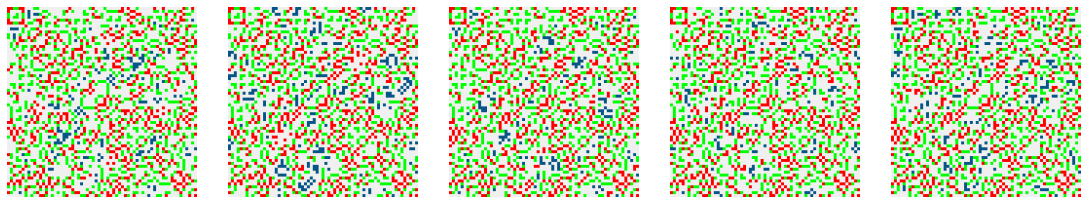
(96)

(97)

(98)

(99)

(100)



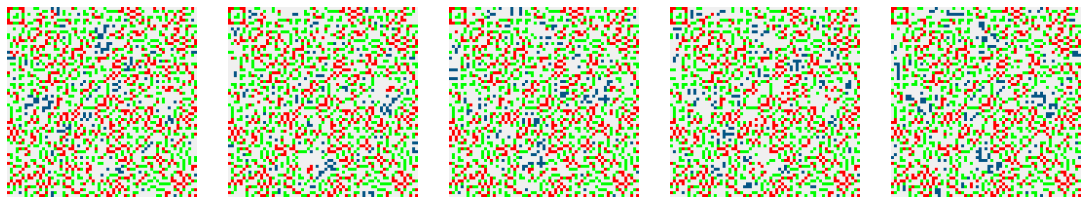
(101)

(102)

(103)

(104)

(105)



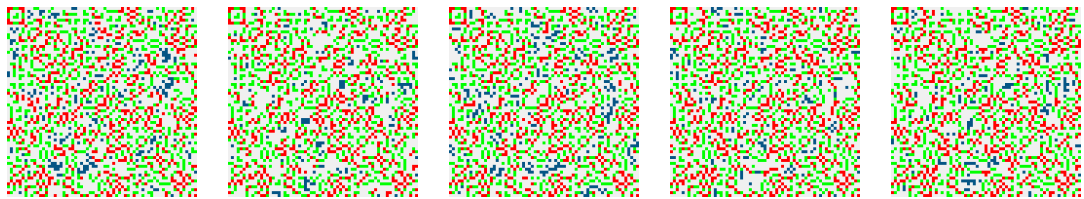
(106)

(107)

(108)

(109)

(110)



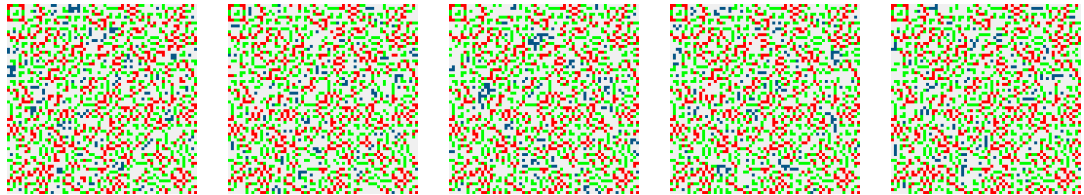
(111)

(112)

(113)

(114)

(115)



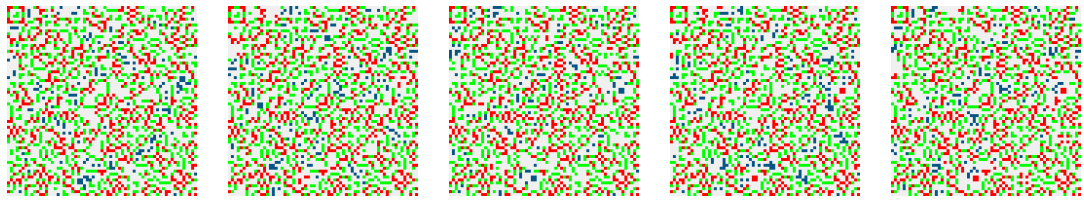
(116)

(117)

(118)

(119)

(120)



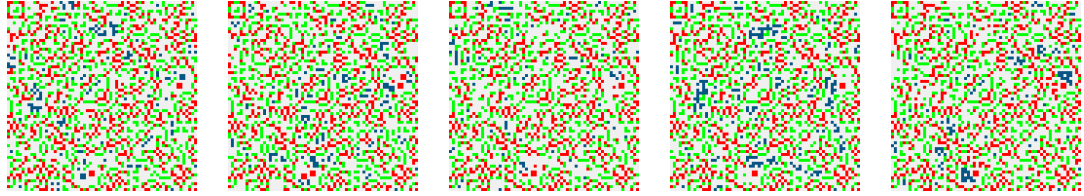
(121)

(122)

(123)

(124)

(125)



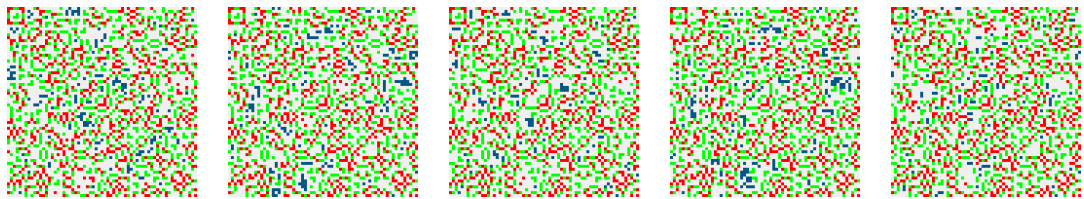
(126)

(127)

(128)

(129)

(130)



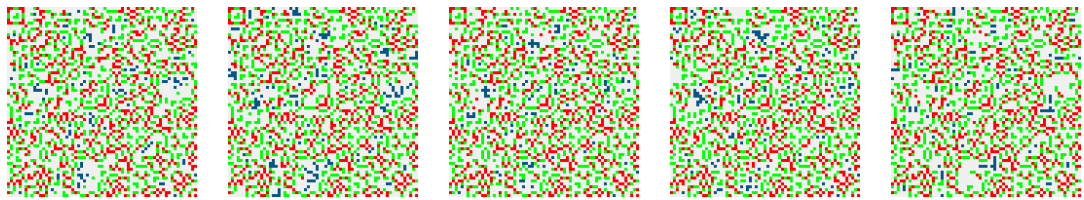
(131)

(132)

(133)

(134)

(135)



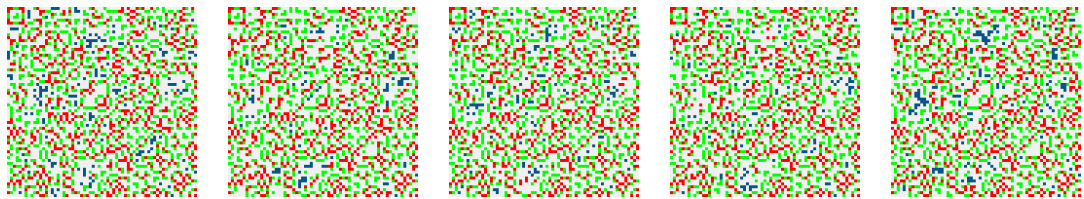
(136)

(137)

(138)

(139)

(140)



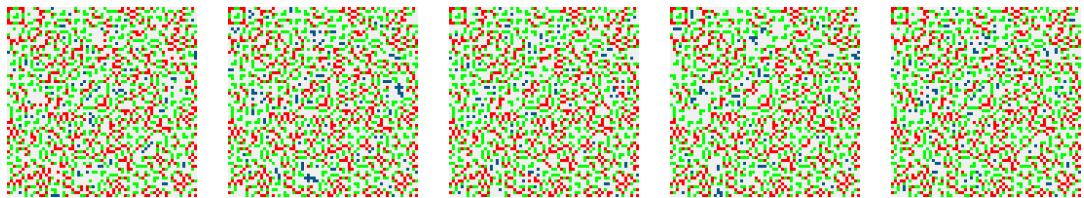
(141)

(142)

(143)

(144)

(145)



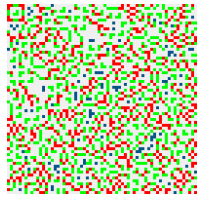
(146)

(147)

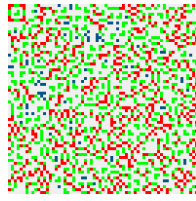
(148)

(149)

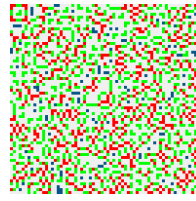
(150)



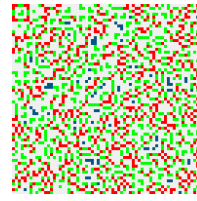
(151)



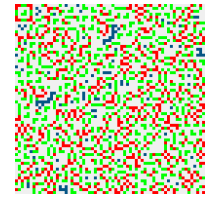
(152)



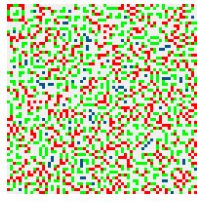
(153)



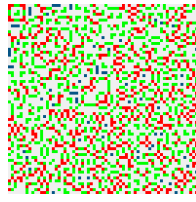
(154)



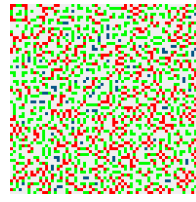
(155)



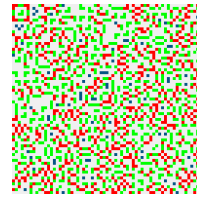
(156)



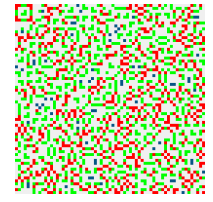
(157)



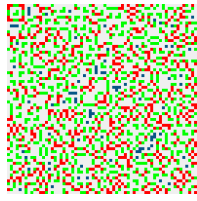
(158)



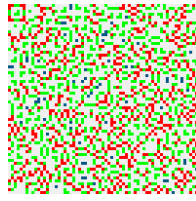
(159)



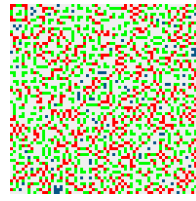
(160)



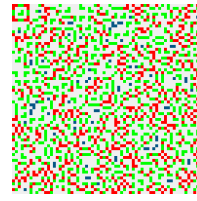
(161)



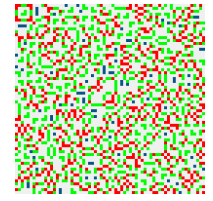
(162)



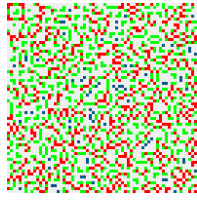
(163)



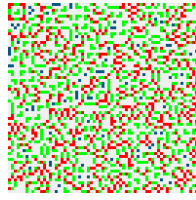
(164)



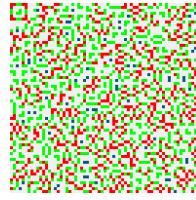
(165)



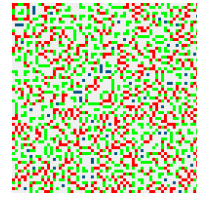
(166)



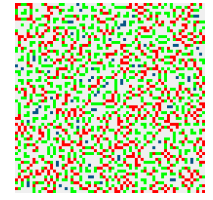
(167)



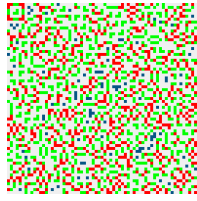
(168)



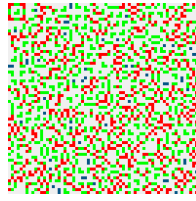
(169)



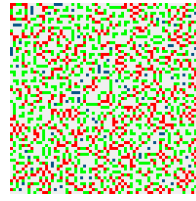
(170)



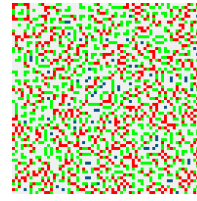
(171)



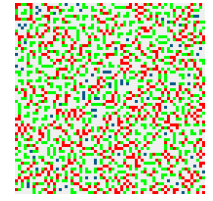
(172)



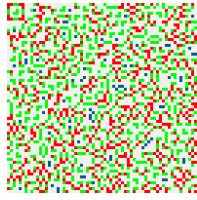
(173)



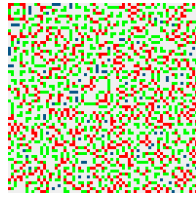
(174)



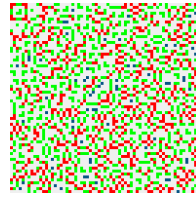
(175)



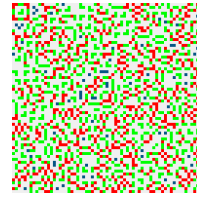
(176)



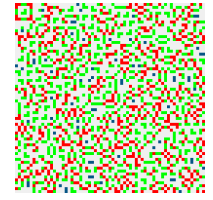
(177)



(178)



(179)



(180)

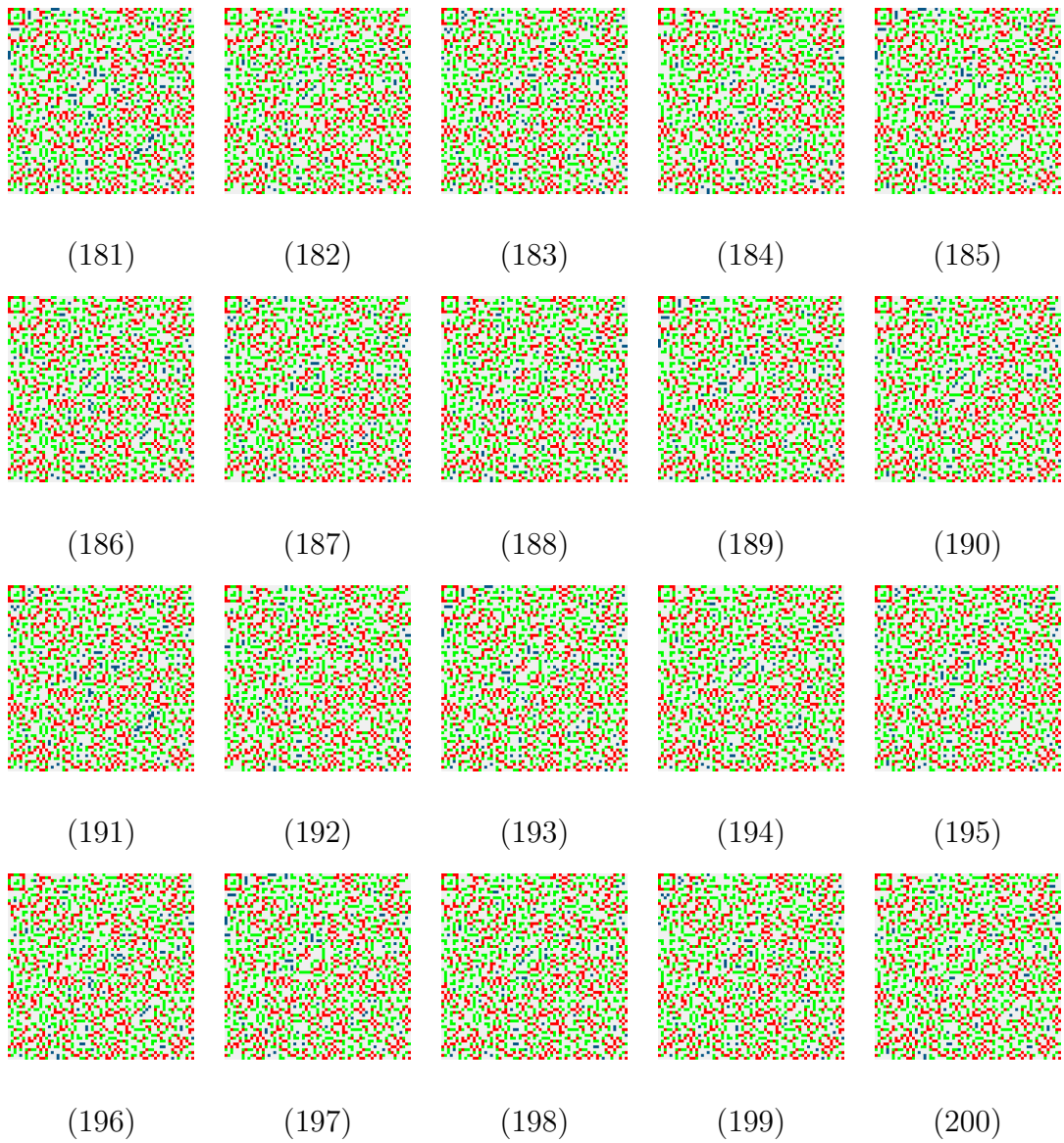
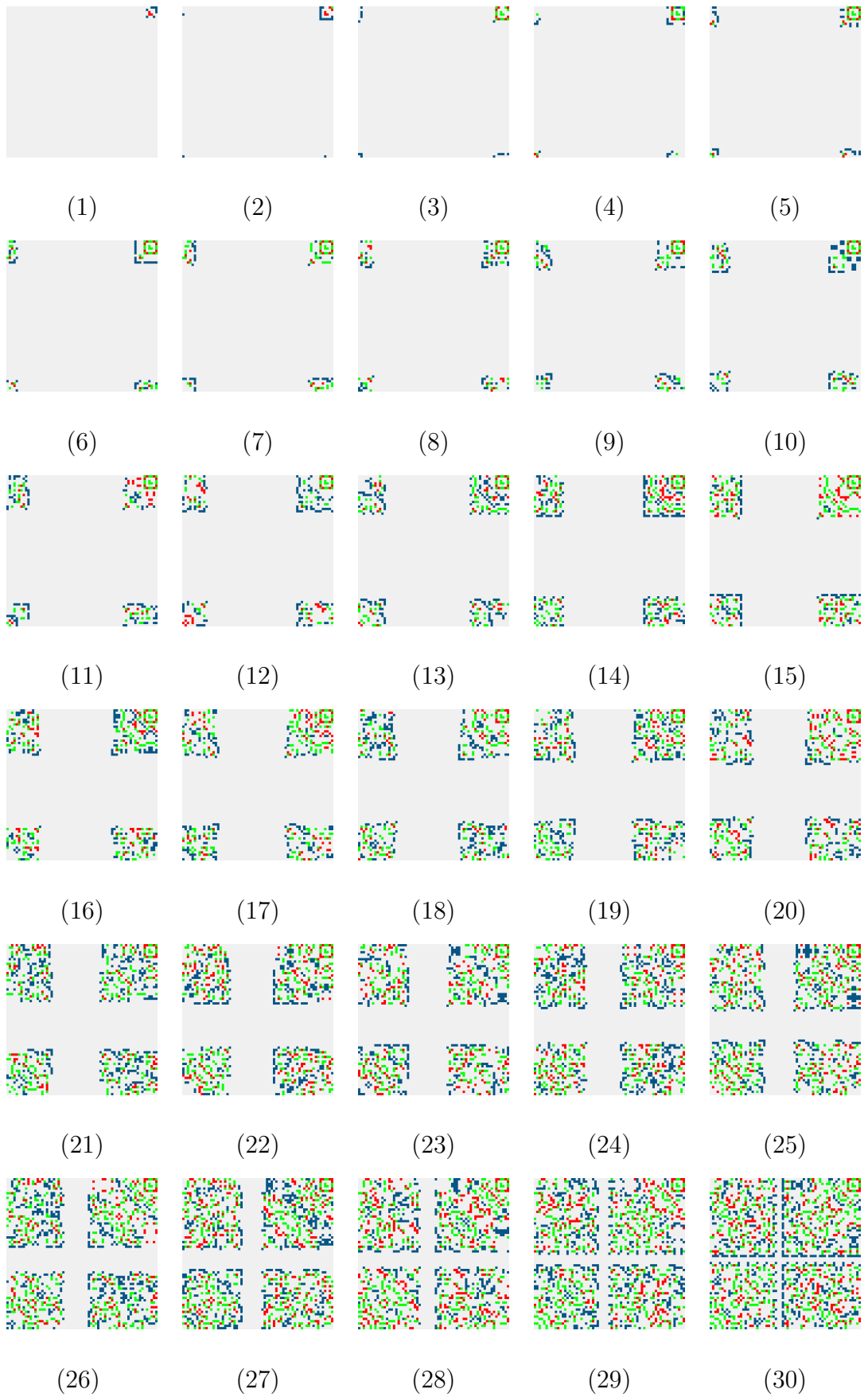
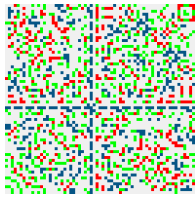
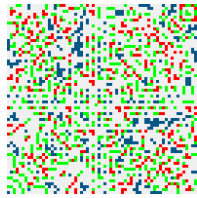


Fig. A.2. *The space-time diagram of cellular automaton 4.6 for 200 time steps starting from 4.19(b) IC.*

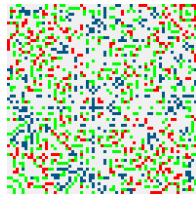




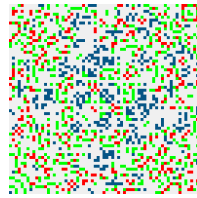
(31)



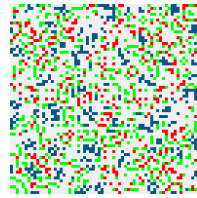
(32)



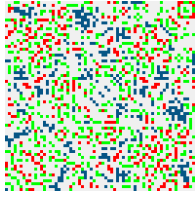
(33)



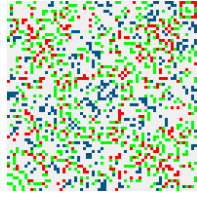
(34)



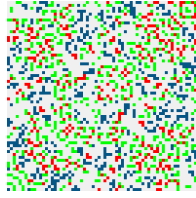
(35)



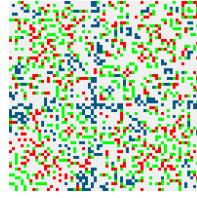
(36)



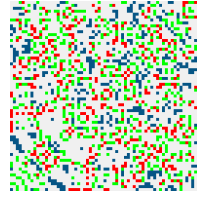
(37)



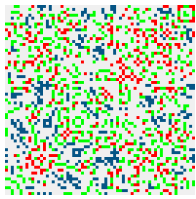
(38)



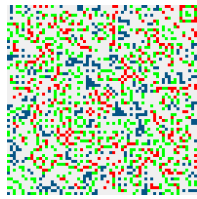
(39)



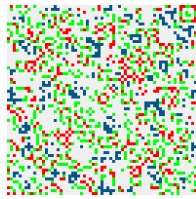
(40)



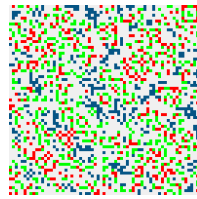
(41)



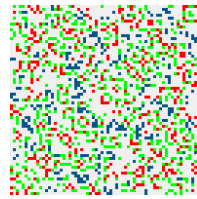
(42)



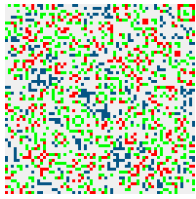
(43)



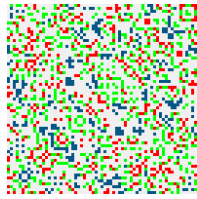
(44)



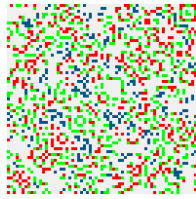
(45)



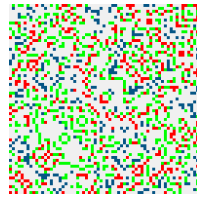
(46)



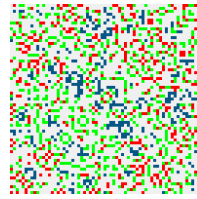
(47)



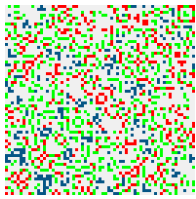
(48)



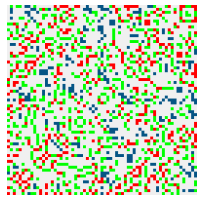
(49)



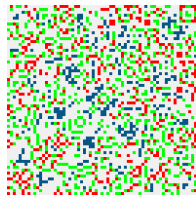
(50)



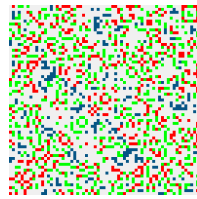
(51)



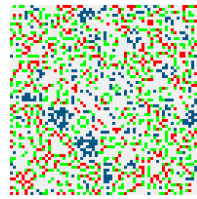
(52)



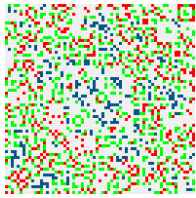
(53)



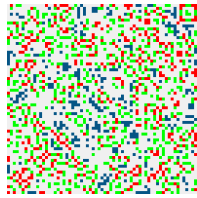
(54)



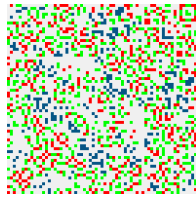
(55)



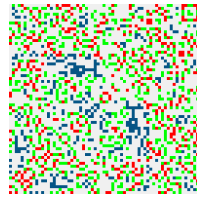
(56)



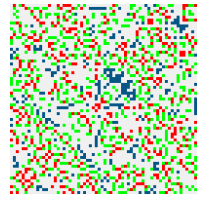
(57)



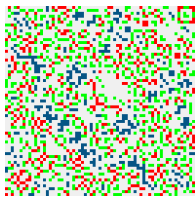
(58)



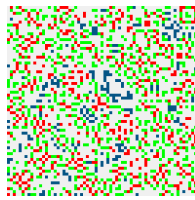
(59)



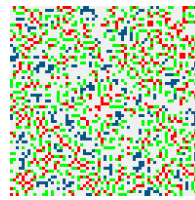
(60)



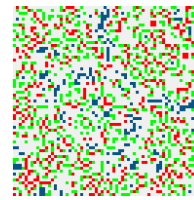
(61)



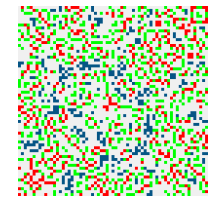
(62)



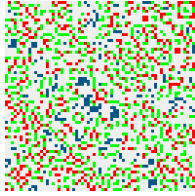
(63)



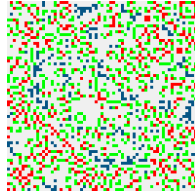
(64)



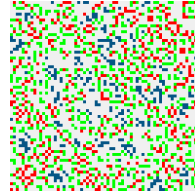
(65)



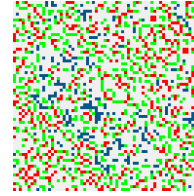
(66)



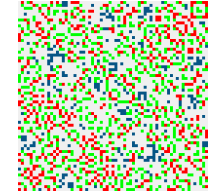
(67)



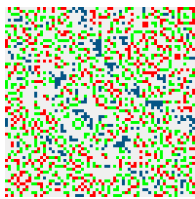
(68)



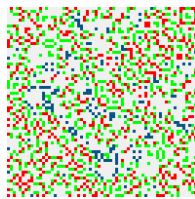
(69)



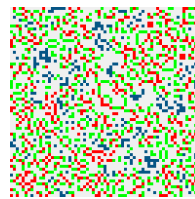
(70)



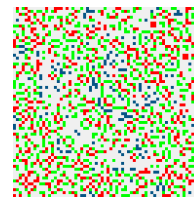
(71)



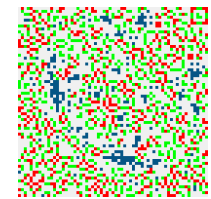
(72)



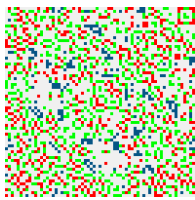
(73)



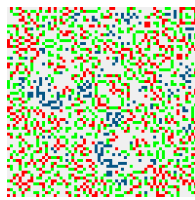
(74)



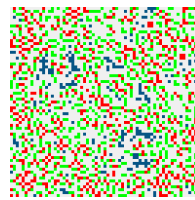
(75)



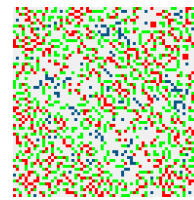
(76)



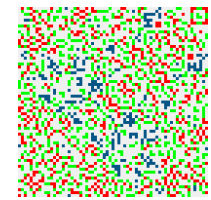
(77)



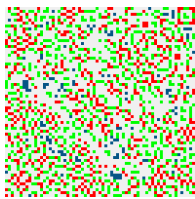
(78)



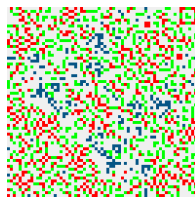
(79)



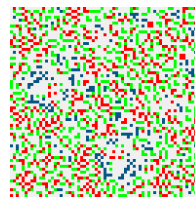
(80)



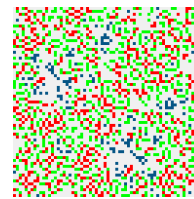
(81)



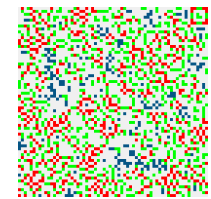
(82)



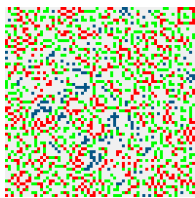
(83)



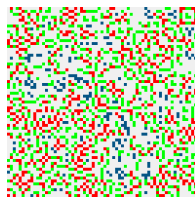
(84)



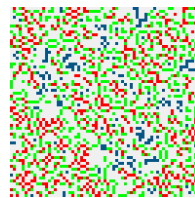
(85)



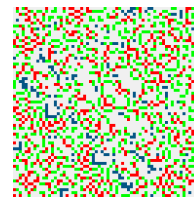
(86)



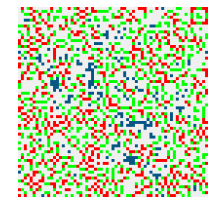
(87)



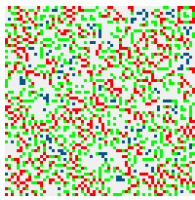
(88)



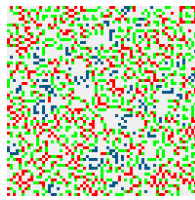
(89)



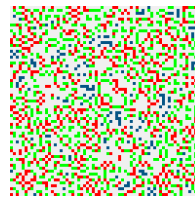
(90)



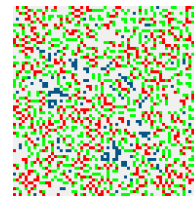
(91)



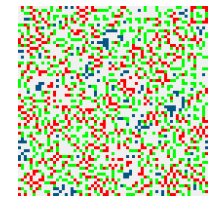
(92)



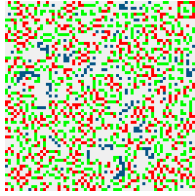
(93)



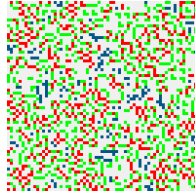
(94)



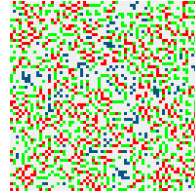
(95)



(96)



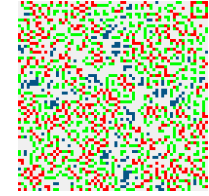
(97)



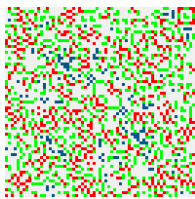
(98)



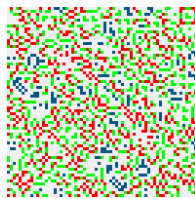
(99)



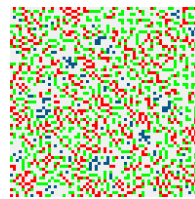
(100)



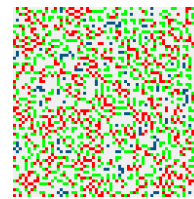
(101)



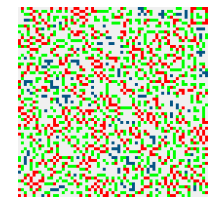
(102)



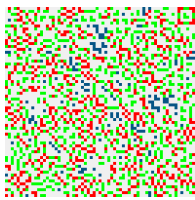
(103)



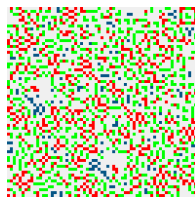
(104)



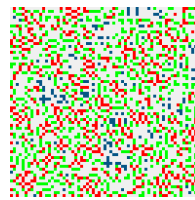
(105)



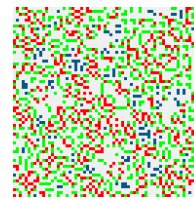
(106)



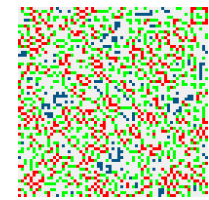
(107)



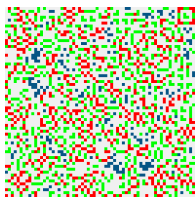
(108)



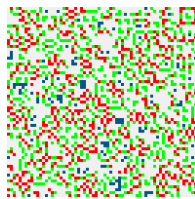
(109)



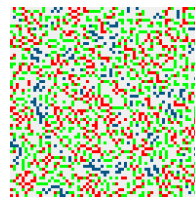
(110)



(111)



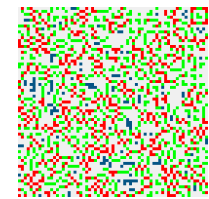
(112)



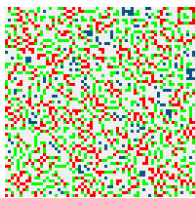
(113)



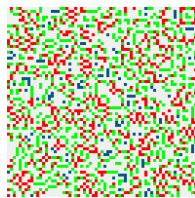
(114)



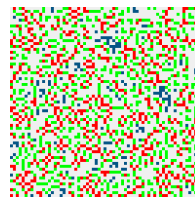
(115)



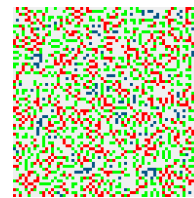
(116)



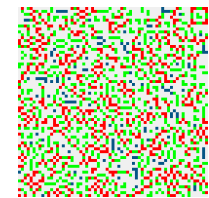
(117)



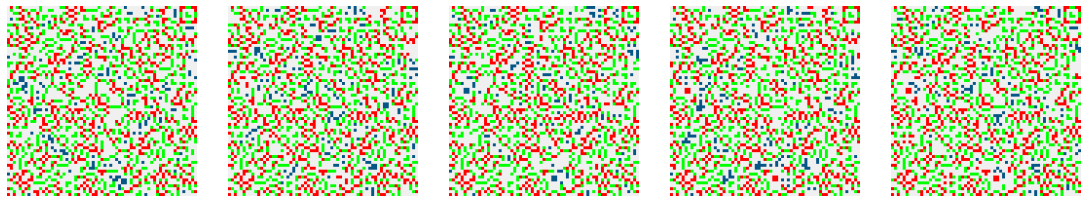
(118)



(119)



(120)



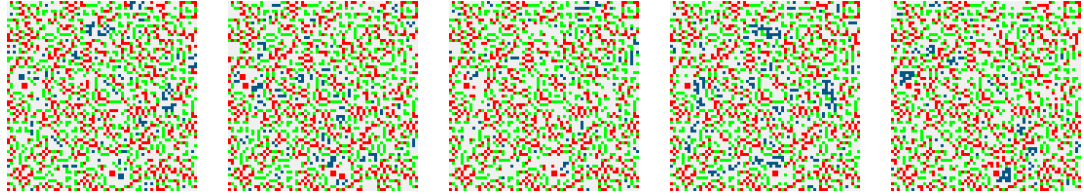
(121)

(122)

(123)

(124)

(125)



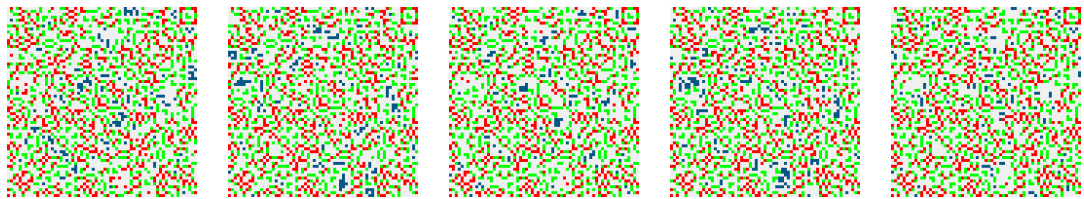
(126)

(127)

(128)

(129)

(130)



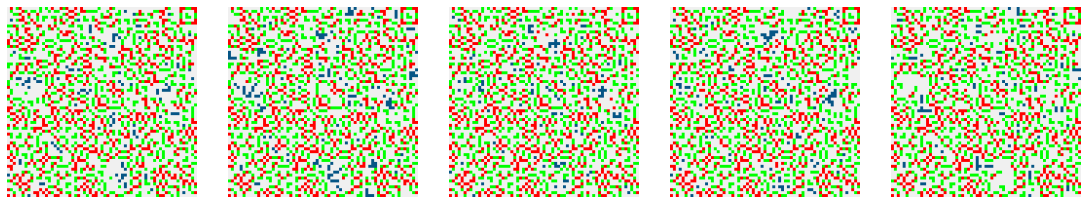
(131)

(132)

(133)

(134)

(135)



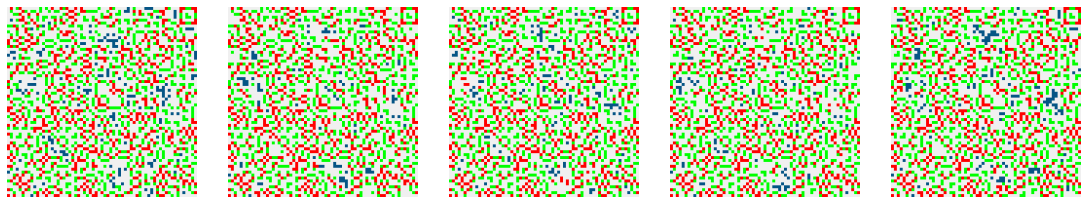
(136)

(137)

(138)

(139)

(140)



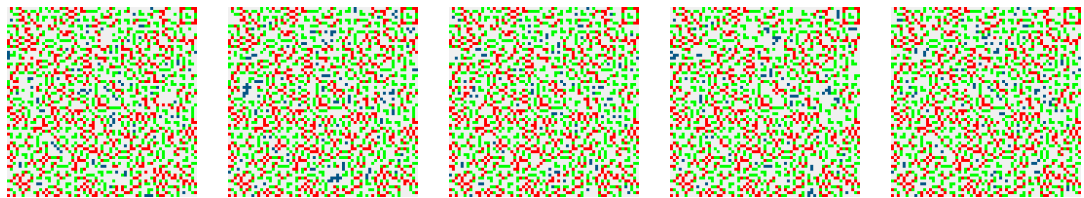
(141)

(142)

(143)

(144)

(145)



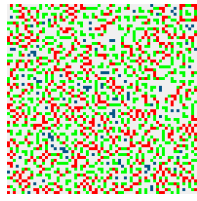
(146)

(147)

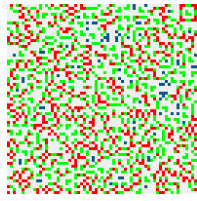
(148)

(149)

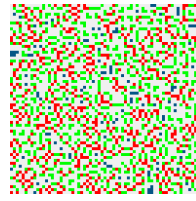
(150)



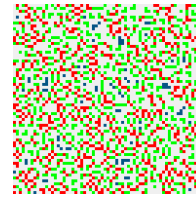
(151)



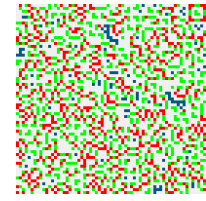
(152)



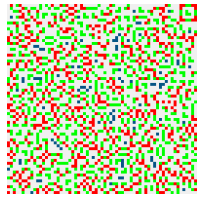
(153)



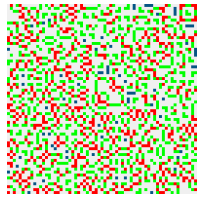
(154)



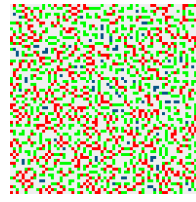
(155)



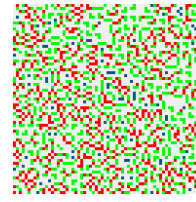
(156)



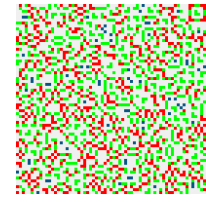
(157)



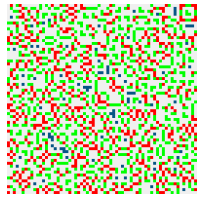
(158)



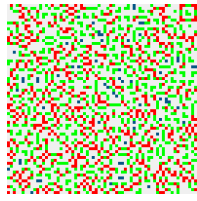
(159)



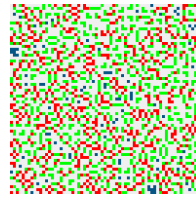
(160)



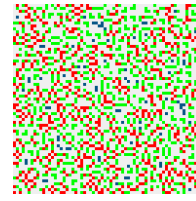
(161)



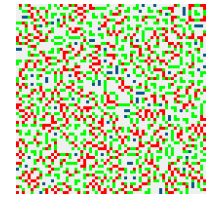
(162)



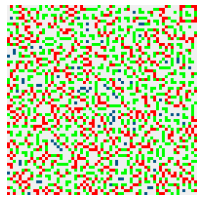
(163)



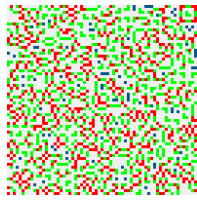
(164)



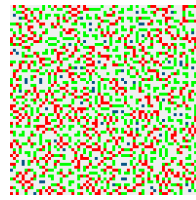
(165)



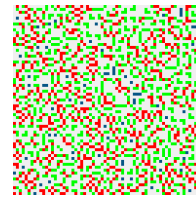
(166)



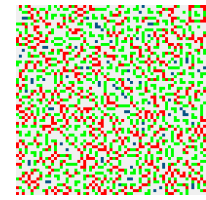
(167)



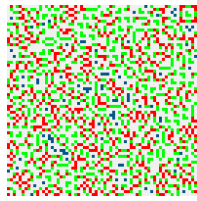
(168)



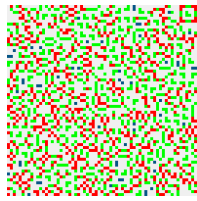
(169)



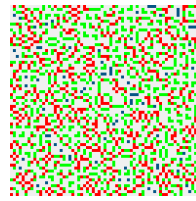
(170)



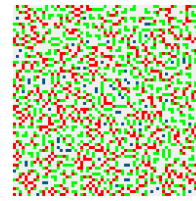
(171)



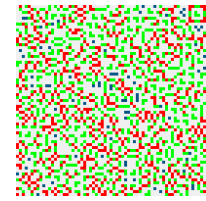
(172)



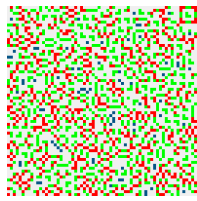
(173)



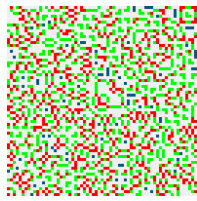
(174)



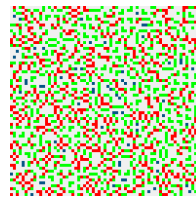
(175)



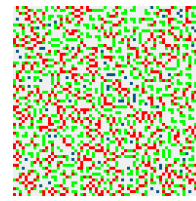
(176)



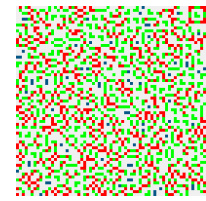
(177)



(178)



(179)



(180)

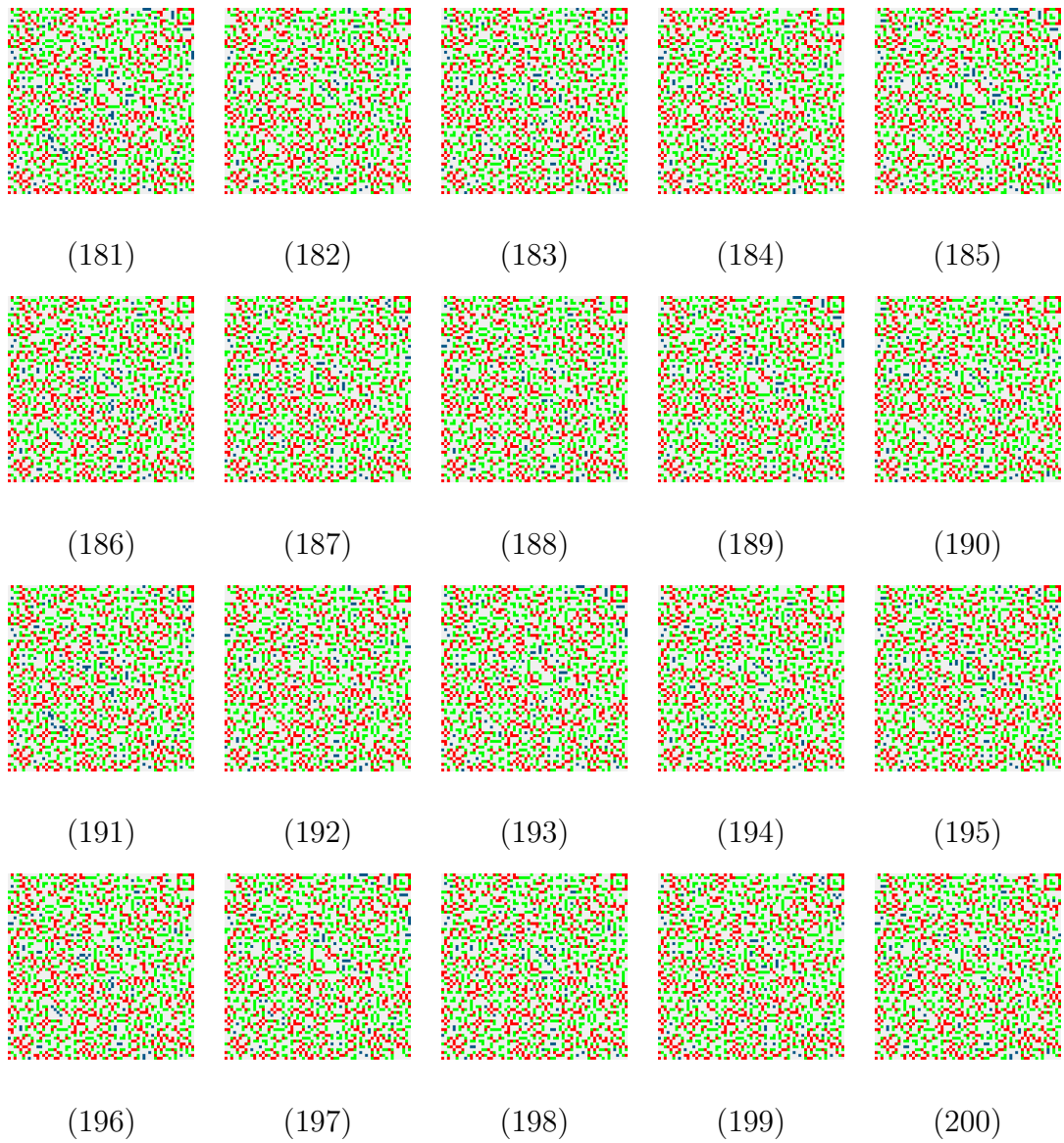
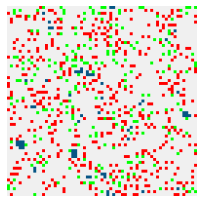
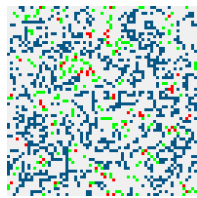


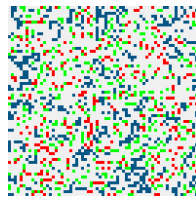
Fig. A.3. *The space-time diagram of cellular automaton 4.6 for 200 time steps starting from 4.19(c) IC.*



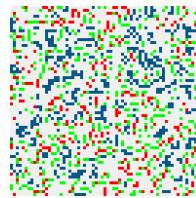
(1)



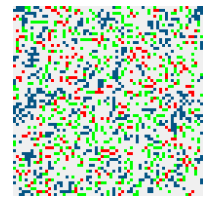
(2)



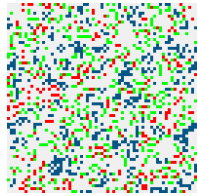
(3)



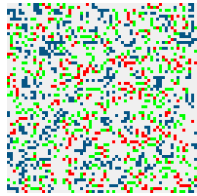
(4)



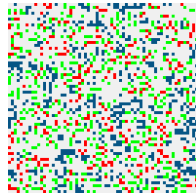
(5)



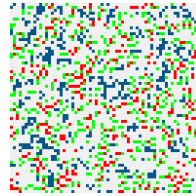
(6)



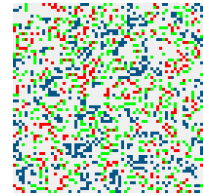
(7)



(8)



(9)



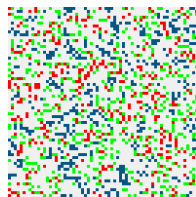
(10)



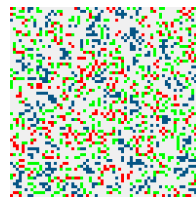
(11)



(12)



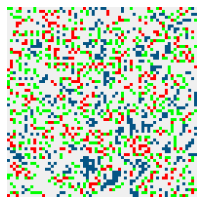
(13)



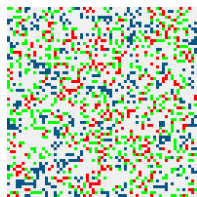
(14)



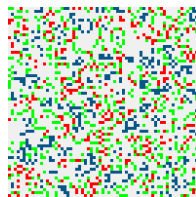
(15)



(16)



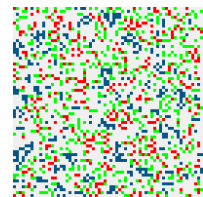
(17)



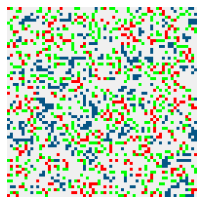
(18)



(19)



(20)



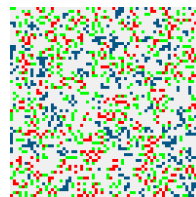
(21)



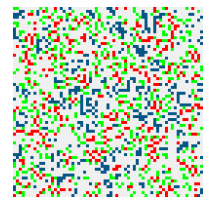
(22)



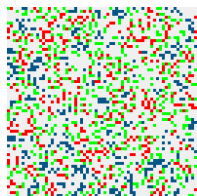
(23)



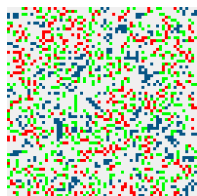
(24)



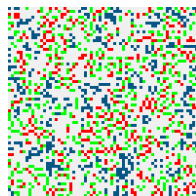
(25)



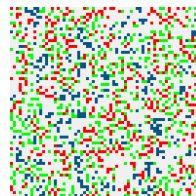
(26)



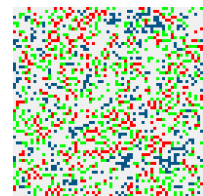
(27)



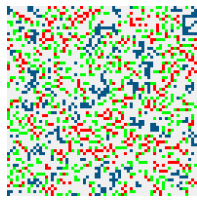
(28)



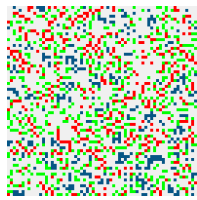
(29)



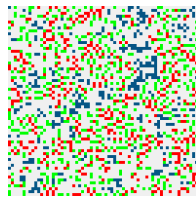
(30)



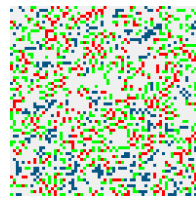
(31)



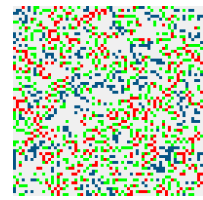
(32)



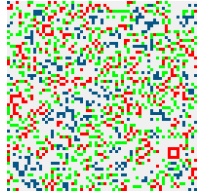
(33)



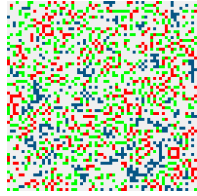
(34)



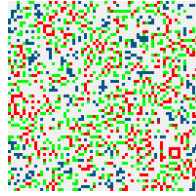
(35)



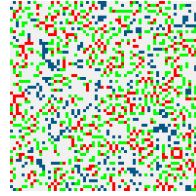
(36)



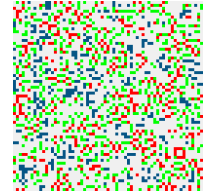
(37)



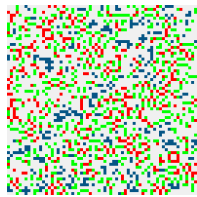
(38)



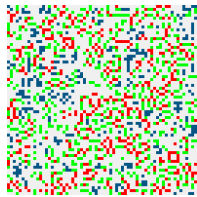
(39)



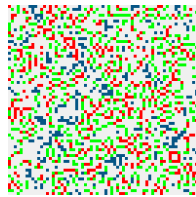
(40)



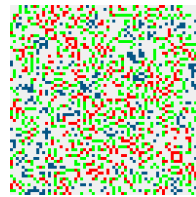
(41)



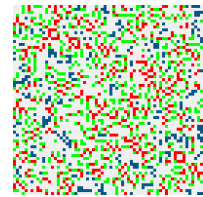
(42)



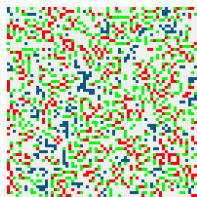
(43)



(44)



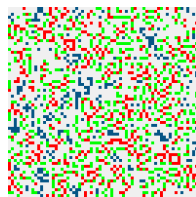
(45)



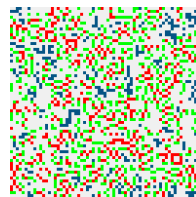
(46)



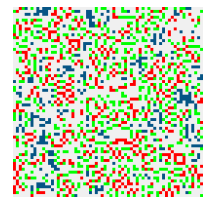
(47)



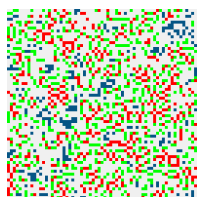
(48)



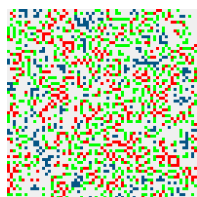
(49)



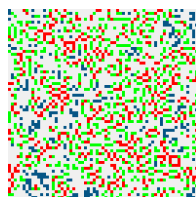
(50)



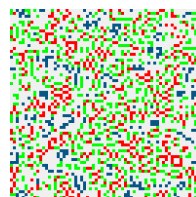
(51)



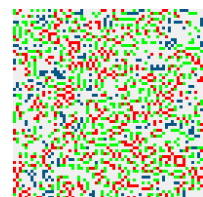
(52)



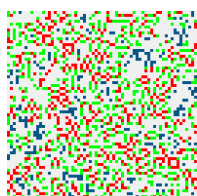
(53)



(54)



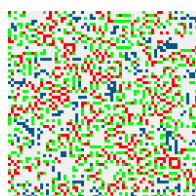
(55)



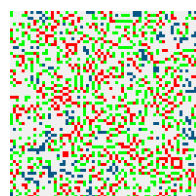
(56)



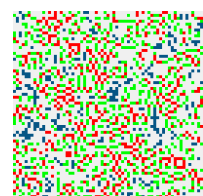
(57)



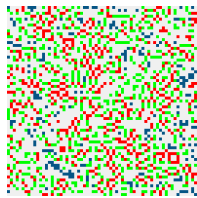
(58)



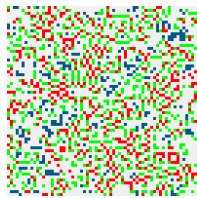
(59)



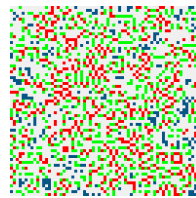
(60)



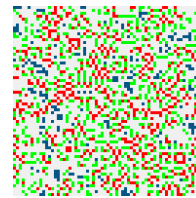
(61)



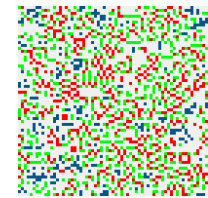
(62)



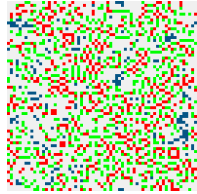
(63)



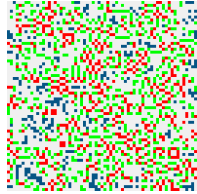
(64)



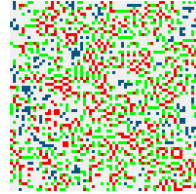
(65)



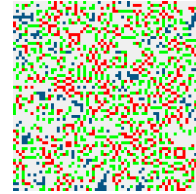
(66)



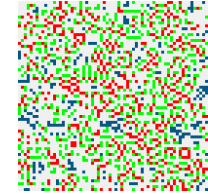
(67)



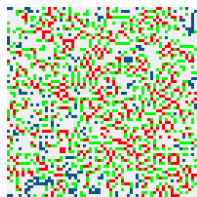
(68)



(69)



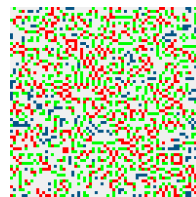
(70)



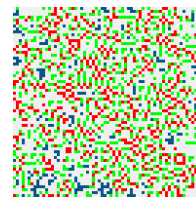
(71)



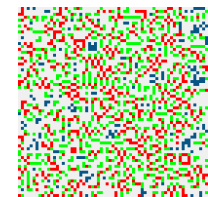
(72)



(73)



(74)



(75)



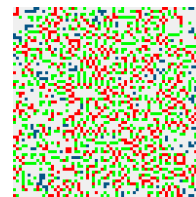
(76)



(77)



(78)



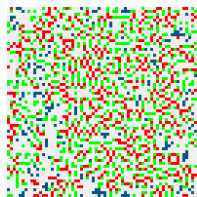
(79)



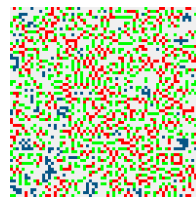
(80)



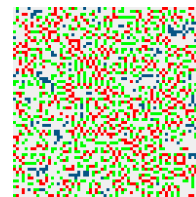
(81)



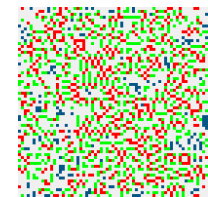
(82)



(83)



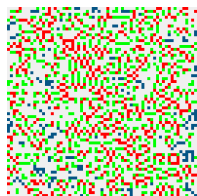
(84)



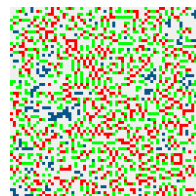
(85)



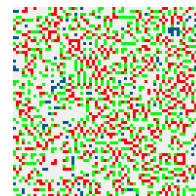
(86)



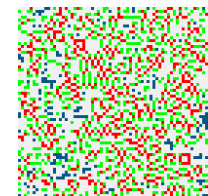
(87)



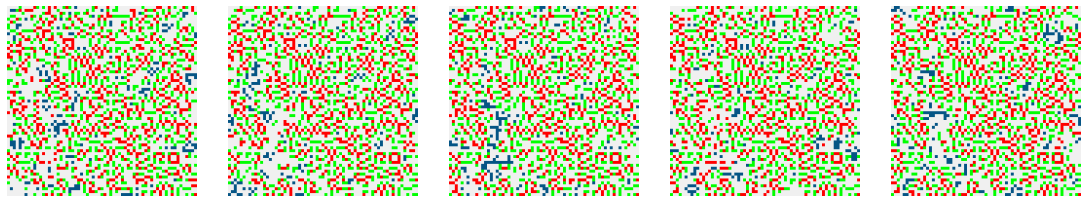
(88)



(89)



(90)



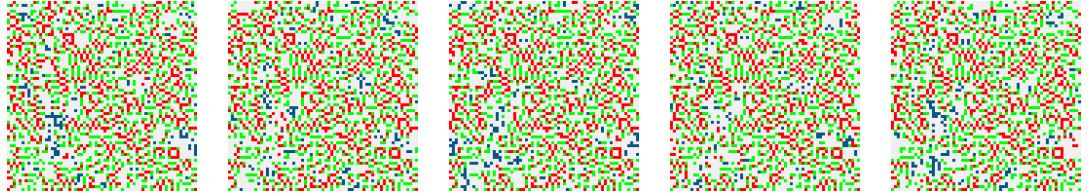
(91)

(92)

(93)

(94)

(95)



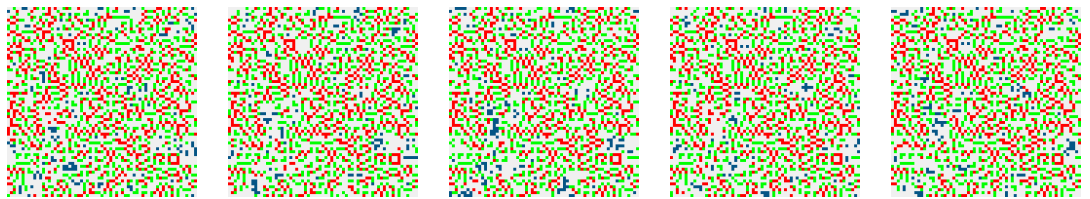
(96)

(97)

(98)

(99)

(100)



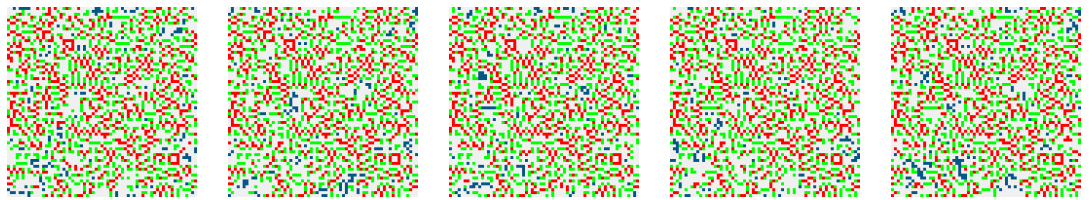
(101)

(102)

(103)

(104)

(105)



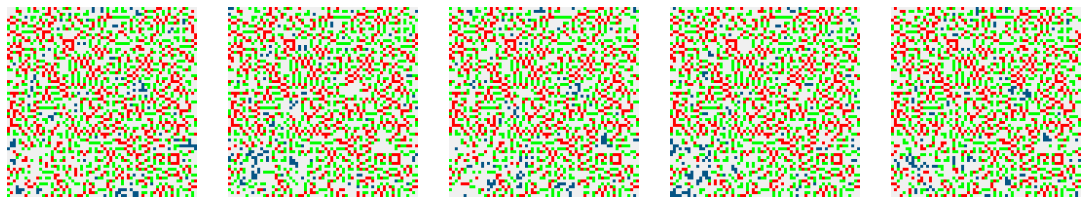
(106)

(107)

(108)

(109)

(110)



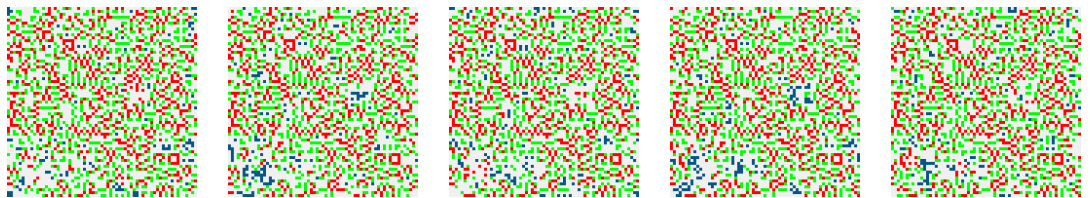
(111)

(112)

(113)

(114)

(115)



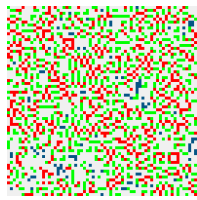
(116)

(117)

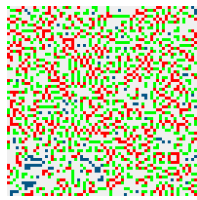
(118)

(119)

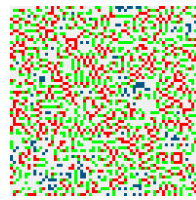
(120)



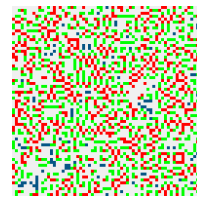
(121)



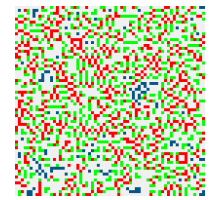
(122)



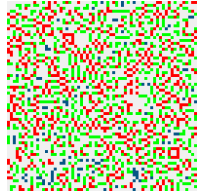
(123)



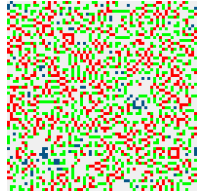
(124)



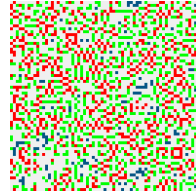
(125)



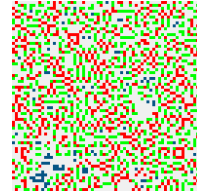
(126)



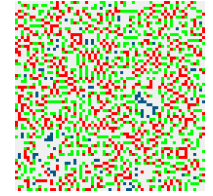
(127)



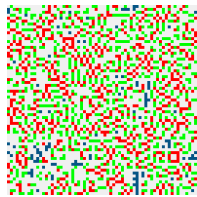
(128)



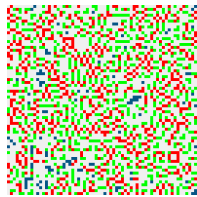
(129)



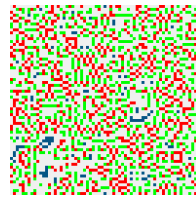
(130)



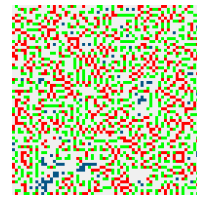
(131)



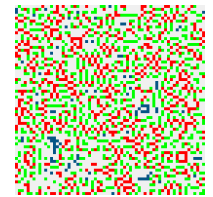
(132)



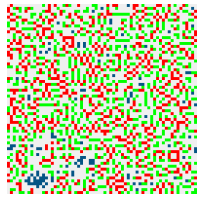
(133)



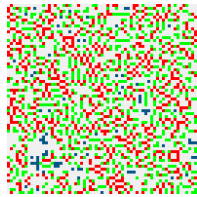
(134)



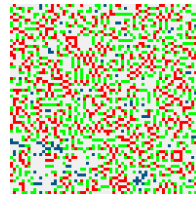
(135)



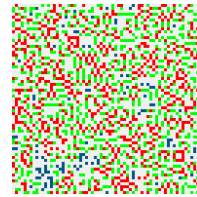
(136)



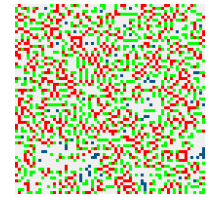
(137)



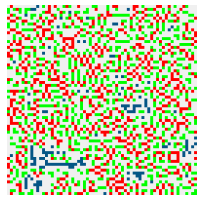
(138)



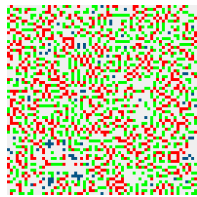
(139)



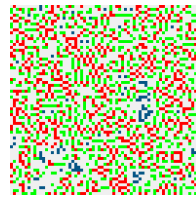
(140)



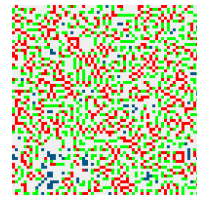
(141)



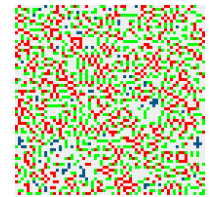
(142)



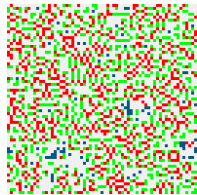
(143)



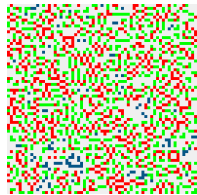
(144)



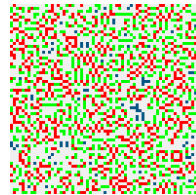
(145)



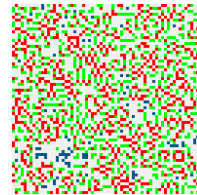
(146)



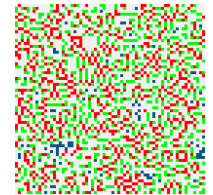
(147)



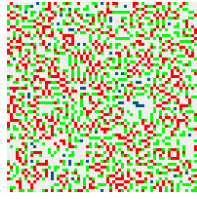
(148)



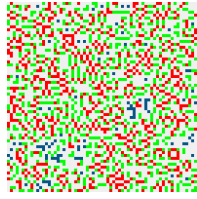
(149)



(150)



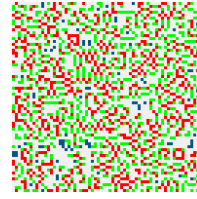
(151)



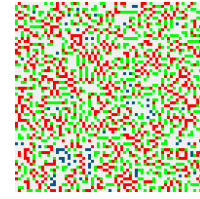
(152)



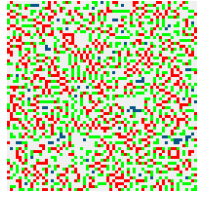
(153)



(154)



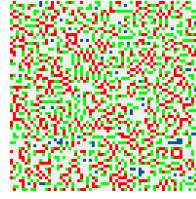
(155)



(156)



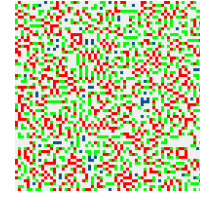
(157)



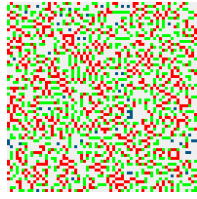
(158)



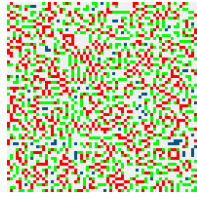
(159)



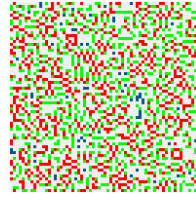
(160)



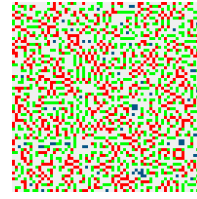
(161)



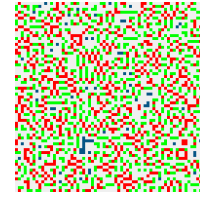
(162)



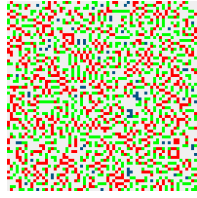
(163)



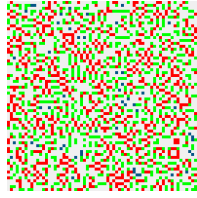
(164)



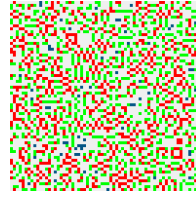
(165)



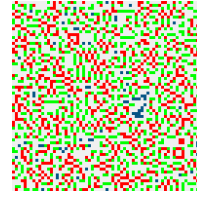
(166)



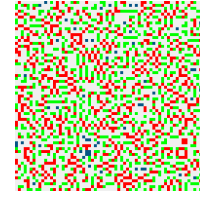
(167)



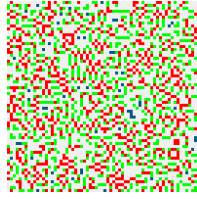
(168)



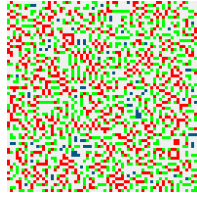
(169)



(170)



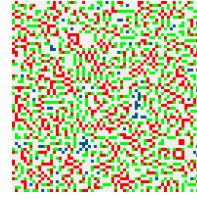
(171)



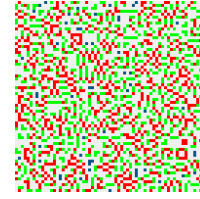
(172)



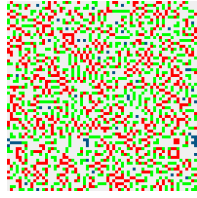
(173)



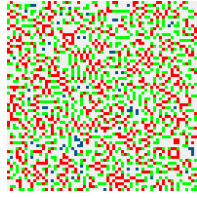
(174)



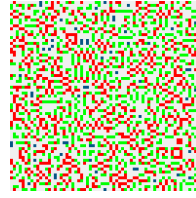
(175)



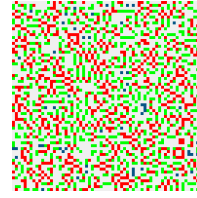
(176)



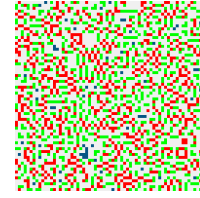
(177)



(178)



(179)



(180)

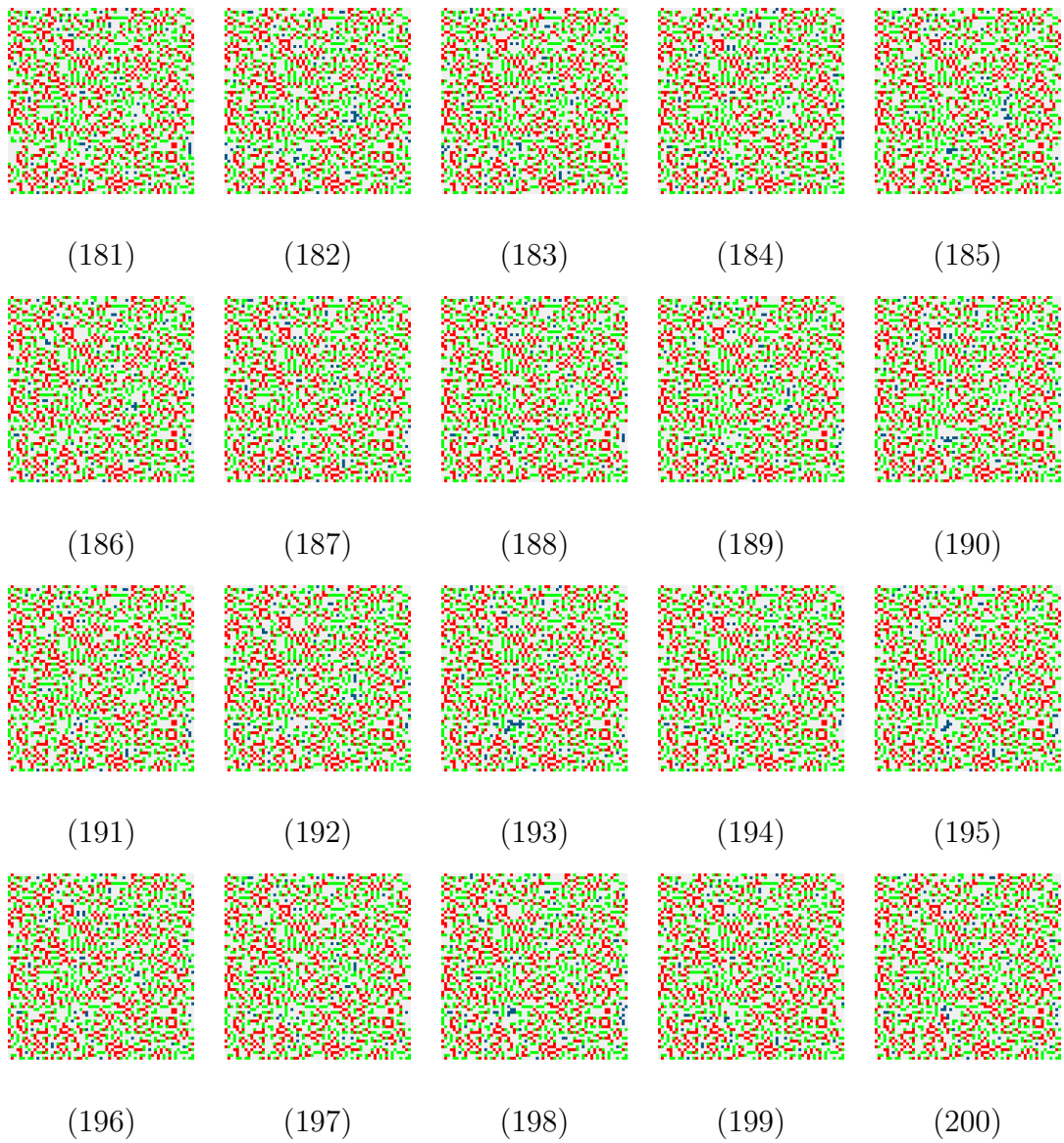


Fig. A.4. *The space-time diagram of cellular automaton 4.6 for 200 time steps starting from the random IC (4.19(d)).*

B Publications

Journal Articles

M. A. Javaheri Javid, W. Alghamdi, A. Ursyn, R. Zimmer, and M. M. al Rifaie, "Swarmic approach for symmetry detection of cellular automata behaviour", *Soft Computing*, vol. 21, no. 21, pp. 5585-5599, 2017.

M. A. Javaheri Javid, T. Blackwell, R. Zimmer, and M. M. al Rifaie, "Analysis of information gain and kolmogorov complexity for structural evaluation of cellular automata configurations," *Connection Science*, vol. 28, no. 02, pp. 155-170, 2016.

Conference Proceedings

M. M. al Rifaie, A. Ursyn, R. Zimmer, and M. A. J. Javid, "On symmetry, aesthetics and quantifying symmetrical complexity," in *Computational Intelligence in Music, Sound, Art and Design: 6th International Conference, EvoMUSART 2017, Amsterdam, The Netherlands, April 19-21, 2017, Proceedings*, J. Correia, V. Ciesielski, and A. Liapis, Eds. Springer International Publishing, 2017, pp. 17-32.

M. A. Javaheri Javid, T. Blackwell, R. Zimmer, and M. M. Al-Rifaie, "Correlation between human aesthetic judgement and spatial complexity measure," in *Proceedings of the 5th International Conference on Evolutionary and Biologically Inspired Music, Sound, Art and Design - Volume 9596*. New York, NY, USA: Springer-Verlag New York, Inc., 2016, pp. 79-91.

M. A. Javaheri Javid, R. Zimmer, A. Ursyn, and M. M. Al-Rifaie, "A quantitative approach for detecting symmetries and complexity in 2D plane," in *Proceedings of the Fourth International Conference on Theory and Practice of Natural Computing - Volume 9477*, ser. TPNC 2015. New York, NY, USA: Springer-Verlag New York, Inc., 2015, pp. 150-160.

M. A. Javaheri Javid, T. Blackwell, M. M. al Rifaie, and R. Zimmer, "Information Gain Measure for Structural Discrimination of Cellular Automata

Configurations,” in *Computer Science and Electronic Engineering Conference (CEEC), 2015 7th*, Colchester, Essex, United Kingdom, Sept 2015, pp. 47-52.

M. A. Javaheri Javid, M. M. al Rifaie, and R. Zimmer, “Detecting Symmetry in Cellular Automata Generated Patterns Using Swarm Intelligence,” in *Theory and Practice of Natural Computing*, ser. Lecture Notes in Computer Science, A.-H. Dediu, M. Lozano, and C. Martí-Vide, Eds., vol. 8890. Springer International Publishing, 2014, pp. 83-94.

M. A. Javaheri Javid, M. M. al Rifaie, and R. Zimmer, “An Informational Model for Cellular Automata Aesthetic Measure,” in *AISB 2015 Symposium on Computational Creativity*, University of Kent, Canterbury, UK, 2015.

M. A. Javaheri Javid, T. Blackwell, R. Zimmer, and M. M. al Rifaie, “Spatial Complexity Measure for Characterising Cellular Automata Generated 2D Patterns,” in *Progress in Artificial Intelligence: 17th Portuguese Conference on Artificial Intelligence, EPIA 2015, Coimbra, Portugal, September 8-11, 2015. Proceedings.*, ser. Lecture Notes in Artificial Intelligence, F. Pereira, P. Machado, E. Costa, E. and A. Cardoso, Eds., vol. 9273. Springer International Publishing, 2015, pp. 201-212.

M. A. J. Javid, M. M. al Rifaie, and R. Zimmer, “Swarm intelligence approach in detecting spatially-independent symmetries in cellular automata,” in *2015 SAI Intelligent Systems Conference (IntelliSys)*, Nov 2015, pp. 632-639.

M. A. Javaheri Javid and R. te Boekhorst, “Cell Dormancy in Cellular Automata,” in *International Conference on Computational Science (3)*, ser. Lecture Notes in Computer Science, V. N. Alexandrov, G. D. van Albada, P. M. A. Sloot, and J. Dongarra, Eds., vol. 3993. Springer, 2006, pp. 367-374.

Bibliography

- [1] D. J. Nurbakhsh, *Divan-e Nurbakhsh: Poems of a Sufi Master*. Khaniqahi Nimatullahi Publications, 2014.
- [2] I. E. Sutherland, “Sketchpad: A man-machine graphical communication system,” Ph.D. dissertation, Massachusetts Institute of Technology, 1963.
- [3] F. Nake, “Art in the time of the artificial,” *Leonardo*, vol. 31, no. 3, pp. 163–164, 1998.
- [4] A. M. Noll, “The digital computer as a creative medium,” *IEEE Spectr.*, vol. 4, no. 10, pp. 89–95, Oct. 1967.
- [5] R. Dawkins, *The blind watchmaker*. New York: W. W. Norton & Company, Inc., 1986.
- [6] S. Todd, W. Latham, and P. Hughes, “Computer sculpture design and animation,” *The Journal of Visualization and Computer Animation*, vol. 2, no. 3, pp. 98–105, Jul.–Sep. 1991.
- [7] K. Sims, “Artificial evolution for computer graphics,” *Computer Graphics*, vol. 25, no. 4, pp. 319–328, July 1991.
- [8] K. Sims, “Interactive evolution of dynamical systems,” in *Toward a practice of autonomous systems: Proceedings of the first European conference on artificial life*, 1992, pp. 171–178.
- [9] K. Sims, “Evolving virtual creatures,” in *Proceedings of the 21st annual conference on Computer graphics and interactive techniques*. ACM, 1994, pp. 15–22.
- [10] G. R. Greenfield *et al.*, “Color dependent computational aesthetics for evolving expressions,” in *Bridges: Mathematical Connections in Art, Music, and Science*. Bridges Conference, 2002, pp. 9–16.
- [11] G. Greenfield, “Evolutionary methods for ant colony paintings,” in *Applications of Evolutionary Computing, EvoWorkshops2005: EvoBIO, EvoCOMNET, EvoHOT, EvoIASP, EvoMUSART, EvoSTOC*, ser. LNCS, F. Rothlauf, J. Branke, S. Cagnoni, D. W. Corne, R. Drechsler, Y. Jin, P. Machado, E. Marchiori, J. Romero, G. D. Smith, and G. Squillero, Eds., vol. 3449. Springer-Verlag, 2005, pp. 478–487.
- [12] A. Dorin, “Aesthetic fitness and artificial evolution for the selection of imagery from the mythical infinite library,” in *Advances in artificial life*. Springer, 2001, pp. 659–668.

- [13] A. Dorin, “A survey of virtual ecosystems in generative electronic art,” in *The Art of Artificial Evolution*. Springer, 2008, pp. 289–309.
- [14] P. Machado, J. Romero, and B. Manaris, “Experiments in computational aesthetics: An iterative approach to stylistic change in evolutionary art,” in *The Art of Artificial Evolution: A Handbook on Evolutionary Art and Music*, J. Romero and P. Machado, Eds. Springer, 2008, pp. 381–415.
- [15] E. den Heijer and A. Eiben, “Evolving art using multiple aesthetic measures,” in *Applications of Evolutionary Computation*. Springer, 2011, pp. 234–243.
- [16] L. Moura and V. Ramos, “Swarm paintings—nonhuman art,” *Architopia: Book, Art, Architecture, and Science*, Institut d’Art Contemporain, Lyon/Villeurbanne, France, pp. 5–24, 2002.
- [17] M. M. al-Rifaie al-Rifaie al-Rifaie, A. Aber, and M. Bishop, “Cooperation of nature and physiologically inspired mechanisms in visualisation,” in *Biologically-Inspired Computing for the Arts: Scientific Data through Graphics*, A. Ursyn, Ed. IGI Global, United States, 2012.
- [18] M. M. al-Rifaie and M. Bishop, “Swarmic sketches and attention mechanism,” in *Evolutionary and Biologically Inspired Music, Sound, Art and Design*, ser. Lecture Notes in Computer Science, P. Machado, J. McDermott, and A. Carballal, Eds. Springer Berlin Heidelberg, 2013, vol. 7834, pp. 85–96.
- [19] P. Prusinkiewicz and A. Lindenmayer, *The Algorithmic Beauty of Plants*. Springer-Verlag New York Inc., 1990.
- [20] P. Prusinkiewicz, M. Hammel, J. Hanan, and R. Mech, “L-systems: from the theory to visual models of plants,” in *Proceedings of the 2nd CSIRO Symposium on Computational Challenges in Life Sciences*, vol. 3, 1996, pp. 1–32.
- [21] J. McCormack, “Interactive evolution of L-system grammars for computer graphics modelling,” in *Complex Systems*, D. Green and T. Bossomaier, Eds. IOS Press, 1993, pp. 118–130.
- [22] J. McCormack, “Aesthetic evolution of l-systems revisited,” in *Applications of Evolutionary Computing, EvoWorkshops2004: EvoBIO, EvoCOMNET, EvoHOT, EvoIASP, EvoMUSART, EvoSTOC*, ser. LNCS, G. R. Raidl, S. Cagnoni, J. Branke, D. W. Corne, R. Drechsler, Y. Jin, C. Johnson, P. Machado, E. Marchiori, F. Rothlauf, G. D. Smith, and G. Squillero, Eds., vol. 3005. Coimbra, Portugal: Springer Verlag, 5-7 apr 2004, pp. 477–488.
- [23] J. McCormack, “Generative modelling with timed l-systems,” *Design Computing and Cognition*, vol. 4, pp. 157–175, 2004.
- [24] A. Witkin and M. Kass, “Reaction-diffusion textures,” *ACM Siggraph Computer Graphics*, vol. 25, no. 4, pp. 299–308, 1991.
- [25] K. C. Knowlton, “A computer technique for producing animated movies,” in *Proceedings of the April 21-23, 1964, spring joint computer conference*. ACM, 1964, pp. 67–87.
- [26] L. Schwartz and L. Schwartz, *The Computer Artist’s Handbook: Concepts, Techniques, and Applications*. W W Norton & Company Incorporated, 1992.

- [27] E. F. Codd, *Cellular Automata*. New York: Academic Press, 1968.
- [28] T. Toffoli, “Occam, turing, von neumann, jaynes: How much can you get for how little?(a conceptual introduction to cellular automata),” in *ACRI 94*, S. D. Gregorio and G. Spezzano, Eds., 1994, pp. 29–30.
- [29] M. Gardner, “Mathematical games - the fantastic combinations of John Conway’s new solitaire game, Life,” *Scientific American*, pp. 120–123, Oct. 1970.
- [30] P. Struycken, “Splash 1972/1974,” in *Artist and computer*, R. Leavitt, Ed. Harmony Books, 1976, pp. 30–31.
- [31] P. Brown, “Stepping stones in the mist,” in *Creative evolutionary systems*, P. Bentley and D. Corne, Eds. Morgan Kaufmann Publishers Inc., 2001, pp. 387–407.
- [32] J. Frazer, *An evolutionary architecture*. Architectural Association Publications, Themes VII, 1995.
- [33] I. Xenakis, *Formalized music: thought and mathematics in composition*. Pendragon Press, 1992.
- [34] E. Miranda, *Composing Music with Computers*, ser. Composing Music with Computers. Focal Press, 2001, no. v. 1.
- [35] S. Wolfram, *A New Kind of Science*. Wolfram Media Inc., 2002.
- [36] A. Findeli, “Rethinking design education for the 21st century: Theoretical, methodological, and ethical discussion,” *Design issues*, vol. 17, no. 1, pp. 5–17, 2001.
- [37] P. F. Smith, *The dynamics of delight: Architecture and aesthetics*. Routledge, 2003.
- [38] A. Lau and A. V. Moere, “Towards a model of information aesthetics in information visualization,” in *Information Visualization, 2007. IV '07. 11th International Conference*, July 2007, pp. 87–92.
- [39] M. Kurosu and K. Kashimura, “Apparent usability vs. inherent usability: experimental analysis on the determinants of the apparent usability,” in *Conference companion on Human factors in computing systems*. ACM, 1995, pp. 292–293.
- [40] N. Tractinsky, “Aesthetics and apparent usability: empirically assessing cultural and methodological issues,” in *Proceedings of the ACM SIGCHI Conference on Human factors in computing systems*. ACM, 1997, pp. 115–122.
- [41] L. E. Udsen and A. H. Jørgensen, “The aesthetic turn: unravelling recent aesthetic approaches to human-computer interaction,” *Digital Creativity*, vol. 16, no. 4, pp. 205–216, 2005.
- [42] F. Hoenig, “Defining computational aesthetics,” in *Workshop on Computational Aesthetics*, L. Neumann, M. Sbert, B. Gooch, and W. Purgathofer, Eds. Girona, Spain: Eurographics Association, 2005, pp. 13–18.

- [43] E. den Heijer and A. E. Eiben, “Comparing Aesthetic Measures for Evolutionary Art,” in *EvoMUSART*, ser. LNCS, C. Di Chio, A. Brabazon, G. A. Di Caro, M. Ebner, M. Farooq, A. Fink, J. Grahl, G. Greenfield, P. Machado, M. O’Neill, E. Tarantino, and N. Urquhart, Eds., vol. 6025. Istanbul: Springer, 7-9Apr. 2010, pp. 311–320.
- [44] “International symposium on computational aesthetics in graphics, visualization, and imaging,” [Online]. Available: <http://www.cs.rug.nl/svcg/cae2009/>, 2009, [Accessed]: Apr, 2017.
- [45] M. A. Javaheri Javid and R. te Boekhorst, “Cell dormancy in cellular automata,” in *International Conference on Computational Science (3)*, ser. Lecture Notes in Computer Science, V. N. Alexandrov, G. D. van Albada, P. M. A. Sloot, and J. Dongarra, Eds., vol. 3993. Springer, 2006, pp. 367–374.
- [46] W. Li, “Complex patterns generated by next nearest neighbors cellular automata,” *Computers & Graphics*, vol. 13, no. 4, pp. 531–537, 1989.
- [47] W. K. Mason, “Art from cellular automata and symmetrized dot-patterns,” *Computers & graphics*, vol. 16, no. 4, pp. 439–441, 1993.
- [48] K. A. Bentley, “Exploring aesthetic pattern formation,” in *Generative Art 2002 conference proceedings*, 2002.
- [49] D. Ashlock and J. Tsang, “Evolved art via control of cellular automata,” in *Evolutionary Computation, 2009. CEC’09. IEEE Congress on*. IEEE, 2009, pp. 3338–3344.
- [50] A. Adamatzky and G. J. Martínez, *Designing Beauty: The Art of Cellular Automata*. Springer, 2016, vol. 20.
- [51] G. Birkhoff, *Aesthetic Measure*. Harvard University Press, 1933.
- [52] D. E. Berlyne, *Conflict, arousal, and curiosity*. McGraw-Hill Book Company, 1960.
- [53] F. Hoenig, “Computational aesthetics and visual preference - an experimental approach,” Ph.D. dissertation, Johannes Kepler Universitaet, Linz, Austria, March 2006.
- [54] J. E. Bates and H. K. Shepard, “Measuring complexity using information fluctuation,” *Physics Letters A*, vol. 172, no. 6, pp. 416–425, 1993.
- [55] R. Wackerbauer, A. Witt, H. Atmanspacher, J. Kurths, and H. Scheingraber, “A comparative classification of complexity measures,” *Chaos, Solitons & Fractals*, vol. 4, no. 1, pp. 133–173, 1994.
- [56] Andrienko, Yu. A., Brilliantov, N. V., and Kurths, J., “Complexity of two-dimensional patterns,” *Eur. Phys. J. B*, vol. 15, no. 3, pp. 539–546, 2000.
- [57] A. N. Kolmogorov, “Three approaches to the quantitative definition of information,” *Problems of information transmission*, vol. 1, no. 1, pp. 1–7, 1965.
- [58] Automaton, “Encyclopadia Britannica Online,” [Online]. Available: <http://www.britannica.com/EBchecked/topic/44951/automaton>, [Accessed]: Apr, 2017.

- [59] H. Henderson, *Encyclopedia of computer science and technology*. Infobase Publishing, 2009.
- [60] M. Arbib, “Automata,” in *The MIT encyclopedia of the cognitive sciences*, R. A. Wilson and F. C. Keil, Eds. MIT press, 1999, pp. 60–63.
- [61] A. M. Turing, “On Computable Numbers, with an application to the Entscheidungsproblem,” *Proceedings of the London Mathematical Society*, vol. 42, no. 2, pp. 230–265, 1936.
- [62] J. von Neumann, “The general and logical theory of automata,” in *Cerebral mechanisms in behavior; the Hixon Symposium*, L. A. Jeffress, Ed., 1951, pp. 1–41.
- [63] R. A. Freitas Jr and R. C. Merkle, *Kinematic self-replicating machines*. Landes Bioscience, 2004.
- [64] S. Levy, *Artificial life: the quest for a new creation*. Penguin Books, 1992.
- [65] J. Von Neumann and A. W. Burks, *Theory of self-reproducing automata*. University of Illinois Press, 1966.
- [66] R. Alonso-Sanz and M. Martín, “Elementary cellular automata with memory,” *Complex Systems*, vol. 14, no. 2, pp. 99–126, 2003.
- [67] C. G. Langton, “Self-reproduction in cellular automata,” *Physica D: Nonlinear Phenomena*, vol. 10, no. 1–2, pp. 135–144, 1984.
- [68] J. Byl, “Self-reproduction in small cellular automata,” *Physica D: Nonlinear Phenomena*, vol. 34, no. 1, pp. 295 – 299, 1989.
- [69] P. Linz, *An introduction to formal languages and automata*. Jones & Bartlett Publishers, 2001.
- [70] H. Gutowitz, *Cellular Automata: Theory and Experiment*, ser. A Bradford book. MIT Press, 1991.
- [71] S. Wolfram, “Universality and complexity in cellular automata,” *Physica D: Nonlinear Phenomena*, vol. 10, no. 1, pp. 1–35, 1984.
- [72] C. G. Langton, “Studying artificial life with cellular automata,” *Physica D: Nonlinear Phenomena*, vol. 22, no. 1, pp. 120–149, 1986.
- [73] C. G. Langton, “Computation at the edge of chaos: phase transitions and emergent computation,” *Physica D: Nonlinear Phenomena*, vol. 42, no. 1, pp. 12–37, 1990.
- [74] A. Ilachinski, *Cellular Automata: A Discrete Universe*. World Scientific Publishing Company Incorporated, 2001.
- [75] S. Willi-Hans, *The Nonlinear Workbook: Chaos, Fractals, Cellular Automata, Genetic Algorithms, Gene Expression Programming, Support Vector Machine, Wavelets, Hidden Markov Models, Fuzzy Logic with C++, Java and Symbolic C++ Programs*. World Scientific Publishing Company Pte Limited, 2014.

- [76] S. Wolfram *et al.*, *Theory and applications of cellular automata*. World scientific Singapore, 1986, vol. 1.
- [77] T. Toffoli, “Cellular automata as an alternative to (rather than an approximation of) differential equations in modeling physics,” *Physica D: Nonlinear Phenomena*, vol. 10, no. 1-2, pp. 117–127, 1984.
- [78] G. Y. Vichniac, “Simulating physics with cellular automata,” *Physica D: Nonlinear Phenomena*, vol. 10, no. 1-2, pp. 96–116, 1984.
- [79] M. Gerhardt and H. Schuster, “A cellular automaton describing the formation of spatially ordered structures in chemical systems,” *Physica D: Nonlinear Phenomena*, vol. 36, no. 3, pp. 209–221, 1989.
- [80] R. M. Baer and H. M. Martinez, “Automata and biology,” *Annual review of biophysics and bioengineering*, vol. 3, no. 1, pp. 255–291, 1974.
- [81] G. B. Ermentrout and L. Edelstein-Keshet, “Cellular automata approaches to biological modeling,” *Journal of theoretical Biology*, vol. 160, no. 1, pp. 97–133, 1993.
- [82] N. J. Savill and P. Hogeweg, “Modelling morphogenesis: from single cells to crawling slugs,” *Journal of Theoretical Biology*, vol. 184, no. 3, pp. 229–235, 1997.
- [83] P. Hogeweg, “Cellular automata as a paradigm for ecological modeling,” *Appl. Math. Comput.*, vol. 27, no. 1, pp. 81–100, Jul. 1988.
- [84] R. Hegselmann and A. Flache, “Understanding complex social dynamics: A plea for cellular automata based modelling,” *Journal of Artificial Societies and Social Simulation*, vol. 1, no. 3, p. 1, 1998.
- [85] C. Waddington and R. J. Cowe, “Computer simulation of a mulluscan pigmentation pattern,” *Journal of Theoretical Biology*, vol. 25, no. 2, pp. 219 – 225, 1969.
- [86] A. Deutsch and S. Dormann, *Cellular automaton modeling of biological pattern formation: characterization, applications, and analysis*. Springer Science & Business Media, 2007.
- [87] N. Margolus, T. Toffoli, and G. Vichniac, “Cellular-automata supercomputers for fluid-dynamics modeling,” *Physical Review Letters*, vol. 56, no. 16, p. 1694, 1986.
- [88] S. Wolfram, “Cellular automaton fluids 1: Basic theory,” *Journal of statistical physics*, vol. 45, no. 3, pp. 471–526, 1986.
- [89] D. H. Rothman, “Cellular-automaton fluids: A model for flow in porous media,” *Geophysics*, vol. 53, no. 4, pp. 509–518, 1988.
- [90] D. N. Ostrov and R. Rucker, “Continuous-valued cellular automata for nonlinear wave equations,” *Complex systems*, vol. 10, no. 2, pp. 91–119, 1996.
- [91] T. Vicsek and A. S. Szalay, “Fractal distribution of galaxies modeled by a cellular-automaton-type stochastic process,” *Physical review letters*, vol. 58, no. 26, p. 2818, 1987.

- [92] M. Fukui and Y. Ishibashi, “Self-organized phase transitions in cellular automaton models for pedestrians,” *Journal of the physical society of Japan*, vol. 68, no. 8, pp. 2861–2863, 1999.
- [93] M. Batty and Y. Xie, “From cells to cities,” *Environment and planning B*, vol. 21, pp. 31–48, 1994.
- [94] M. Batty, *Cities and complexity: understanding cities with cellular automata, agent-based models, and fractals*. The MIT press, 2007.
- [95] Y. Liu, *Modelling urban development with geographical information systems and cellular automata*. CRC Press, 2008.
- [96] A. R. Kansal, S. Torquato, G. Harsh, E. Chiocca, and T. Deisboeck, “Simulated brain tumor growth dynamics using a three-dimensional cellular automaton,” *Journal of theoretical biology*, vol. 203, no. 4, pp. 367–382, 2000.
- [97] K. Christensen, H. C. Fogedby, and H. Jeldtoft Jensen, “Dynamical and spatial aspects of sandpile cellular automata,” *Journal of statistical physics*, vol. 63, no. 3, pp. 653–684, 1991.
- [98] K. Nagel and M. Schreckenberg, “A cellular automaton model for freeway traffic,” *Journal de physique I*, vol. 2, no. 12, pp. 2221–2229, 1992.
- [99] P. Bak and C. Tang, “Earthquakes as a self-organized critical phenomenon,” *J. geophys. Res*, vol. 94, no. 15, pp. 635–15, 1989.
- [100] P. Akishin, M. Altaisky, I. Antoniou, A. Budnik, and V. Ivanov, “Simulation of earthquakes with cellular automata,” *Discrete Dynamics in Nature and Society*, vol. 2, no. 4, pp. 267–279, 1998.
- [101] I. Karafyllidis and A. Thanailakis, “A model for predicting forest fire spreading using cellular automata,” *Ecological Modelling*, vol. 99, no. 1, pp. 87–97, 1997.
- [102] T. Welberry and R. Galbraith, “A two-dimensional model of crystal-growth disorder,” *Journal of Applied Crystallography*, vol. 6, no. 2, pp. 87–96, 1973.
- [103] N. H. Packard, “Lattice models for solidification and aggregation,” *First International Symposium for Science on Form*, 1986.
- [104] M. d’Inverno and R. Saunders, “Agent-based modelling of stem cell self-organisation in a niche,” in *International Workshop on Engineering Self-Organising Applications*. Springer, 2004, pp. 52–68.
- [105] G. C. Sirakoulis and A. Adamatzky, *Robots and Lattice Automata*. Springer, 2015.
- [106] S. Gobron and N. Chiba, “3D surface cellular automata and their applications,” *The Journal of Visualization and Computer Animation*, vol. 10, no. 3, pp. 143–158, 1999.
- [107] S. Wolfram, “Cryptography with cellular automata,” in *Conference on the Theory and Application of Cryptographic Techniques*. Springer, 1985, pp. 429–432.

- [108] S. Nandi, B. Kar, and P. P. Chaudhuri, "Theory and applications of cellular automata in cryptography," *IEEE Transactions on computers*, vol. 43, no. 12, pp. 1346–1357, 1994.
- [109] K. Preston, M. J. Duff, S. Levialedi, P. E. Norgren, and J. Toriwaki, "Basics of cellular logic with some applications in medical image processing," *Proceedings of the IEEE*, vol. 67, no. 5, pp. 826–856, 1979.
- [110] P. Sahota, M. F. Daemi, and D. G. Elliman, "Training genetically evolving cellular automata for image processing," in *Speech, Image Processing and Neural Networks, 1994. Proceedings, ISSIPNN '94., 1994 International Symposium on*, Apr 1994, pp. 753–756 vol.2.
- [111] J. Dittmann, A. Steinmetz, and R. Steinmetz, "Content-based digital signature for motion pictures authentication and content-fragile watermarking," in *Multimedia Computing and Systems, 1999. IEEE International Conference on*, vol. 2. IEEE, 1999, pp. 209–213.
- [112] T. Toffoli and N. Margolus, *Cellular Automata Machines: A new environment for modelling*. MIT press, 1987.
- [113] B. Chopard, A. Dupuis, A. Masselot, and P. Luthi, "Cellular automata and lattice boltzmann techniques: An approach to model and simulate complex systems," *Advances in complex systems*, vol. 5, no. 2, pp. 1–144, 2002.
- [114] N. Ganguly, B. K. Sikdar, A. Deutsch, G. Canright, and P. P. Chaudhuri, "A survey on cellular automata," Dresden University of Technology, Bengal Engineering College, Telenor Research and Development, Tech. Rep., 2003.
- [115] C. Emmeche, *The Garden in the Machine: The Emerging Science of Artificial Life*. Princeton University Press, 1996.
- [116] M. A. Nowak, *Evolutionary dynamics: exploring the equations of life*. Harvard University Press, 2006.
- [117] K. Sims, "Interactive evolution of equations for procedural models," *The Visual Computer*, vol. 9, no. 8, pp. 466–476, 1993.
- [118] G. Birkin, "Art & complexity: an exploration of aesthetics," in *Proceedings of the 6th ACM SIGCHI conference on Creativity & cognition*. ACM, 2007, pp. 278–278.
- [119] G. Birkin, "Aesthetic complexity: Practice and perception in art & design," Ph.D. dissertation, Nottingham Trent University, October 2010.
- [120] R. Rucker, *Seek!: Selected Nonfiction*. Running Press Book Publishers, 1999.
- [121] T. O. Roth and A. Deutsch, "Universal synthesizer and window: Cellular automata as a new kind of cybernetic image," in *Imagery in the 21st Century*, O. G. with Thomas Veigl, Ed. The MIT Press, 2011, pp. 269–288.
- [122] R. Thornhill and S. W. Gangestad, "Human fluctuating asymmetry and sexual behavior," *Psychological Science*, vol. 5, no. 5, pp. 297–302, 1994.

- [123] S. W. Gangestad, R. Thornhill, and R. A. Yeo, “Facial attractiveness, developmental stability, and fluctuating asymmetry,” *Ethology and Sociobiology*, vol. 15, no. 2, pp. 73–85, 1994.
- [124] P. Møller A. and T. R., “Bilateral symmetry and sexual selection: a meta-analysis,” *Am. Nat.*, vol. 151, no. 2, pp. 174–192, 1998.
- [125] M. A. Javaheri Javid, T. Blackwell, R. Zimmer, and M. M. al Rifaie, “Spatial complexity measure for characterising cellular automata generated 2D patterns,” in *Progress in Artificial Intelligence: 17th Portuguese Conference on Artificial Intelligence, EPIA 2015, Coimbra, Portugal, September 8-11, 2015. Proceedings.*, ser. Lecture Notes in Artificial Intelligence, F. Pereira, P. Machado, E. Costa, and A. Cardoso, Eds., vol. 9273. Springer International Publishing, 2015, pp. 201–212.
- [126] B. Julesz, “Binocular depth perception of computer-generated patterns.” *Bell System Technical Journal*, vol. 39, no. 5, pp. 1125–1162, 1960.
- [127] K. C. Knowlton, “Explor—a generator of images from explicit patterns, local operations, and randomness,” in *Proceedings of 9th Meeting of UAIDE*, 1970, pp. 544–583.
- [128] K. Knowlton, “Mini-explor: A fortran-coded version of the explor language for mini (and larger) computers,” *SIGGRAPH Comput. Graph.*, vol. 9, no. 3, pp. 31–42, sep 1975.
- [129] L. Geurts and L. Meertens, “Crystallization,” *Computers and Automation*, no. 8, p. 22, 1970.
- [130] J. Scala, “Joseph scala,” in *Artist and computer*, R. Leavitt, Ed. Harmony Books, 1976, pp. 70–72.
- [131] I. R. Scha, “Kunstmatige Kunst,” *De Commectie*, vol. 2, no. 1, pp. 4–7, 2006.
- [132] H. Beddard and D. Dodds, *Digital Pioneers*, ser. V&A Pattern. V&A Publishing, 2009.
- [133] E. Regis, *Who got Einstein’s office?: eccentricity and genius at the Institute for Advanced Study*. Basic Books, 1988.
- [134] S. Wolfram, “Computer software in science and mathematics.” *Scientific American*, vol. 251, no. 3, 1984.
- [135] S. Wolfram, “Cellular automata as models of complexity,” *Nature*, vol. 311, no. 5985, pp. 419–424, 1984.
- [136] B. P. Hoke, “Cellular automata and art,” [Online]. Available: <http://www.dartmouth.edu/~matc/math5.pattern/FinalProject/Hoke.html>, 1996, [Accessed]: Apr, 2017.
- [137] E. F. S. Jr, “John f. simon jr,” [Online]. Available: <http://www.numeral.com/>, 2017, [Accessed]: Apr, 2017.
- [138] D. Terdiman, “When leds and math equal high art,” [Online]. Available: http://news.cnet.com/8301-13772_3-20017310-52.html?tag=mncol;1n, Sept 2011, [Accessed]: Apr, 2017.

- [139] R. Espericueta, “Rafael espericueta,” [Online]. Available: <http://www.imagekind.com/MemberProfile.aspx?MID=95734473-9596-4182-850D-57F862AAF2C4>, 2017, [Accessed]: Apr, 2017.
- [140] R. J. Krawczyk, “Architectural interpretation of cellular automata,” in *The 5th International Conference on Generative Art*, 2002, pp. 7–1.
- [141] E. Driessen and M. Verstappen, “Erwin driessen and maria verstappen,” [Online]. Available: <https://notnot.home.xs4all.nl/>, 2017, [Accessed]: Apr, 2017.
- [142] G. Fechner, *Vorschule der aesthetik* [Preschool of aesthetics], ser. Vorschule der Aesthetik. Breitkopf & Härtel, 1876, vol. 1-2.
- [143] R. Arnheim, *Art and visual perception: A psychology of the creative eye*. Univ of California Press, 1954.
- [144] D. Berlyne, *Studies in the new experimental aesthetics: steps toward an objective psychology of aesthetic appreciation*, ser. Halsted Press Book. Hemisphere Pub. Corp., 1974.
- [145] S. Zeki and J. Nash, *Inner vision: An exploration of art and the brain*. Oxford University Press Oxford, 1999, vol. 415.
- [146] D. Dutton, “Aesthetics and evolutionary psychology,” *The Oxford handbook for aesthetics*, pp. 693–705, 2003.
- [147] D. Dutton, *The Art Instinct: Beauty, Pleasure, and Human Evolution*. Oxford University Press, 2009.
- [148] H. Kawabata and S. Zeki, “Neural correlates of beauty,” *Journal of neurophysiology*, vol. 91, no. 4, pp. 1699–1705, 2004.
- [149] V. Ramachandran and W. Hirstein, “The science of art: a neurological theory of aesthetic experience,” *Journal of Consciousness Studies*, vol. 6, no. 6-7, pp. 15–51, 1999.
- [150] R. Thornhill, “Darwinian aesthetics informs traditional aesthetics,” in *Evolutionary Aesthetics*, E. Voland and K. Grammer, Eds. Springer-Verlag Berlin and Heidelberg, 2003, ch. I The Problem.
- [151] A. Slater, C. V. der Schulten, E. Brown, M. Badenoch, G. Butterworth, S. Parsons, and C. Samuels, “Newborn infants prefer attractive faces,” *Infant Behavior and Development*, vol. 21, no. 2, pp. 345–354, 1998.
- [152] K. GRAMMER, B. FINK, A. P. MØLLER, and R. THORNHILL, “Darwinian aesthetics: sexual selection and the biology of beauty,” *Biological reviews*, vol. 78, no. 3, pp. 385–407, 2003.
- [153] G. Greenfield, “On the origins of the term “computational aesthetics”,” in *Proceedings of the First Eurographics Conference on Computational Aesthetics in Graphics, Visualization and Imaging*, ser. Computational Aesthetics’05. Aire-la-Ville, Switzerland: Eurographics Association, 2005, pp. 9–12.
- [154] P. Galanter, “Computational aesthetic evaluation: Past and future,” in *Computers and Creativity*, J. McCormack and M. d’Inverno, Eds. Berlin, Heidelberg: Springer Berlin Heidelberg, 2012, pp. 255–293.

- [155] P. Galanter, “Computational aesthetic evaluation: automated fitness functions for evolutionary art, design, and music,” in *Proceeding of the fifteenth annual conference companion on Genetic and evolutionary computation conference companion*, ser. GECCO '13 Companion. ACM, 2013, pp. 1005–1038.
- [156] E. den Heijer, “Autonomous evolutionary art,” Ph.D. dissertation, Vrije Universiteit, Amsterdam, 2013.
- [157] R. De Rosa, *Descartes and the puzzle of sensory representation*. Oxford University Press, 2010.
- [158] E. Prettejohn, *Beauty and Art, 1750-2000*. Oxford University Press, 2005.
- [159] A. Baumgarten, *Aesthetica scripsit Alexand. Gottlieb Baumgarten*. Impens. I.C. Kleyb, 1750.
- [160] A. Panizo and E. F. Rustia, *Introduction to Art Appreciation and Aesthetics: An Approach to the Humanities*. Rex Printing Company, Inc. Manila, Philippines, 1969.
- [161] G. Fechner, *Elemente der Psychophysik* [Elements of Psychophysics]. Breitkopf & Härtel, 1860.
- [162] W. M. Wundt, *Grundzüge de physiologischen Psychologie* [Outline of physiological psychology]. W. Engelman, Leipzig, Germany, 1874.
- [163] H. Munsinger and W. Kessen, “Uncertainty, structure, and preference.” *Psychological Monographs: General and Applied*, vol. 78, no. 9, p. 1, 1964.
- [164] D. E. Berlyne, “Novelty, complexity, and hedonic value,” *Perception & Psychophysics*, vol. 8, no. 5, pp. 279–286, 1970.
- [165] P. J. Silvia, *Exploring the psychology of interest*. Oxford University Press, 2006.
- [166] S. S. Stevens, “On the psychophysical law,” *Psychological review*, vol. 64, no. 3, p. 153, 1957.
- [167] A. Nieder and E. K. Miller, “7 neural correlates of numerical cognition in the neocortex of nonhuman primates,” in *From Monkey Brain to Human Brain: A Fyssen Foundation Symposium*. MIT Press, 2005, p. 117.
- [168] D. E. Berlyne, “Conflict and information-theory variables as determinants of human perceptual curiosity,” *Journal of experimental psychology*, vol. 53, no. 6, p. 399, 1957.
- [169] E. Whittaker, “George David Birkhoff,” *Journal of the London Mathematical Society*, vol. 20, no. 2, pp. 121–128, 1945.
- [170] G. Birkhoff, “Mathematics of aesthetics,” in *The World of Mathematics*, J. Newman, Ed., vol. 4. Simon and Schuster, N.Y., 1956, pp. 2185–2208.
- [171] R. Scha and R. Bod, “Computationele esthetica [computational esthetics],” *Informatie en Informatiebeleid*, vol. 11, no. 1, pp. 54–63, 1993.

- [172] T. Staudek, “On Birkhoff’s aesthetic measure of vases,” *Faculty of Information, Masaryk University Report Series (FIMU-RS-99-06)*, 1999.
- [173] T. Staudek, “Exact aesthetics. object and scene to message,” Ph.D. dissertation, Faculty of Informatics, Masaryk University of Brno, 2002.
- [174] D. J. Wilson, “An experimental investigation of Birkhoff’s aesthetic measure,” *The Journal of Abnormal and Social Psychology*, vol. 34, no. 3, p. 390, July 1939.
- [175] H. J. Eysenck, “The empirical determination of an aesthetic formula.” *Psychological Review*, vol. 48, no. 1, p. 83, 1941.
- [176] H. J. Eysenck, “An experimental study of aesthetic preference for polygonal figures,” *The Journal of General Psychology*, vol. 79, no. 1, pp. 3–17, 1968.
- [177] H. J. Eysenck, “The experimental study of the ‘good gestalt’ –a new approach.” *Psychological Review*, vol. 49, no. 4, p. 344, 1942.
- [178] C. Shannon, “A mathematical theory of communication,” *The Bell System Technical Journal*, vol. 27, pp. 379–423 & 623–656, Oct. 1948.
- [179] T. M. Cover and J. A. Thomas, *Elements of Information Theory (Wiley Series in Telecommunications and Signal Processing)*. Wiley-Interscience, 2006.
- [180] A. Newell, J. C. Shaw, and H. A. Simon, “Elements of a theory of human problem solving,” *Psychological review*, vol. 65, no. 3, p. 151, 1958.
- [181] H. W. Franke, “A cybernetic approach to aesthetics,” *Leonardo*, vol. 10, no. 3, pp. 203–206, 1977.
- [182] A. A. Moles, *Théorie de l’information et perception esthétique* [Information theory and esthetic perception]. Flammarion & C, 1958.
- [183] M. Bense, *Aesthetica: Programmierung des Schönen, allgemeine Texttheorie und Textästhetik* [Aesthetica : Programming of beauty, general text theory and aesthetics]. Agis-Verlag, 1960.
- [184] M. Bense and G. Nee, “Computer grafik,” in *Edition Rot*, M. Bense and E. Walther, Eds. Walther, Stuttgart, 1965, vol. 19.
- [185] M. Bense, *Kleine abstrakte ästhetik* [small abstract aesthetics], ser. Edition Rot. E. Walther, March 1969, vol. 38.
- [186] R. Arnheim, “Towards a psychology of art/entropy and art an essay on disorder and order,” *The Regents of the University of California*, 1966.
- [187] R. Arnheim, *Visual thinking*. Univ of California Press, 1969.
- [188] M. Bense, *Aesthetica, Einführung in die neue Aesthetik* [Aesthetica introduction to the new aesthetics]. Agis-Verlag, Baden-Baden, 1965.
- [189] F. Nake, “Information aesthetics: An heroic experiment,” *Journal of Mathematics and the Arts*, vol. 6, no. 2-3, pp. 65–75, 2012.

- [190] R. Gunzenhäuser, *Ästhetisches Mass und ästhetische Information: Einführung in die Theorie GD Birkhoffs und die Redundanztheorie ästhetischer Prozesse* [Aesthetic measure and aesthetic information: introduction to the theory of G. D. Birkhoff and the redundancy theory of aesthetic processes]. Schnelle Quickborn, 1962.
- [191] P. Machado and A. Cardoso, “Computing aesthetics,” in *Advances in Artificial Intelligence*. Springer, 1998, pp. 219–228.
- [192] J. Rigau, M. Feixas, and M. Sbert, “Informational aesthetics measures,” *Computer Graphics and Applications, IEEE*, vol. 28, no. 2, pp. 24–34, 2008.
- [193] H. Leder, B. Belke, A. Oeberst, and D. Augustin, “A model of aesthetic appreciation and aesthetic judgments,” *British journal of psychology*, vol. 95, no. 4, pp. 489–508, 2004.
- [194] D. J. Graham and C. Redies, “Statistical regularities in art: Relations with visual coding and perception,” *Vision Research*, vol. 50, no. 16, pp. 1503 – 1509, 2010.
- [195] R. Arnheim, *Entropy and art: An essay on disorder and order*. Univ of California Press, 1974.
- [196] E. Navratil, I. Zelinka, and R. Senkerik, “Preliminary results of deterministic chaos control through complexity measures,” in *20th European Conference on Modelling and Simulation ECMS 2006: Modelling Methodologies and Simulation: Key Technologies in Academia and Industry*. European Council for Modelling and Simulation (ECMS), 2006.
- [197] M. Li, *An introduction to Kolmogorov complexity and its applications*. Springer, 1997.
- [198] J. Ziv and A. Lempel, “Compression of individual sequences via variable-rate coding,” *Information Theory, IEEE Transactions on*, vol. 24, no. 5, pp. 530–536, 1978.
- [199] T. Jacobsen and L. Höfel, “Aesthetic judgments of novel graphic patterns: analyses of individual judgments,” *Perceptual and motor skills*, vol. 95, no. 3, pp. 755–766, 2002.
- [200] R. Likert, “A technique for the measurement of attitudes.” *Archives of psychology*, vol. 15, no. 140, pp. 1–55, 1932.
- [201] C. Spearman, “The proof and measurement of association between two things,” *The American Journal of Psychology*, vol. 15, no. 1, pp. 72–101, 1904.
- [202] M. A. Javid, T. Blackwell, R. Zimmer, and M. M. Al-Rifaie, “Correlation between human aesthetic judgement and spatial complexity measure,” in *Proceedings of the 5th International Conference on Evolutionary and Biologically Inspired Music, Sound, Art and Design - Volume 9596*. New York, NY, USA: Springer-Verlag New York, Inc., 2016, pp. 79–91.